

DESIGN OF A NON-TRANPOSED POWER TRANSMISSION
LINE MODEL

Kenneth A. Schmidt

LIBRARY

NAVAL POSTGRADUATE SCHOOL

MONTEREY, CALIF. 93940

DESIGN OF A NON-TRANPOSED
POWER TRANSMISSION LINE MODEL

by

Kenneth A. Schmidt
B.A., Vanderbilt University
(1964)

SUBMITTED IN PARTIAL FULFILLMENT
OF THE REQUIREMENTS FOR THE
DEGREES OF
NAVAL ENGINEER
and
MASTER OF SCIENCE IN ELECTRICAL ENGINEERING

at the

MASSACHUSETTS INSTITUTE OF TECHNOLOGY

June, 1971



DESIGN OF A NON-TRANPOSED
POWER TRANSMISSION LINE MODEL

by

Kenneth A. Schmidt

Submitted to the Departments of Naval Architecture and Marine Engineering and Electrical Engineering on May 14, 1971, in partial fulfillment of the requirements for the degrees of Naval Engineer and Master of Science in Electrical Engineering.

ABSTRACT

This thesis describes the design and construction of a wide band (60-3060 Hz), three phase (including zero sequence), non-transposed, lumped element, power transmission line model. The model consists of from 15 to 65 "three phase L sections" - depending upon the length of the actual line being modeled - and includes trimming features to model both horizontal and vertical configurations of lines in the 345 kV to 1500 kV range.

To predict the performance of the model and determine the number of sections required to model a given line, the poles of the driving point impedance of various numbers of L-sections in series is determined by computer and compared with the corresponding poles of the actual line being modeled. For either an open or short circuited termination, the performance specification is that in the range from 60 to 400 miles long, the percent error between the poles of the model and those of the actual line shall not exceed 5 percent. This criterion results in the requirement for 15 to 65 L-sections. Thirty sections are of 4 mile "length" and thirty five are of 8 mile "length".

With the number and "length" of the model sections determined, electrical parameter data for a number of typical extra high voltage (EHV) lines are suitably scaled to select a base value of model inductance and capacitance for the 4 mile and 8 mile sections. The effects of non-transposition are modeled by incorporating two mutual inductors between the phases. Zero-sequence inductance is modeled by a specially designed low Q inductor whose inductance decreases appropriately with increasing frequency.

To ensure that the overall quality factor of the model remains greater than or equal to that of actual lines for all frequencies between 60 Hz and 3060 Hz; low loss, powdered molybdenum-nickel-iron toroid cores are selected for the inductors, and low dissipation factor polystyrene capacitors form the basic capacitance of each section. With the designed quality factor of the model exceeding that of most EHV lines in operation, the Q of the model is brought into correspondence with actual lines (at 60 Hz) by suitably inserting resistance into each section.

Thesis Supervisor: Gerald L. Wilson
Title: Associate Professor of Electrical Engineering

Thesis Reader: Warren C. Dietz
Title: Associate Professor of Marine Engineering

TABLE OF CONTENTS

	<u>page</u>
TITLE PAGE	1
ABSTRACT	2
TABLE OF CONTENTS	4
LIST OF FIGURES	7
LIST OF TABLES	9
ACKNOWLEDGMENTS	11
CHAPTER 1 <u>INTRODUCTION</u>	12
1.1 Transmission System Simulators	12
1.2 General Model Parameters and Constraints	12
1.3 Features and Scope of the Design	13
1.4 Extensions of the Design Concept	14
CHAPTER 2 <u>MODEL CONFIGURATIONS</u>	15
2.1 General Non-Transposed Models	15
2.2 Transposed Models	20
2.2.1 Symmetrical Component Equivalent Circuits for a Transposed Model	22
CHAPTER 3 <u>NATURAL FREQUENCY ANALYSIS</u>	24
3.1 Methods and Criteria for Predicting Model and Actual Line Correspondence	24
3.2 Driving Point Impedance of Continuous Lines	27
3.3 Driving Point Impedance of L-Section Model	30
3.3.1 Inductor Input L-Section Model (Shorted)	32
3.3.2 Capacitor Input L-Section Model (Shorted)	37
3.3.3 L-Section Model, Open Termination	43
3.4 Driving Point Impedance of π -Section Models	45
3.4.1 π -Section Model (Shorted)	45
3.4.2 π -Section Model (Open)	48
3.5 Conclusions	48
3.6 Applications and Recommendations	53
CHAPTER 4 <u>PARAMETERS OF EHV LINES AND MODELS</u>	55
4.1 Parameters of Representative EHV Lines	55
4.2.1 Line/Model Scale Factors and General Model Parameters	65
4.2.2 Selection of Model Mutual Inductance Parameters	73
4.2.3 Selection of Model Resistance Parameters	75
4.2.4 Selection of Model Capacitance Parameters	75
4.3 Summary Remarks	76

	<u>page</u>
CHAPTER 5 <u>INDUCTOR DESIGN</u>	77
5.1 Model Inductor Requirements	77
5.2 Inductor Core Selection and Core Properties	78
5.3 Design of Model Self Inductors	85
5.4 Design of Model Mutual Inductors	89
CHAPTER 6 <u>CAPACITOR SELECTION</u>	94
6.1 Factors Determining Capacitor Selection	94
6.2 Capacitors Selected for Model Sections	99
CHAPTER 7 <u>RESISTANCE AND LOSS CONSIDERATIONS</u>	102
7.1 Overall Q Considerations	102
7.2 Resistance Selection	105
CHAPTER 8 <u>MODEL PHYSICAL CONSTRUCTION</u>	109
8.1 Electrical Construction of a Typical Section	109
8.2 T.L.M. Physical Construction	109
CHAPTER 9 <u>SUMMARY AND RECOMMENDATIONS</u>	114
9.1 Summary	114
9.2 Recommendations	117
APPENDIX A <u>MODEL TRANSFORMATIONS</u>	121
A.1 Equations of the General Non-Transposed Model	121
A.2 Transformation of the General Non-Transposed Model to a "Balanced Mutual" Model	121
A.3 Transformation of the General Non-Transposed Model to a "Transposed Model"	122
APPENDIX B <u>MODEL IMPEDANCE DERIVATIONS</u>	128
B.1.1 Derivation of L-Section Model Impedance, Inductor Input, Shorted Termination	128
B.1.2 Solution for the Poles of the L-Section Model, Inductor Input, Shorted Termination	130
B.2 Derivation of L-Section Model Impedance, Capacitor Input, Shorted Termination	133
B.3 Derivation of L-Section Model Impedance, Open Termination	135
B.4 Derivation of π -Section Model Impedance, Shorted Termination	136
B.5 Derivation of π -Section Model Impedance, Open Termination	139

	<u>page</u>
APPENDIX C <u>SOLUTIONS FOR THE POLES OF THE MODEL IMPEDANCE FUNCTIONS</u>	140
C.1 Model Impedance Functions	140
C.2 Generation of Impedance Function Denominator Polynomial	142
C.2.1 Polynomial for L-Section Model, Inductor Input, Shorted	145
C.2.2 Polynomial for L-Section Model, Capacitor Input, Shorted	147
C.2.3 Polynomial for L-Section Model, Open	148
C.2.4 Polynomial for π -Section Model, Shorted	148
C.2.5 Polynomial for π -Section Model, Open	149
APPENDIX D <u>COMPUTER PROGRAM LISTINGS</u>	150
D.1 Pole Error Program, Inductor Input, Shorted Termination, L-Section Model	150
D.2 Pole Error Program, Capacitor Input, Shorted Termination, L-Section Model	154
D.3 Pole Error Program, Open Termination, L-Section Model	158
D.4 Pole Error Program, Shorted Termination, π -Section Model	162
D.5 Pole Error Program, Open Termination, π -Section Model	166
D.6 Pole Error Program, Zero Sequence, Shorted Termination, Lossy L-Section Model	170
LIST OF REFERENCES	174

LIST OF FIGURES

<u>Figure</u>	<u>Title</u>	<u>Page</u>
2.1	Section of General Non-Transposed Line Model.	16
2.2	Section of a "Balanced Mutual", Non-Transposed Line Model.	18
2.3	Section of Transposed Line Model.	21
3.1a	Schematic of L-Section Model, Positive-Sequence Components.	25
3.1b	Schematic of L-Section Model, Zero-Sequence Components.	25
3.2	Diagram of a General Transmission Line of Length, ℓ .	28
3.3	Schematic of L-Section Model Inductor Input, Positive Sequence Component, Shorted Termination.	31
3.4a	Plot of Pole Error vs. Pole No., L-Section Line, Inductor Input, Shorted Termination, Lossy Line and Model. (765 kV <u>Positive-Sequence</u>).	34
3.4b	Plot of Pole Error vs. Pole No., L-Section Line, Inductor Input, Shorted Termination, Lossless Line and Model.	36
3.5	Plot of Pole Error vs. Pole No., L-Section Line, Inductor Input, Shorted Termination, Lossy Line. (765 kV <u>Zero-Sequence</u>).	39
3.6	Schematic of L-Section Model, Lossless, Capacitor Input, Positive-Sequence Component (Shorted).	40
3.7	Plot of Pole Error vs. Pole No. L-Section Line, Capacitor Input, Shorted Termination.	42
3.8	Plot of Pole Error vs. Pole No., L-Section Line, Open Termination.	44
3.9	Plot of Pole Error vs. Pole No., π -Section Line, Shorted Termination.	47
3.10	Plot of Pole Error vs. Pole No., π -Section Line, Open Termination.	49
3.11	Examples of an "Error Band-Error Bound" Plot for a Twelve Section L-Model.	51
4.1	Graph of Positive-Sequence Q vs. Frequency for Representative EHV Lines.	62

4.2	Graph of Zero-Sequence Q vs. Frequency for Representative EHV Lines.	63
4.3	Graph of Zero-Sequence Inductance vs. Frequency for a Typical 765 kV Line.	64
4.4	Graph of Zero-Sequence Inductance vs. Frequency of a 4-Mile Model Section When Modeling a Typical 765 kV Line.	71
5.1	Graph of Q vs. Frequency of T.L.M. Inductors and Sections.	81
5.2	Circuit For Measuring T.L.M. Inductor Q at 59 Hz.	82
5.3	Graph of Permeability vs. AC Flux Density for T.L.M. Inductors.	88
7.1	Test Circuit for Measuring Resistance of Banana Jacks and Plugs.	104
8.1	Electrical Schematic of Typical Section.	110
8.2	Typical Section Chassis Construction.	111
8.3	Operating Panel of Typical T.L.M. Section.	112
8.4	Drawing of T.L.M. Console.	113
A.1	Illustration of One Cycle of Transposed Line.	123
B.1	Schematic of Lossless π -Section Model.	137

LIST OF TABLES

<u>Table</u>	<u>Title</u>	<u>Page</u>
3.1	Table of Pole Frequencies for a Shorted, Typical 765 kV Line (Positive Sequence-Lossless).	38
3.2	Table of Pole Frequencies for an Open, Typical 765 kV Line (Positive-Sequence-Lossless).	46
4.1	Table of Positive Sequence Parameters for Some Typical EHV Line Configurations (at 60 Hz).	57
4.2	Table of Positive-Sequence Q and Zero-Sequence Parameters of Some Typical EHV Line Configurations.	58
4.3	Table of Unscaled Parameters for Model of Representative EHV Lines.	59
4.4a	Table of Scaled Parameters Implied For a 4-Mile Model Section ("Horizontal" Lines).	68
4.4b	Table of Scaled Parameters Implied For a 4-Mile Model Section ("Vertical" Lines).	69
4.5	Self Inductance Designed Into the 4-Mile Sections.	72
4.6	Table of Mutual Inductance Values Designed Into the 4-Mile Sections.	74
5.1	Turns Required in 4-Mile T.L.M. Inductors.	86
5.2	Turns Required in 8-Mile T.L.M. Inductors.	86
5.3	Table of L_{ab} and $(L_{ab})_s$ For T.L.M. 4-Mile Sections.	91
5.4	Table of L_{bc} and $(L_{bc})_s$ For T.L.M. 4-Mile Sections.	92
5.5	Table of Mutual Inductance Values Designed Into the 8-Mile Sections.	93
6.1	Table of Capacitance Parameters to be Spanned by the 4 and 8-Mile Model Sections.	95
6.2	Table of Capacitor Values Provided in the T.L.M. Capacitor Banks.	100
7.1	Table of Q Values Provided in the T.L.M. Sections.	106

7.2	Table of Operating Panel Resistance Values Corresponding to Q's of Table 7.1.	106
7.3	Table of Resistors in the T.L.M. Sections.	107
B.1	Table of Expansions of $\sinh m\lambda$.	130
B.2	Table of Expansions of $\cosh m\lambda$.	131
B.3	Table of Expansions of Impedance Function Denominator (L-Section Line, Inductor Input, Shorted Termination).	131
C.1	Table of Impedance Functions for Which Poles Are Sought.	141

ACKNOWLEDGEMENTS

I wish to express first of all my gratitude to the U.S. Navy for providing the time and finances for the entire seven years of my college education. I wish to thank Professor Gerald L. Wilson, my thesis supervisor, for the initial concept and direction of the project, for his constant availability and interest, and for his timely suggestions, comments, criticisms, and guidance throughout the design. Many of the important ideas in the design are those of Professor Wilson. I wish to thank also Dr. John D. Glover for his help in the implementation of the polynomial generator program. Finally, I wish to thank Mrs. Barbara Morton for her weeks of effort in typing a very difficult manuscript.

The direct funding of this project was provided by the American Electric Power Service Corporation. It is hoped that the results described herein will merit their continued confidence and support.

CHAPTER 1

INTRODUCTION

1.1 Transmission System Simulators

The three phase power transmission line model to be designed will form part of a power transmission system simulator (TSS) for use in the M.I.T. Electric Power Systems Engineering Laboratory. Knowledge of the transient behavior of power system networks is essential to the system designer and planner in order to correctly dimension or rate the various components of a power system. Circuit breakers and insulators, for example, cannot be correctly sized without some knowledge of the magnitude and duration of system fault currents or switching overvoltages. With 765 kV systems already in operation, and 1100 kV and 1500 kV systems proposed for the future, it is particularly important to know the magnitude and shape of over-voltage transients caused by routine switching operations. Models for 1100-1500 kV lines still in the design stage are of obvious value, and the very limited access to extra high voltage (EHV) lines in operation makes a model of these lines highly desirable.

1.2 General Model Parameters and Constraints

A transmission line model (t.l.m.) is only one part of a TSS. Most simulators include, in addition, models of power system generators, transformers, compensating reactors, lightning arresters, circuit breakers, ground fault neutralizers, etc. In the present t.l.m. design, the requirement for interface with other TSS components places certain constraints upon the model. In particular, compatibility

with existing TSS transformers dictates that the nominal operating voltage of the t.l.m. be 138V line-to-line and that nominal phase current be 38.6 ma. Other required features for the t.l.m. are that it be capable of modeling vertical, horizontal, transposed, and non-transposed EHV line configurations from 60 to 400 miles in length, have quality factors exceeding those of existing EHV lines from 60 to 3060 Hz, model the variation of zero sequence inductance with frequency over the range 60 to 3060 Hz, and model lines in the voltage range from 345 kV to 1500 kV. In addition, the positive sequence inductance and capacitance of the t.l.m. must remain essentially constant over the range 60 Hz to 3060 Hz, and inductance must remain constant with varying current in the range from 0 to at least one ampere-thus ensuring constant model inductance up to 25 p.u. fault current.

1.3 Features and Scope of Design

One of the more unique features of this t.l.m. design is that it is to be capable of modeling non-transposed power transmission lines. Numerous transmission line models in simulators are presently in operation¹⁻⁴, but all in the U.S., at least, are transposed models. A literature search covering the period subsequent to 1960 disclosed only a limited literature on t.l.m.'s - all relating to transposed models. Many actual lines are, in fact, not transposed. Previously, with relatively lower voltage transmission lines, it was assumed that the small effects of non transposition could be ignored. Non-transposed lines were mathematically and physically modeled as though they were transposed, and model results

were considered to agree satisfactorily with actual lines. Recent studies⁵ on EHV lines indicate, however, that the effects of non-transposition can no longer be ignored. This thesis is an attempt to design a t.l.m. which will include the effects of non-transposition and document the design in sufficient detail that persons other than the designer can construct and operate the model.

1.4 Extensions of the Design Concept

The t.l.m. design discussed in this thesis is intended specifically for the modeling of electric utility power transmission systems for which the X_C/X_L ratio (per unit length) at 60 Hz is of the order of 230,000-270,000 mi^2 (X_C = positive-sequence capacitive reactance; X_L = positive-sequence inductive reactance). The design concept, however, is not at all limited to utility lines. As will become clear in later sections of the discussion, any band of X_C/X_L ratios could have been provided - had it been desirable or necessary. With the proper selection of model components, any audio range power transmission system involving inductive and capacitive coupling could be accommodated. Thus, the model concept is equally suited to modeling, for example, under ground power cables, long ship-board or industrial plant cable runs or long synchro cable runs, etc.. In addition, the mathematical approach developed in Chapter 3 for the solution of the impedance polynomial has application in any area where the impedance concept has validity - including, for example, the mechanical impedance in mechanical vibrations problems.

CHAPTER 2

MODEL CONFIGURATIONS

2.1 General Non-Transposed Models

A section of a general, lumped-element, three-phase transmission line is shown in Figure 2.1. The electrical parameters of the model follow directly from the inductance, capacitance, and resistance matrices of the actual line. With the matrices of the line defined as

$$[L] = \begin{bmatrix} L_{aa} & L_{ab} & L_{ac} \\ L_{ab} & L_{bb} & L_{bc} \\ L_{ac} & L_{bc} & L_{cc} \end{bmatrix}, \quad (2-1)$$

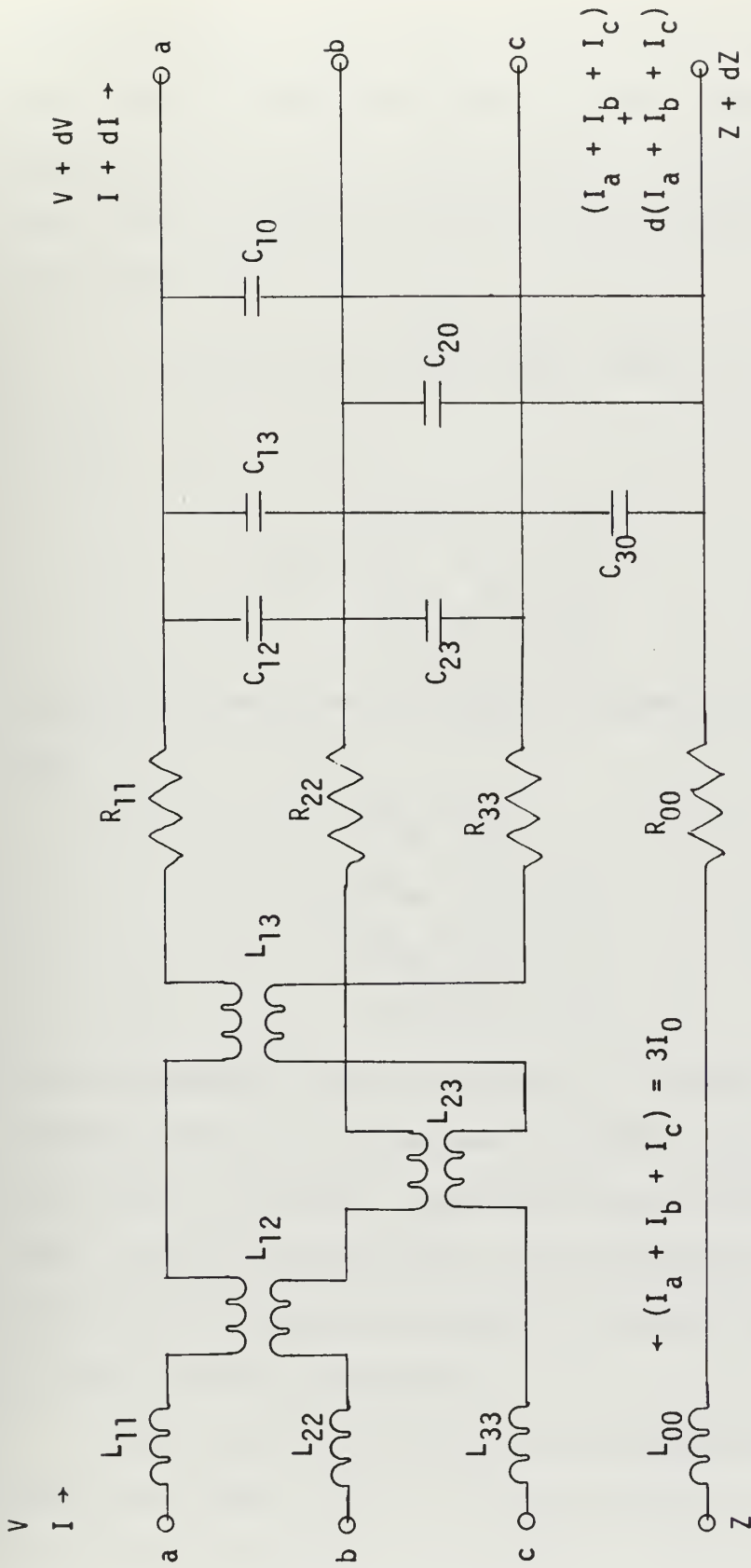
$$[C] = \begin{bmatrix} C_{aa} & -C_{ab} & -C_{ac} \\ -C_{ab} & C_{bb} & -C_{bc} \\ -C_{ac} & -C_{bc} & C_{cc} \end{bmatrix},$$

and

$$[R] = \begin{bmatrix} R_{aa} & R_{ab} & R_{ac} \\ R_{ab} & R_{bb} & R_{bc} \\ R_{ac} & R_{bc} & R_{cc} \end{bmatrix},$$

the correspondence between line and model inductance and capacitance parameters is as follows (See Appendix A.1):

$$\begin{aligned} L_{aa} &= L_{11} + L_{00} & L_{ab} &= L_{12} + L_{00} \\ L_{bb} &= L_{22} + L_{00} & L_{bc} &= L_{23} + L_{00} \\ L_{cc} &= L_{33} + L_{00} & L_{ac} &= L_{13} + L_{00} \\ C_{ab} &= C_{12} & C_{aa} &= C_{12} + C_{13} + C_{10} \\ C_{ac} &= C_{13} & C_{bb} &= C_{12} + C_{23} + C_{20} \\ C_{bc} &= C_{23} & C_{cc} &= C_{13} + C_{23} + C_{30} \end{aligned} \quad (2-2)$$



Section of General Non-Transposed Line Model

Figure 2.1

The resistance R_{00} in the model represents only an approximate modeling of line inter-phase resistances. Rather than providing three separate inter-phase resistance circuits in the model, each of the three line inter-phase resistances is approximated by the average of the three i.e.,

$$R_{ab} \approx R_{bc} \approx R_{ac} \approx \frac{R_{ab} + R_{bc} + R_{ac}}{3} = R_m. \quad (2-3)$$

So that,

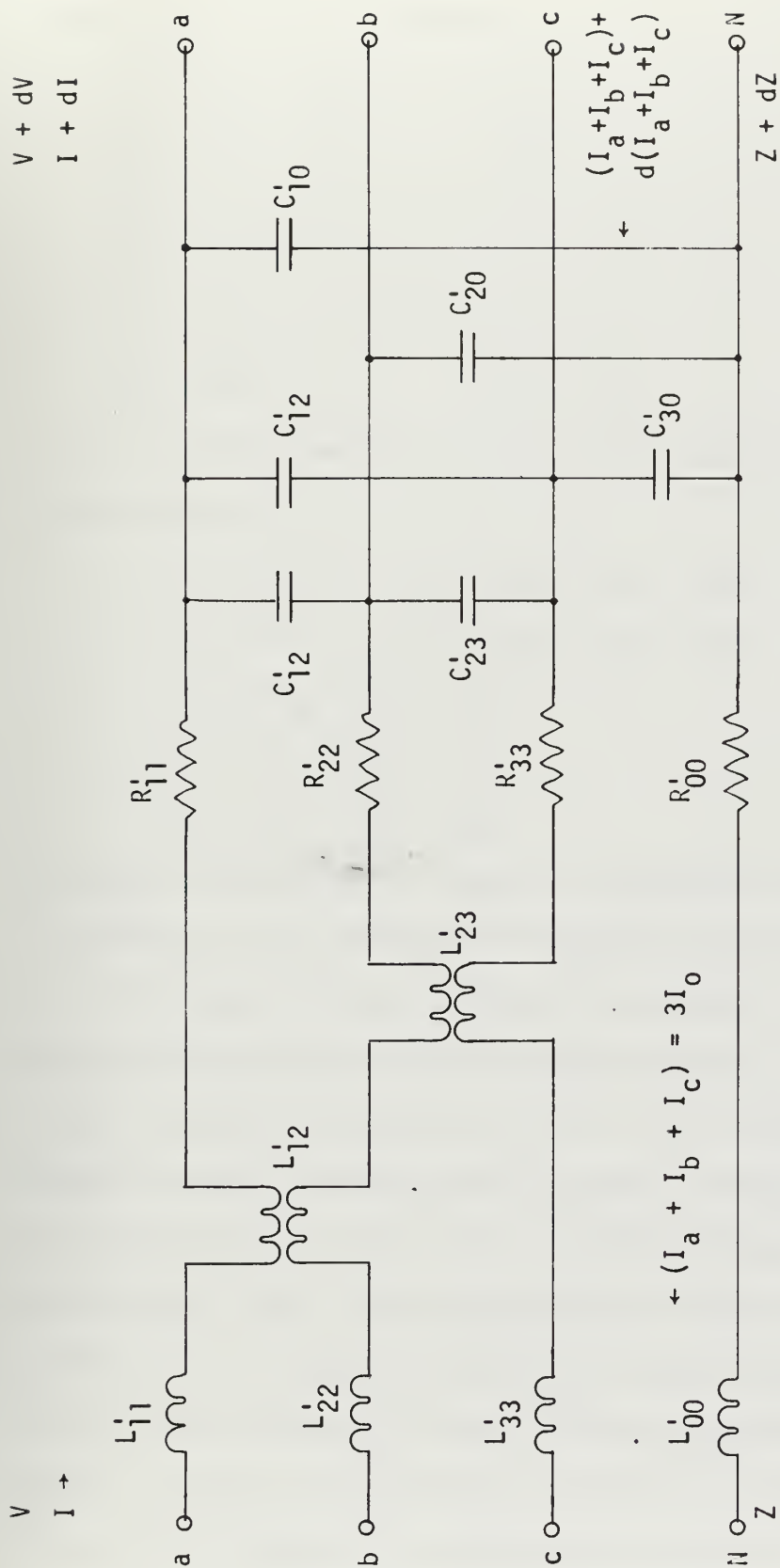
$$[R] \approx \begin{bmatrix} R_{aa} & R_m & R_m \\ R_m & R_{bb} & R_m \\ R_m & R_m & R_{cc} \end{bmatrix}. \quad (2-4)$$

Comparing line equations with those of Appendix (A.1), it is found that:

$$\begin{aligned} R_{00} &= R_m \\ R_{aa} &= R_{11} + R_m \\ R_{bb} &= R_{22} + R_m \\ R_{cc} &= R_{33} + R_m \end{aligned} \quad (2-5)$$

The line parameters given in equation (2-1) include the effect of ground wires, so that the model parameters also include ground wire effects. The mutual inductances shown in Figure 2.1 represent "ideal" mutual inductors adding no self inductance to the lines. The value of the mutual inductances is nominally about ten percent or less of the self inductances.

The circuit of Figure 2.1 can be transformed by simple algebra (See Appendix A.2) to the configuration of Figure 2.2. The circuit of Figure 2.2 is as general as that of Figure 2.1 but has one less mutual inductor. In Figure 2.2 the transformed



Section of a "Balanced Mutual", Non-Transposed Line Model

Figure 2.2

quantities, in terms of Figure 2.1, are:

$$\begin{array}{lll}
 L'_{11} = L_{11} - L_{13} & L'_{12} = L_{12} - L_{13} & C'_{10} = C_{10} \\
 L'_{22} = L_{22} - L_{13} & L'_{23} = L_{23} - L_{13} & C'_{20} = C_{20} \\
 L'_{33} = L_{33} - L_{13} & L'_{00} = L_{00} + L_{13} & C'_{30} = C_{30} \\
 C'_{12} = C_{12} & R'_{11} = R_{11} & R'_{00} = R_{00} \\
 C'_{13} = C_{13} & R'_{22} = R_{22} & \\
 C'_{23} = C_{23} & R'_{33} = R_{33} & (A-4)
 \end{array}$$

If the line being modeled is of horizontal configuration; then for both circuits:

$$\begin{array}{l}
 L'_{12} = (L_{12} - L_{13}) = L'_{23} = (L_{23} - L_{13}) \\
 L'_{11} = (L_{11} - L_{13}) = L'_{33} = (L_{33} - L_{13}) \\
 C'_{10} = C_{10} = C'_{30} = C_{30} \\
 C'_{12} = C_{12} = C'_{23} = C_{23} \\
 R'_{11} = R_{11} = R'_{33} = R_{33}
 \end{array}$$

The model section shown in Figure 2.2 (hereafter referred to as "the model") is the configuration selected for the design. While it is by no means the only configuration possible, this model has a number of advantages over other possible models of equal generality. First, it should be pointed out that in order to economize on the number of cores to be purchased, the mutual inductors are wound over the self inductors in the line. The configuration of Figure 2.2 requires four cores, and incorporates the feature that no self-inductor will be required to physically accept more than one mutual winding (the self winding leaves sufficient window area for only one mutual). Second, the configuration in Figure 2.2 ensures that no phase line is required to incorporate the resistance of more than

one mutual winding. (The resistance of each phase line must be kept to a minimum to keep Q high.) Third, when modeling horizontal lines, the mutual inductances of the Figure 2.2 configuration are equal-thus incorporating into the model the symmetry which actually exists in the line being modeled. (This would not be true of some other non-transposed models.⁶⁾)

2.2 Transposed Models

As mentioned in Chapter 1, it is common practice to simplify the analysis of non-transposed lines by assuming that they are transposed. In most non-transposed lines the values of the three self inductances of the phase conductors are approximately the same, and the values of all inter-phase parameters are not too different from one another. As shown in Appendix A.3, the transformation to a transposed view-point "averages" the line parameters and "re-distributes" them uniformly among the three phases. The result is a balanced, symmetrical model which for many applications is a good approximation to what is in reality a non-transposed line. A schematic of a transposed line model section resulting from the transformation of Appendix A.3 is shown in Figure 2.3. In terms of the general model of Figure 2.1, the parameters of Figure 2.3 are:

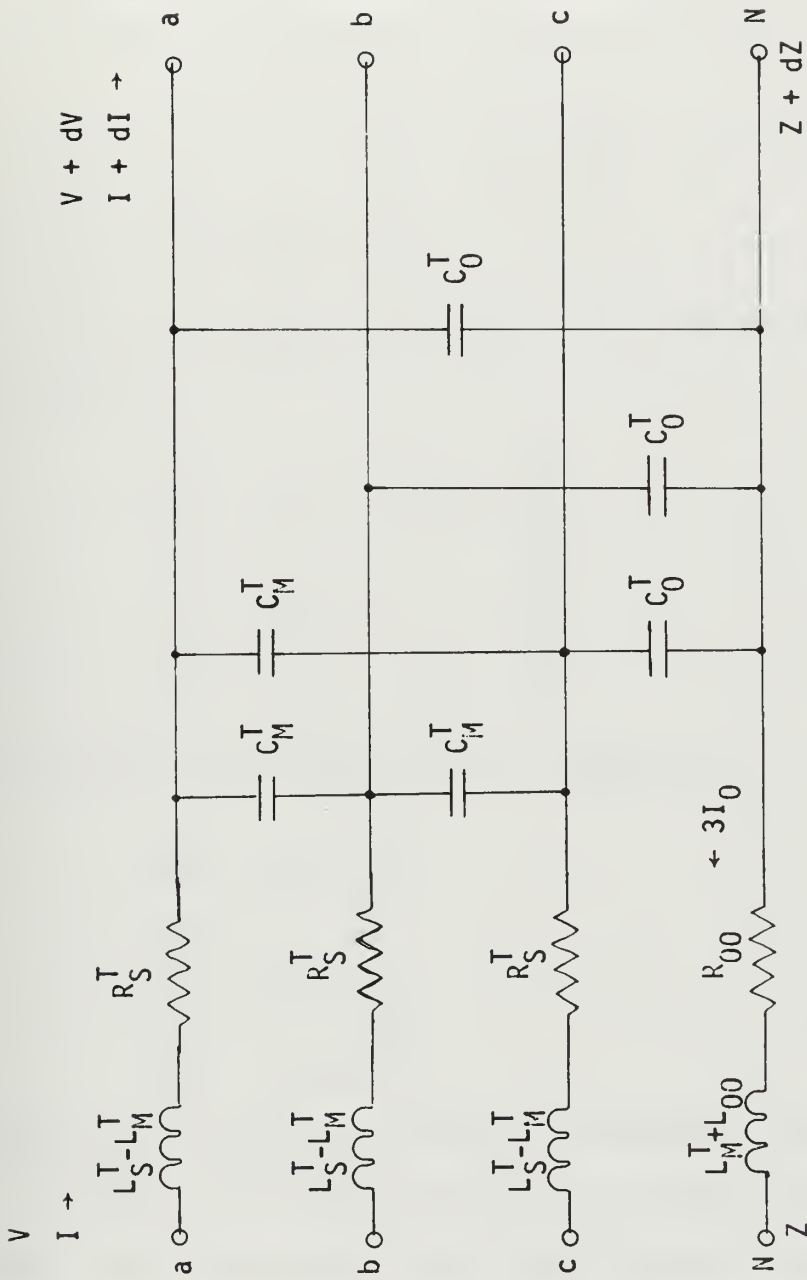
$$C_0^T = \frac{C_{10} + C_{20} + C_{30}}{3} \quad (A-5c)$$

$$C_M^T = \frac{C_{12} + C_{23} + C_{13}}{3} \quad (A-5d)$$

$$R_S^T = \frac{R_{11} + R_{22} + R_{33}}{3} \quad (A-5e)$$

$$L_S^T = \frac{L_{11} + L_{22} + L_{33}}{3} \quad (A-5a)$$

$$L_M^T = \frac{L_{12} + L_{23} + L_{13}}{3} \quad (A-5b)$$



Section of Transposed Line Model

Figure 2.3

2.2.1 Symmetrical Component Equivalent Circuits for Transposed Model

In Appendix A.3 it is shown that the transposed line model can be reduced to two symmetrical component models. The results are repeated here for continuity. With the definitions

$$\begin{aligned} R_{P.S.} &= R_S^T & R_{Z.S.} &= R_S^T + 3R_{00} & C_{P.S.} &= C_0^T + 3C_M^T \\ C_{Z.S.} &= C_0^T & L_{P.S.} &= L_S^T - L_M^T \\ \text{and } L_{Z.S.} &= L_S^T + 2L_M^T + 3L_{00}, \end{aligned}$$

the transposed line equations (A-7) - with positive sequence currents only-reduce to:

$$\begin{aligned} -\frac{\partial V_a}{\partial z} &= R_{P.S.} I_a + L_{P.S.} \frac{\partial I_a}{\partial t} \\ -\frac{\partial V_b}{\partial z} &= R_{P.S.} I_b + L_{P.S.} \frac{\partial I_b}{\partial t} \\ -\frac{\partial V_c}{\partial z} &= R_{P.S.} I_c + L_{P.S.} \frac{\partial I_c}{\partial t} . \end{aligned} \tag{A-8}$$

And The Current Law equations (A-11) reduce to:

$$\begin{aligned} -\frac{\partial I_a}{\partial z} &= C_{P.S.} \frac{\partial V_a}{\partial t} \\ -\frac{\partial I_b}{\partial z} &= C_{P.S.} \frac{\partial V_b}{\partial t} \\ -\frac{\partial I_c}{\partial z} &= C_{P.S.} \frac{\partial V_c}{\partial t} . \end{aligned} \tag{A-12}$$

These results show that for positive (or negative) sequence voltages and currents, the transposed line may be viewed as three identical single phase circuits (the 120° phase difference understood).

Similar conclusions apply to zero sequence voltages and currents where it can be shown (Appendix A.3) that under these conditions the transposed line equations reduce to:

$$\begin{aligned}
- \frac{\partial V_a}{\partial z} &= R_{Z.S.} I_a + L_{Z.S.} \frac{\partial I_a}{\partial t} \\
- \frac{\partial V_b}{\partial z} &= R_{Z.S.} I_b + L_{Z.S.} \frac{\partial I_b}{\partial t} \\
- \frac{\partial V_c}{\partial z} &= R_{Z.S.} I_c + L_{Z.S.} \frac{\partial I_c}{\partial t} ,
\end{aligned} \tag{A-9}$$

and

$$\begin{aligned}
- \frac{\partial I_a}{\partial z} &= C_{Z.S.} \frac{\partial V_a}{\partial t} \\
- \frac{\partial I_b}{\partial z} &= C_{Z.S.} \frac{\partial V_b}{\partial t} \\
- \frac{\partial I_c}{\partial z} &= C_{Z.S.} \frac{\partial V_c}{\partial t}
\end{aligned} \tag{A-13}$$

Thus, the non-transposed model can be approximated by a transposed model, and the transposed model can, in turn, be analyzed into two symmetrical component equivalent circuits - one for positive-sequence and another for zero-sequence.

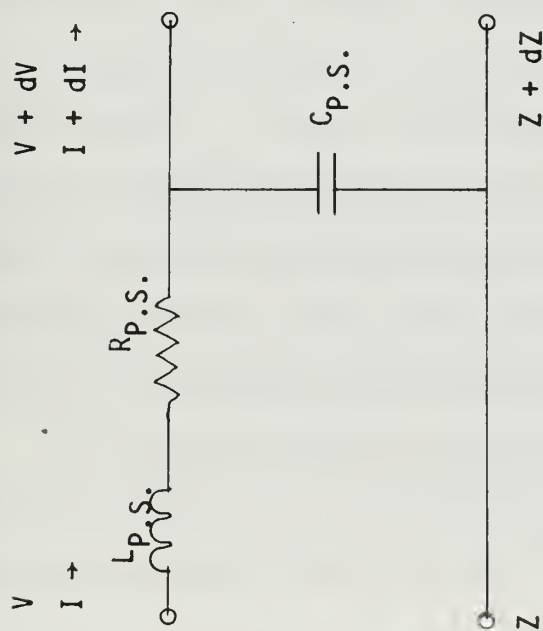
CHAPTER 3

NATURAL FREQUENCY ANALYSIS

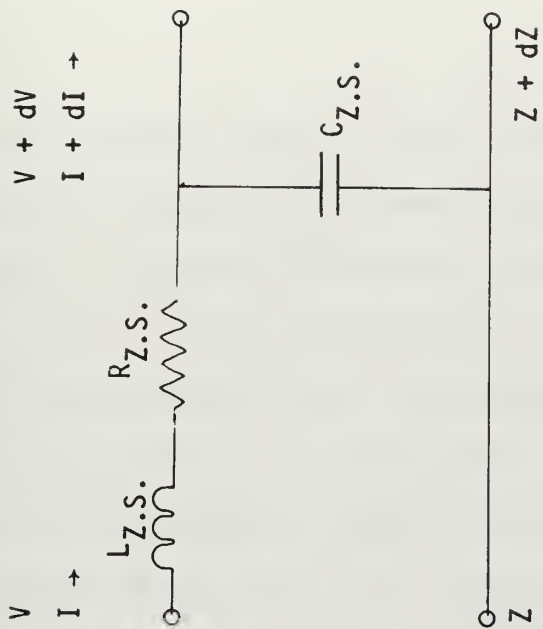
3.1 Methods and Criteria for Predicting Model and ActualLine Correspondence

As discussed in Chapter 2 and Appendix A, the transposed line can be analyzed into two, symmetrical component, single-phase equivalent circuits. A single-phase L-section model as "seen" by positive (or negative) sequence voltages and currents is shown in Figure 3.1a. A similar L-section model as seen by zero-sequence quantities is shown in Figure 3.1b. Figures 3.1a and 3.1b reflect the basic "L" configuration implied by the three-phase models of Figures 2.1, 2.2 and 2.3, but " π " or "T" section models are equally valid. In fact, under certain circumstances and with certain loads, the " π " or "T" configurations may have advantages over the "L" models - these circumstances will be discussed more fully in later sections.

One of the purposes for which the transposed line approximation can be used is that of establishing a "math-model-predictor" for comparison of an actual line and its proposed models. Some of the early questions in the design of a lumped element t.l.m. are: How many sections are required? How "accurate" is the model with ten-twenty-forty sections? Should the sections be "L" or " π "? What should be the "length" of each model section? For what frequency band must the model "correspond" to the actual line? Exactly what is it that should "correspond" between model and line-to what "accuracy"? A method of theoretically comparing an actual line and its proposed models is clearly desirable. If a t.l.m.



Schematic of L-Section Model
Positive Sequence Component.



Schematic of L-Section Model,
Zero-Sequence Component.

Figure 3.1a

Figure 3.1b

could be constructed to exactly duplicate in magnitude and phase the impedance function of the actual line for all frequencies, then the model could be said to have "perfect accuracy". Perfect accuracy would probably require more lumped element sections than economically practical, so that some compromise is required.

As the first, and perhaps the simplest, approach toward answering the questions above, this design uses as a comparison "device" the poles of the driving point impedance functions. The poles of a given length of actual line are compared to the poles of a proposed m -section model. The number of sections, m , in the model is "adjusted" until the frequency difference between corresponding poles of the model and actual line is sufficiently small. In each case, the actual line and model compared are the transposed, symmetrical-component equivalents of the three-phase systems. This simplification is sufficient for design analysis since it is not the detailed nature (e.g. "splitting") of the poles that is sought, but rather, a reasonably accurate estimate of their mean position in the frequency spectrum. The mean positions can then be compared to estimate the difference between the actual line and model. The transposed, symmetrical-component approximation is applied to both the mathematical model of the actual line and that of the t.l.m., so that errors introduced by this approximation are self compensating.

In analyzing the driving point impedance function of both the line and models, it is convenient and sufficient to consider two possible extremes as terminations. Both the sources and loads connected to the terminals of the line are non-linear devices (at least under some conditions of operation or fault) so that, as

viewed from the line, the terminals of the line may simultaneously appear as a high impedance to some transient components and a low impedance to other components. This "high-low" terminal impedance characteristic is provided for in the analysis to follow by considering both open and short circuit terminations. The decision as to what is a "sufficiently" small difference between the line and the model is deferred to a point later in the analysis where it can be made to appear a little less arbitrary.

3.2 Driving Point Impedance of Continuous Lines

The relations describing the driving point impedance of continuous lines are well known and will not be derived for this discussion. Readers interested in the details of the derivation may consult any good text on transmission lines such as references 7, 8, or 9. For the general transmission line circuit shown in Figure 3.2, the pertinent impedance relations for a length, ℓ , are:

$$Z_{s.c.} = Z_0 \tanh \gamma \ell \quad (3-1)$$

$$Z_{o.c.} = Z_0 \coth \gamma \ell. \quad (3-2)$$

Where

$Z_{s.c.}$ = Impedance at $Z = \ell$ with a short circuit termination.

$Z_{o.c.}$ = Impedance at $Z = \ell$ with an open circuit termination

$$Z_0 = \sqrt{\frac{R + sL}{sC}} \quad (3-3)$$

$$\gamma = \sqrt{(R + sL)sC} \quad (3-4)$$

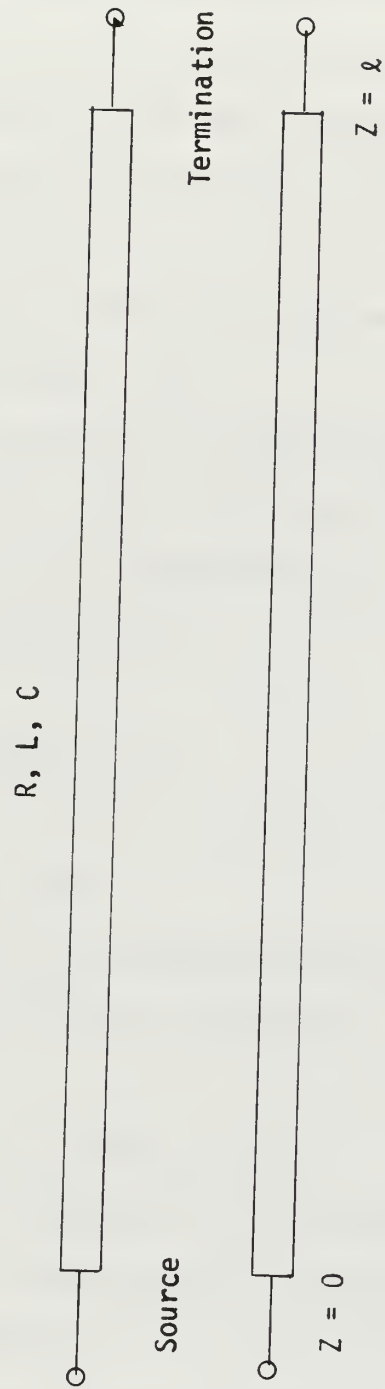


Diagram of a General Transmission Line of Length- ℓ .

Figure 3.2

s = Complex phase constant

R = Positive or zero-sequence resistance per unit length

L = Positive or zero-sequence inductance per unit length

C = Positive or zero-sequence capacitance per unit length

The shunt conductance, G , has been ignored in these relations. In the short circuit case, the poles are seen to occur when

$$\cosh \gamma \ell = 0. \quad (3-5)$$

Setting $\gamma = \gamma_r + j\gamma_i$, equation (3-5) can be expanded as follows:

$$\begin{aligned} \cosh(\gamma_r + j\gamma_i)\ell &= 0 \\ \cosh(\gamma_r \ell) \cosh(j\gamma_i \ell) + \sinh(\gamma_r \ell) \sinh(j\gamma_i \ell) &= 0 \\ \cosh(\gamma_r \ell) \cos \gamma_i \ell + j \sinh(\gamma_r \ell) \sin \gamma_i \ell &= 0. \end{aligned}$$

Thus, for $\cosh \gamma \ell = 0$ it is necessary that

$$\cosh(\gamma_r \ell) \cos \gamma_i \ell = 0, \quad (3-6)$$

and

$$\sinh(\gamma_r \ell) \sin \gamma_i \ell = 0. \quad (3-7)$$

Case No. 1:

Suppose $\gamma_r = 0$

Then eq. (3-7) is satisfied and eq. (3-6)

$$\text{implies } \gamma \ell = j\gamma_i \ell = \pm j(2n+1)\pi/2 \quad n=0,1,2,\dots \quad (3-8)$$

Case No. 2:

Suppose $\gamma_r \neq 0$ but $\gamma_i \ell = \pm \frac{n\pi}{2} \quad n=0,1,2,\dots$

Then eqs. (3-6) and (3-7) are never both satisfied.

Therefore Case No. 1 gives the only solutions for γ which result in the poles of equation (3-1). A similar development applied to equation (3-2) gives for the open line:

$$\gamma \ell = \pm jn\pi \quad n = 0,1,2,\dots \quad (3-9)$$

If equations (3-8) and (3-9) are expanded and solved for the complex phase constant, s , there results:

$$s_{s.c.} = - \left(\frac{R}{2L} \right) \pm \sqrt{\left(\frac{R}{2L} \right)^2 - \frac{(2n+1)^2 \pi^2}{4\ell^2 LC}} \quad n=0,1,2,\dots \quad (3-10)$$

$$s_{o.c.} = - \left(\frac{R}{2L} \right) \pm \sqrt{\left(\frac{R}{2L} \right)^2 - \frac{n^2 \pi^2}{\ell^2 LC}} \quad n=0,1,2,\dots \quad (3-11)$$

If the line shown in Figure 3.2 is lossless ($R = 0$) then:

$$Z_{s.c.} = jZ_0 \tan \beta \ell \quad (3-12)$$

$$Z_{o.c.} = -jZ_0 \cot \beta \ell \quad (3-13)$$

$$Z_0 = \sqrt{\frac{L}{C}} \quad (3-14)$$

$$\beta = \omega \sqrt{LC} = \text{phase constant} \quad (3-15)$$

$$\omega_{s.c.} = \pm \frac{(2n+1)\pi}{2\ell \sqrt{LC}} \quad n=0,1,2,\dots \quad (3-16)$$

$$\omega_{o.c.} = \pm \frac{n\pi}{\ell \sqrt{LC}} \quad n=0,1,2,\dots \quad (3-17)$$

3.3 Driving Point Impedance of L-Section Models

A schematic diagram of an L-section model for modeling the line of Figure 3.2 is shown in Figure 3.3. Both figures refer to the symmetrical component equivalent circuits of their respective three-phase systems. Thus, both figures represent a "transposed-line-approximation" to their respective non-transposed, three-phase counterparts. In the case that the L-section line is shorted, a clear distinction must be made as to which end is the source and which is the termination. In the first case, a short can be placed across the last capacitor-removing it from the circuit. This case is referred to as "inductor input". In the second case, the short can be placed to connect the "last" inductor to ground. This case is referred to as "capacitor input".

3.3.1 Inductor Input L-Section Model (Shorted)

The inductor input case is that shown in Figure 3.3. The derivation of the driving point impedance expression is rather lengthy and is shown in detail in Appendix B.1. The lumped element parameters of Figure 3.3 are defined in terms of the distributed parameters of Figure 3.2 as:

$$R_s = \frac{R\ell}{m} \quad (3-18)$$

$$L_s = \frac{L\ell}{m} \quad (3-19)$$

$$C_s = \frac{C\ell}{m} . \quad (3-20)$$

Where "m" is the number of sections in the model. The result from Appendix B.1 for an m-section; lossy model is:

$$Z_{s.c.} = \frac{(R_s + L_s) \sinh m\lambda}{\sinh m\lambda - \sinh(m-1)\lambda} . \quad (B-16)$$

The denominator of equation (B-16) is a polynomial in the real variable $\cosh \lambda$ so that the solutions, $[\cosh \lambda]_{\text{root}}$, to the equation $\sinh m\lambda - \sinh(m-1)\lambda = 0$ yield the propagation constants in the propagation relation

$$[\cosh \lambda]_{\text{root}} = 1 + \frac{s^2 L_s C_s}{2} + \frac{s R_s C_s}{2} . \quad (B-7)$$

Solving equation (B-7) for s gives:

$$s_{s.c.} = - \left(\frac{R}{2L} \right) \pm \sqrt{\left(\frac{R}{2L} \right)^2 - \frac{2m^2}{\ell^2 LC} [1 - (\cosh \lambda)_{\text{root}}]} \quad (B-26)$$

If the model of Figure 3.3 is lossless ($R_s = 0$),

$$Z_{s.c.} = \frac{j\omega L_s \sinh m\lambda}{\sinh m\lambda - \sinh(m-1)\lambda} \quad m=1,2,3,\dots \quad (B-17)$$

$$\cosh \lambda = 1 - \frac{\omega^2 L_s C_s}{2} \quad (\text{B-18})$$

$$\omega_{s.c.} = \frac{m}{\ell} \sqrt{\frac{2}{LC} [1 - (\cosh \lambda)_{\text{root}}]} \quad m=1,2,3 \quad (\text{B-27})$$

For an example application, suppose there are seven sections in a proposed model. Then $m=7$; there are six values of $[\cosh \lambda]_{\text{root}}$, and six values of $s_{s.c.}$ or $\omega_{s.c.}$. The six poles of the model given by equations (B-26) or (B-27) are compared to the first six poles of the actual line given by equations (3-10) or (3-16). The difference in frequency between two corresponding poles is a measure of the error of the model for that pole number. Equations (B-16), (B-26), and (3-10) were implemented on the computer, as shown in Appendices C and D, for various numbers of sections up to about forty. A plot of the resulting pole error vs. pole number is shown in Figure 3.4a. The percent error in Figure 3.4a is defined as

$$\% \text{ Error} = 100 \frac{I_m[\text{equation (B-26)}] - I_m[\text{equation (3-10)}]}{I_m[\text{equation (3-10)}]} \quad (3-21)$$

The parameters used in equations (B-26) and (3-10) for Figure 3.4a are the positive sequence values of a 765 kV "typical aluminum tower" configuration:

$$\ell = 100 \text{ miles} \quad (3-22)$$

$$R = .0251 \text{ ohms/mi} \quad (3-23)$$

$$C = .021 \text{ } \mu\text{f/mi} \quad (3-24)$$

$$L = 1.45 \text{ mh/mi} \quad (3-25)$$

The pole number shown in Figure 3.4a is, of course, a discreet integer variable with pole no. 1 corresponding to the pole of lowest frequency in either the actual line or model. The curve for a given

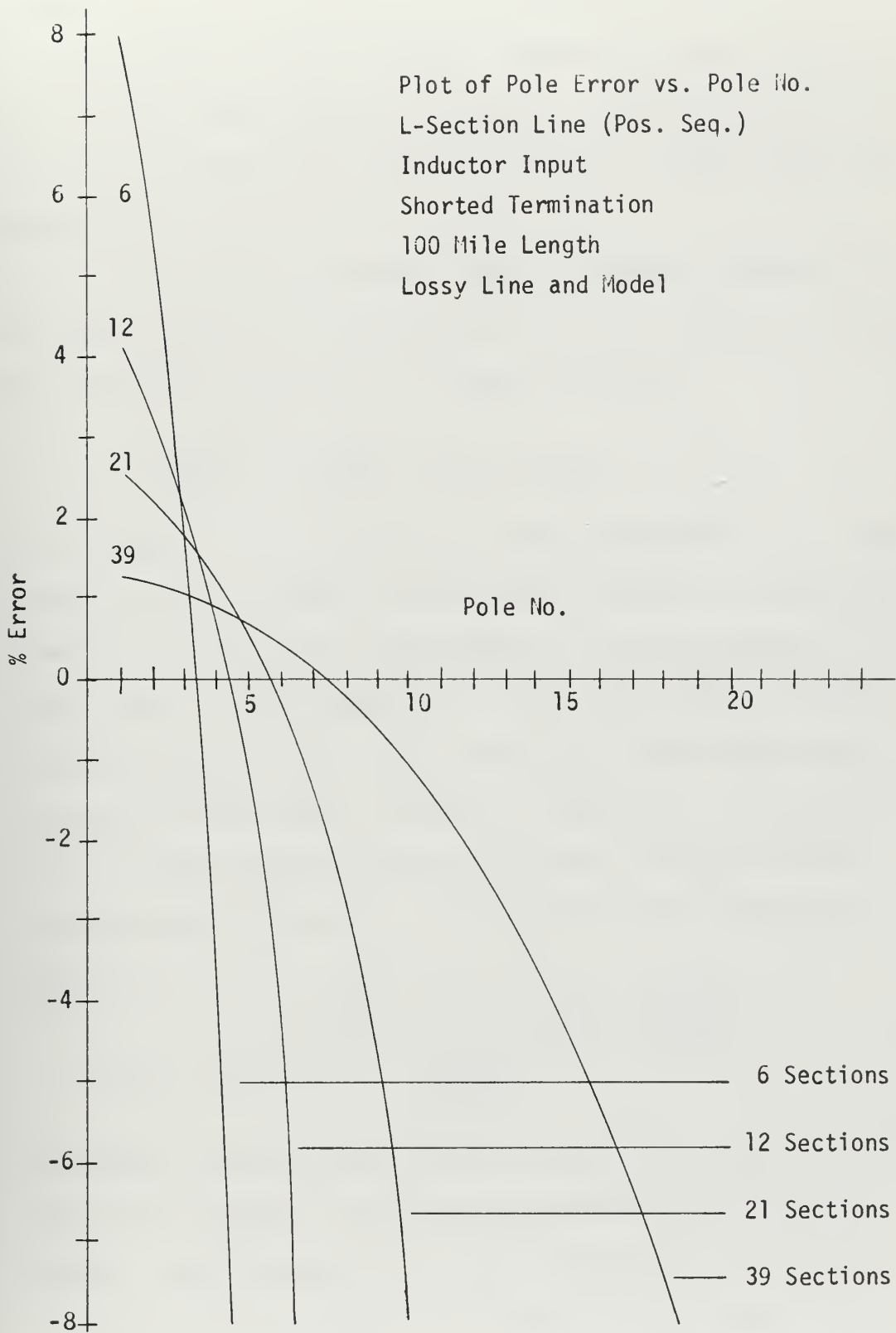


Figure 3.4a

number of sections in the model is a series of discrete points but is drawn continuous to avoid confusion. Figure 3.4a shows, for example, that at least twelve sections are required to model the line if it is desired to keep all of the first five poles of the model within five percent error.

If the typical parameter values of equations (3-22)-(3-25) are substituted directly into equations (3-10) or (B-26), it is found that the term $\frac{R}{2L}$ is of order 10^{-1} whereas the terms

$$\frac{(2n+1)^2 \pi^2}{4\ell^2 LC} \quad \text{or} \quad \frac{2m^2}{\ell^2 LC} [1 - \cosh \lambda]_{\text{root}}$$

are of order 10^7 or 10^8 for even the lowest values of m or n . This suggests that for purposes of a pole error analysis, the resistance terms can be neglected when considering the positive sequence of the lines. This, in turn suggests that a pole error analysis using the lossless equations (B-17), (B-27), and (3-16) should give results very similar to the lossy case shown in Figure 3.4a. The results for the lossless case paralleling the analysis leading to Figure 3.4a are shown in Figure 3.4b. The percent error in Figure 3.4b is defined as

$$\% \text{ Error} = 100 \frac{\frac{m}{\ell} \sqrt{\frac{2}{LC}} [1 - (\cosh \lambda)_{\text{root}}] - \frac{(2n+1)\pi}{2\ell \sqrt{LC}}}{\frac{(2n+1)\pi}{2\ell \sqrt{LC}}} . \quad (3-26)$$

As expected, Figures 3.4a and 3.4b are practically identical so that losses will be ignored throughout the remainder of the pole error analysis. Note that equation (3-26) is independent of ℓ , L , and C , so that the pole error curves of Figure 3.4b apply to any line and model provided the model is "inductor input", L-section, and both

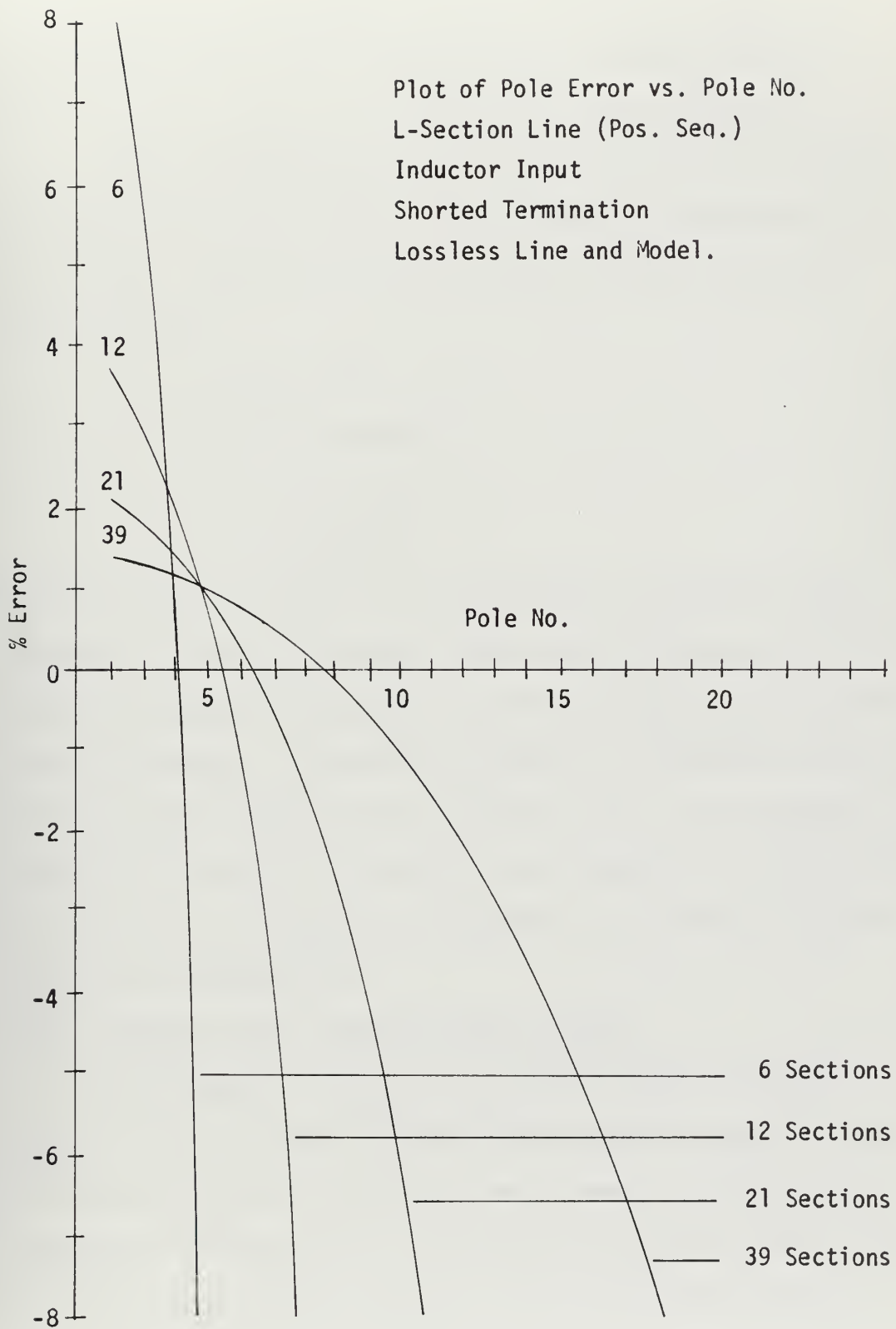


Figure 3.4b

line and model are terminated in a short. The pole frequencies corresponding to the first fifteen poles of a shorted, typical 765 kV line, for various line lengths are shown in Table 3.1.

Equations (B-26) and (3-10) for the configuration of Figure 3.3 were also run using zero sequence values of a typical 100 mile 765 kV line. The pole error results for this case are shown in Figure 3.5 with

$$\ell = 100 \text{ miles} \quad (3-27)$$

$$R = .51 \text{ ohms/mile} \quad (3-28)$$

$$C = .0143 \text{ } \mu\text{f/mile} \quad (3-29)$$

$$L = 4.2 \text{ mh/mile} \quad (3-30)$$

The percent error in Figure 3.5 is as defined by equation (3-21). A comparison of Figures 3.4a and 3.5 shows that the pole error for zero sequence parameters is practically identical to the error for positive sequence parameters. In addition, Figure 3.5 is practically identical with the lossless results shown in Figure 3.4b. Thus, throughout the remainder of the pole error analysis, the lossy line and zero sequence pole error will be assumed to be the same as the lossless line error of any given configuration.

3.3.2 Capacitor Input L-Section Model (Shorted)

If the model of Figure 3.3 is turned around so that the capacitor is at the input, the result (lossless) is shown in Figure 3.6. The derivation of the driving point impedance of this line is carried out in Appendix B.2. The analysis considers only the lossless case since, as discussed in section 3.3.1, the effect of resistance can be neglected in the pole error analysis. The results from

Table 3.1

Short Circuit Pole Frequencies (Pos. Seq.)

Pole No.	60 Mi	100 Mi	200 Mi	300 Mi	400 Mi
1	760 Hz	456 Hz	228 Hz	152 Hz	114 Hz
2	2,280	1,370	685	456	343
3	3,800	2,280	1,140	760	570
4	5,345	3,200	1,600	1,054	800
5	6,840	4,100	2,050	1,370	1,025
6	8,335	5,020	2,560	1,675	1,257
7	9,850	5,920	2,960	1,975	1,480
8	11,390	6,840	3,420	2,275	1,710
9	12,900	7,750	3,880	2,580	1,940
10	14,400	8,650	4,325	2,880	2,160
11	15,950	9,580	4,790	3,190	2,390
12	17,410	10,470	5,235	3,490	2,620
13	18,950	11,390	5,695	3,790	2,840
14	20,500	12,300	6,150	4,100	3,075
15	22,000	13,200	6,600	4,400	3,300

Table of Pole Frequencies for Shorted, Typical
765 kV Line (Positive Sequence-Lossless)

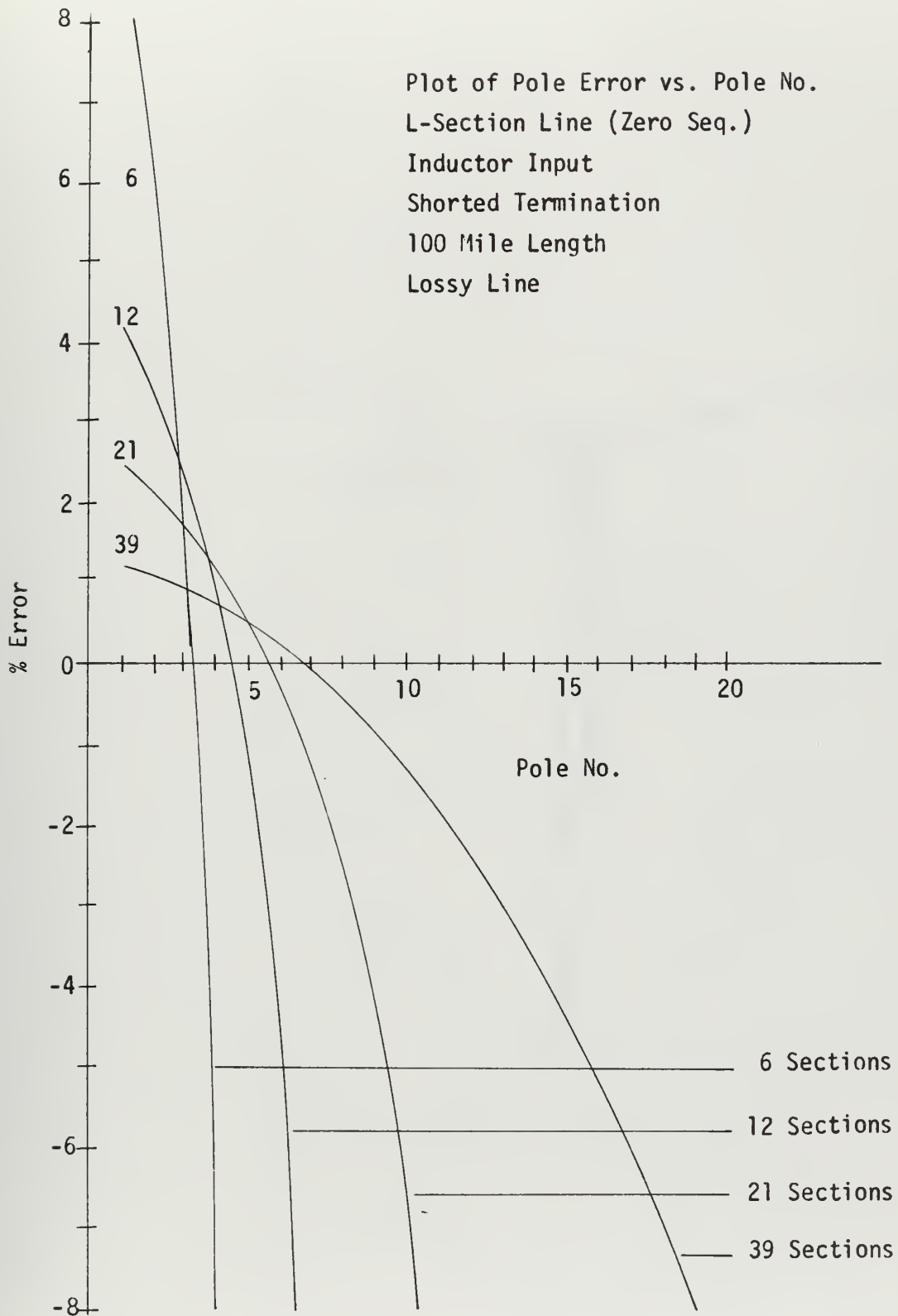
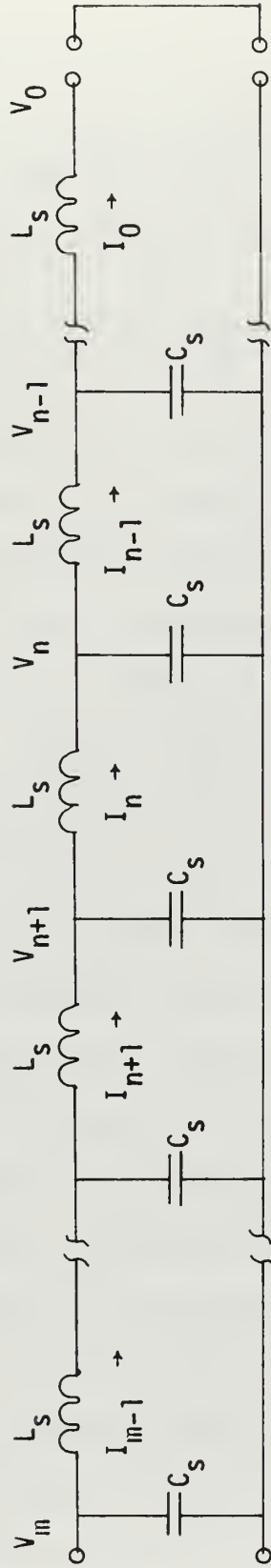


Figure 3.5



Schematic of L-Section Model Lossless, Capacitor Input, Positive Sequence Component (Shorted)

Figure 3.6

Appendix B.2 are,

$$Z_{s.c.} = \frac{j\omega L_s \sinh m\lambda}{\sinh(m+1)\lambda - \sinh m\lambda} \quad m=1,2,\dots \quad (B-39)$$

$$\cosh \lambda = 1 - \frac{\omega^2 L_s C_s}{2} \quad (B-33)$$

$$\omega_{s.c.} = \frac{m}{\ell} \sqrt{\frac{2}{LC} [1 - (\cosh \lambda)_{\text{root}}]} \quad m=1,2,3,\dots \quad (B-40)$$

Note that equation (B-39) is not the same as equation (B-17), so that the values of $(\cosh \lambda)_{\text{root}}$ obtained from (B-39) for use in (B-40) will be different from the roots obtained from (B-17) for use in (B-27).

Equations (B-39), (B-40), and (3-16) were solved with the computer as shown in Appendices C and D. A plot of the resulting pole error vs. pole number is shown in Figure 3.7. Having neglected resistance, the poles of the model are given by equation (B-40) and those of the actual line by equation (3-16). The percent error in Figure 3.7 is defined by equation (3-26). Figure 3.7 shows that the error behavior for the capacitor input case is radically different from that of the inductor input. The capacitor input model consistently under-estimates the actual pole frequency, whereas the inductor input model over-estimates the frequency of the lower order poles, and, throughout its range, yields pole frequencies higher than the capacitor input model. The inductor input model gives higher pole frequencies due to the fact that the shorted termination removes the last capacitor from the model-thus reducing overall model capacity and increasing the model's natural frequencies. Note also, that the capacitor input model errors are larger at lower order poles and smaller at higher order poles than corresponding lengths of inductor

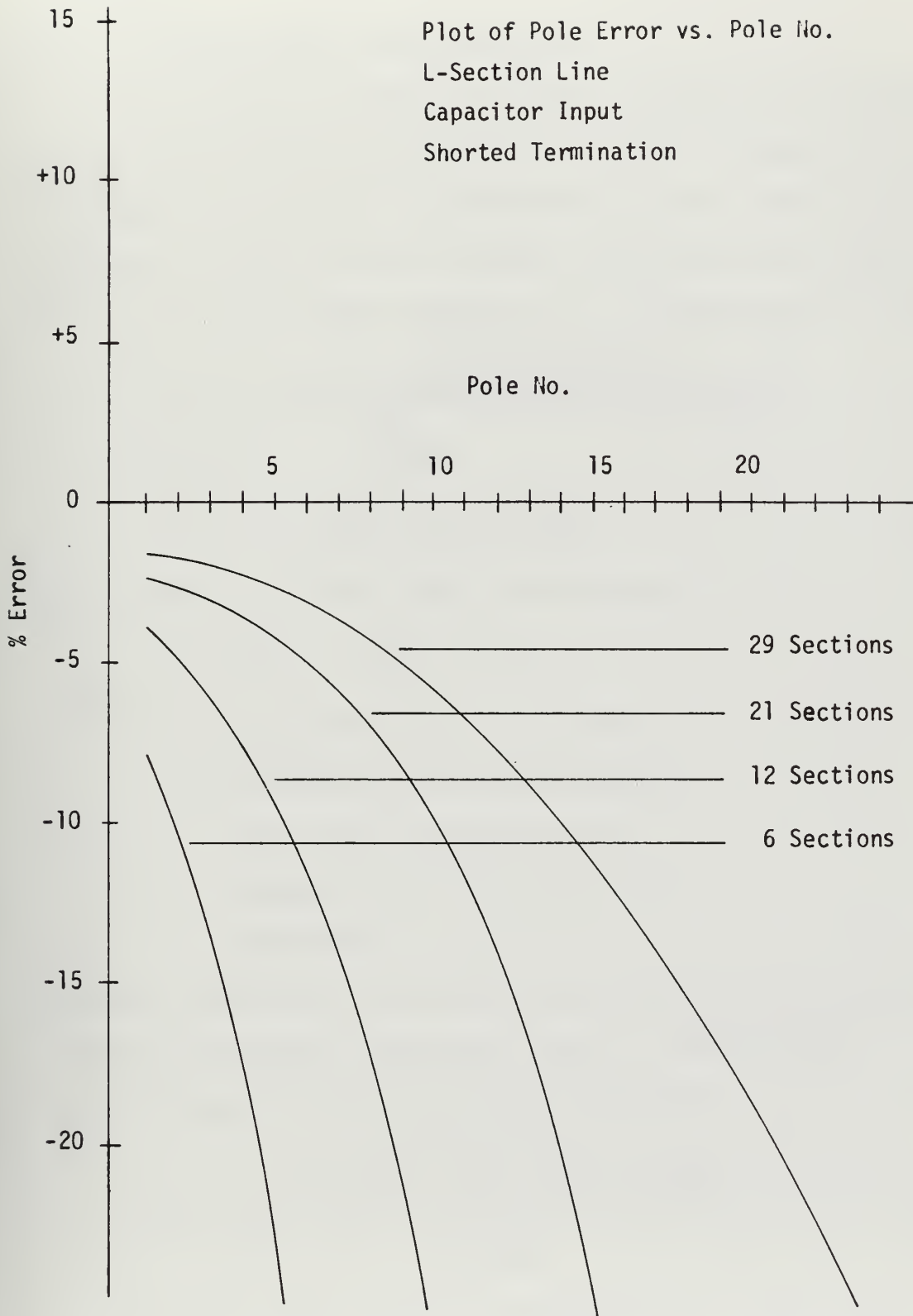


Figure 3.7

input model.

3.3.3 L-Section Model, Open Termination

In the case of an open termination, the poles are unaffected by which terminals are considered to be the input or output, and only one analysis is required. The schematic of the open circuit case is just Figure 3.3 with the short removed. The driving point impedance for this case is derived in Appendix B.3. The results are ($R_s = 0$):

$$Z_{o.c.} = j\omega L_s \left[\frac{\sinh(m+1)\lambda - \sinh m\lambda}{2 \sinh m\lambda - \sinh(m+1)\lambda - \sinh(m-1)\lambda} \right] \quad (B-46)$$

$$\cosh \lambda = 1 - \frac{\omega^2 L_s C_s}{2} \quad (B-18)$$

$$\omega_{o.c.} = \frac{m}{\ell} \sqrt{\frac{2}{LC} [1 - (\cosh \lambda)_{\text{root}}]} \quad (B-47)$$

Where, again, use has been made of the fact that,

$$L_s = \frac{L\ell}{m}, \quad C_s = \frac{C\ell}{m}, \quad R_s = 0,$$

m = number of sections in the model,

ℓ = length of the line being modeled,

and L and C are the electrical

parameters per unit length of any

given line.

Equations (B-46), (B-47), and (3-17) were solved with the aid of a computer as discussed in Appendices C and D. The results are shown in Figure 3.8 with the pole error defined as

$$\% \text{ Error} = 100 \frac{\frac{m}{\ell} \sqrt{\frac{2}{LC} [1 - (\cosh \lambda)_{\text{root}}]} - \frac{n\pi}{\ell\sqrt{LC}}}{\frac{n\pi}{\ell\sqrt{LC}}} \quad (3-31)$$

As in equation (3-26), (3-31) is independent of ℓ , L , and C , and

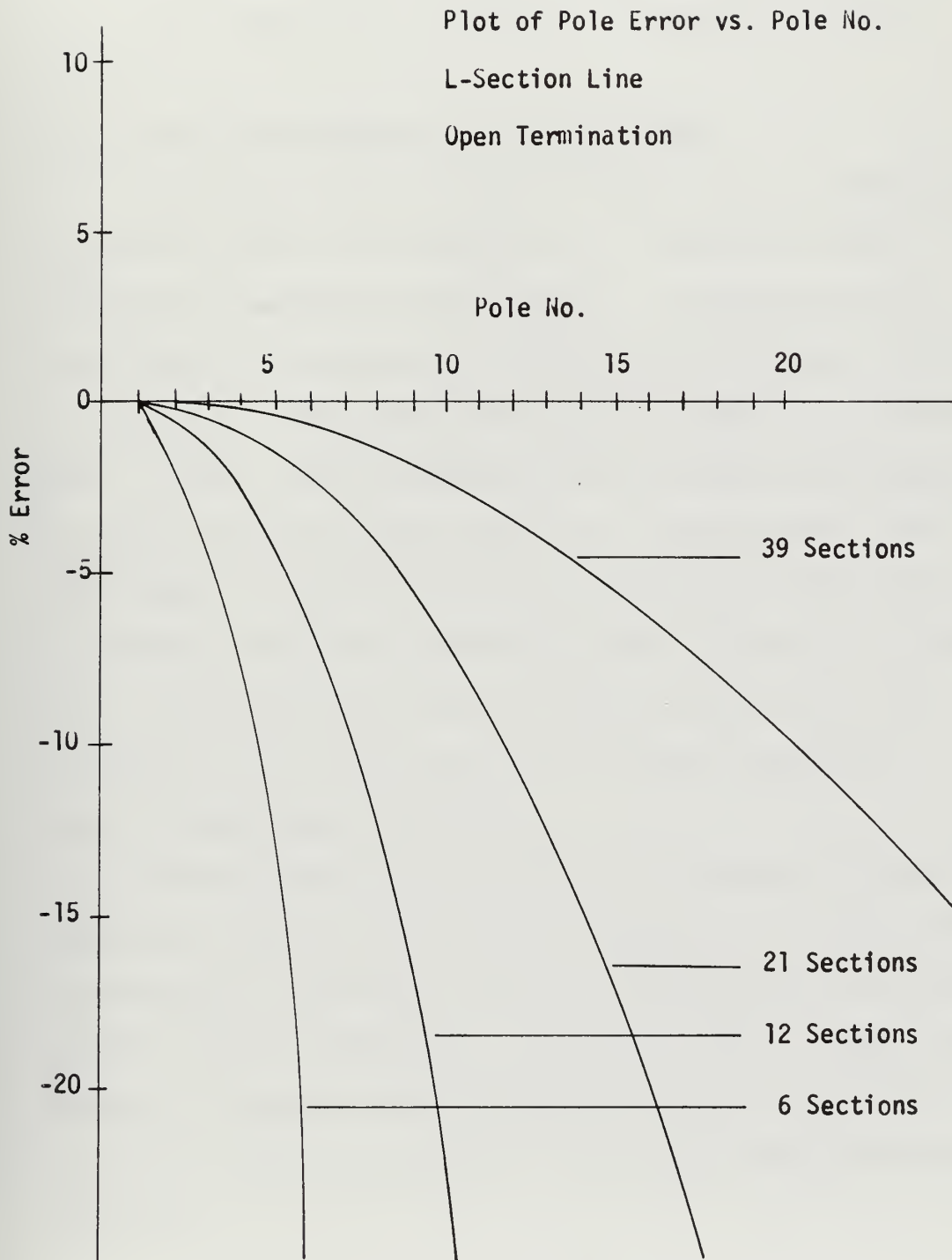


Figure 3.8

depends only upon line configuration. Again, the values of the roots are different from what they were for either of the preceeding cases. The pole frequencies corresponding to the first fifteen poles of an open, typical 765 kV line, for various line lengths is shown in Table 3.2.

3.4 Driving Point Impedance of π -Section Models

Referring to the line shown in Figure 3.6, it is seen that the L-section model can be converted to a π model by a simple adjustment of the first and last sections. If the capacitor at the m th node is replaced by one of value $C_s/2$, and another capacitor of value $C_s/2$ is added at the "0"th node, the result is a π -section model. A similar type of adjustment could be made using inductors of value $L_s/2$, and the result would be a T-section model. The π and T-models are reciprocal networks, whereas the L-model is not. A pole error analysis for π -sections follows in sections 3.4.1 and 3.4.2. The analysis for T-sections is not included since it is assumed that it will add little to all the cases considered.

3.4.1 π -Section Model (Shorted)

The derivation of the driving point impedance relations for the shorted, π -model are carried out in Appendix B.4 and the solution is carried out in Appendices C and D. The result for the shorted π -model is shown in Figure 3.9. The percent error in Figure 3.9 is defined as in equation (3-26), but again it should be noted that the values of $[\cosh \lambda]_{\text{root}}$ differ for each line configuration and termination.

Table 3.2

Pole No.	Open Circuit Pole Frequencies				
	60 Mi	100 Mi	200 Mi	300 Mi	400 Mi
1	0 Hz	0 Hz	0 Hz	0 Hz	0 Hz
2	1,510	905	452	315	226
3	3,020	1,810	905	604	402
4	4,540	2,720	1,360	906	680
5	6,040	3,620	1,810	1,205	905
6	7,550	4,540	2,270	1,510	1,135
7	9,055	5,440	2,770	1,810	1,385
8	10,580	6,350	3,175	2,120	1,585
9	12,090	7,250	3,625	2,420	1,815
10	13,600	8,175	4,092	2,720	2,046
11	15,050	9,050	4,525	3,070	2,260
12	16,600	9,998	4,999	3,325	2,500
13	18,200	10,900	5,450	3,640	2,725
14	19,650	11,800	5,900	3,940	2,950
15	21,200	12,700	6,350	4,240	3,175

Table of Pole Frequencies for Open, Typical
765 kV Line (Positive Sequence-Lossless)

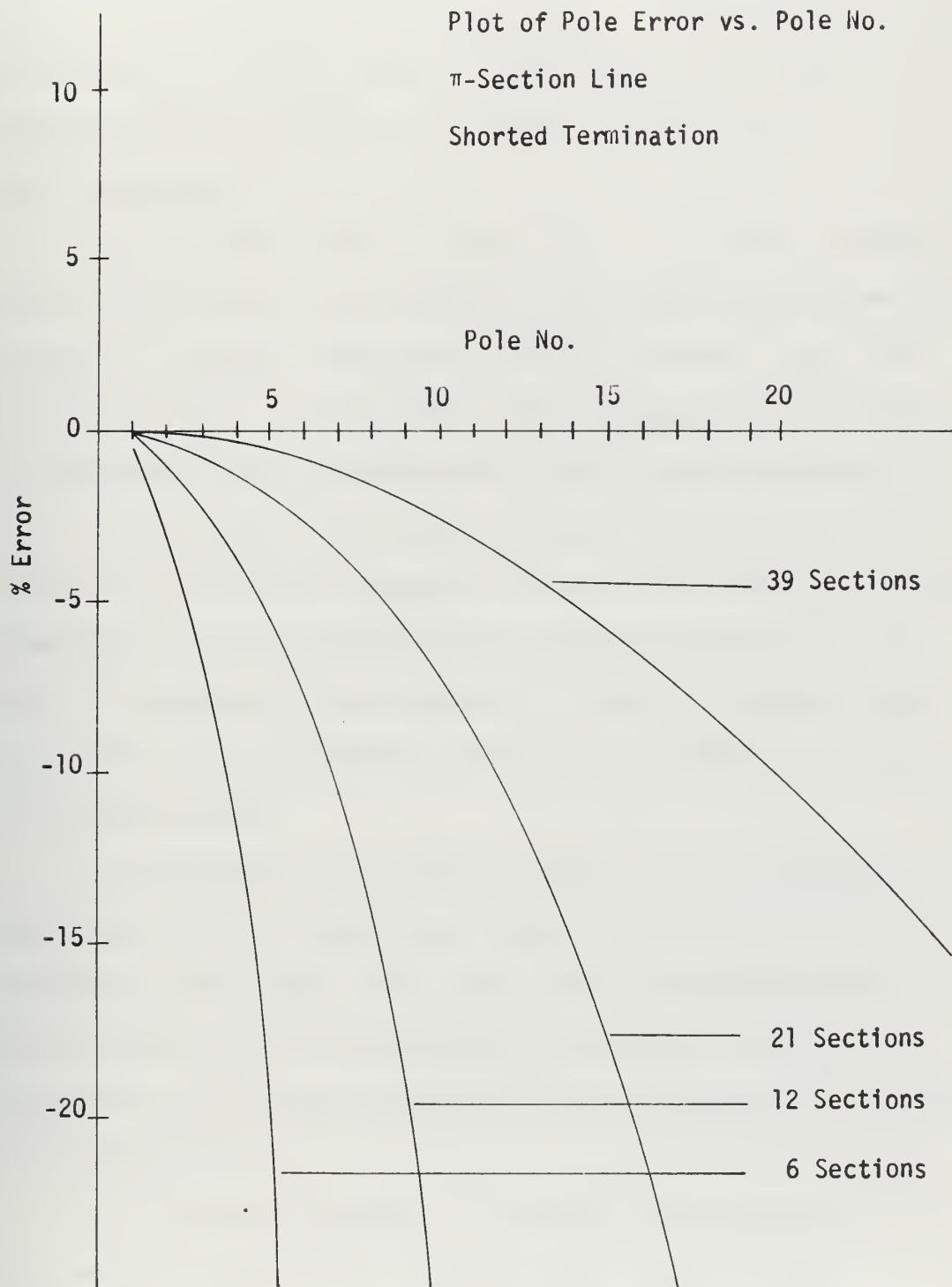


Figure 3.9

3.4.2 π -Section Model (Open)

The open circuit case is derived in Appendix B.5 and solved in Appendices C and D. The results are as shown in Figure 3.10. For Figure 3.10, the percent error is as defined in equation (3-31) with due recognition that the values of $(\cosh \lambda)_{\text{root}}$ in this case are different from their values in the opened, L-section line.

3.5 Conclusions

1. The results shown in Figures 3.4a, 3.4b, and 3.5 indicate that for typical EHV lines and models, the percent error between lines and models is largely independent of losses in either. Thus, the percent error for either positive or zero-sequence is the same for a given number of model sections and a given type of termination.

2. The results indicated by Figures 3.4b and 3.7 show that due to the non-reciprocal character of the L-section model, the error between model and line depends greatly upon which terminals of the model are considered input or output. In fact, the capacitor input case is seen to be considerably inferior to the inductor input case for low order poles.

3. Comparison of the shorted L-model with the shorted π -model shows that the L-model has a rather more complicated error pattern than the π -model. The L-model first over estimates the true pole position for low order poles - then under estimates for higher order. The π -model consistently under estimates the position of the actual pole.

4. The open circuited π and L-models give practically identical pole error plots. (Actually, each π -model has one additional pole higher than the highest pole of the corresponding

Plot of Pole Error vs. Pole No.

π -Section Line

Open Termination

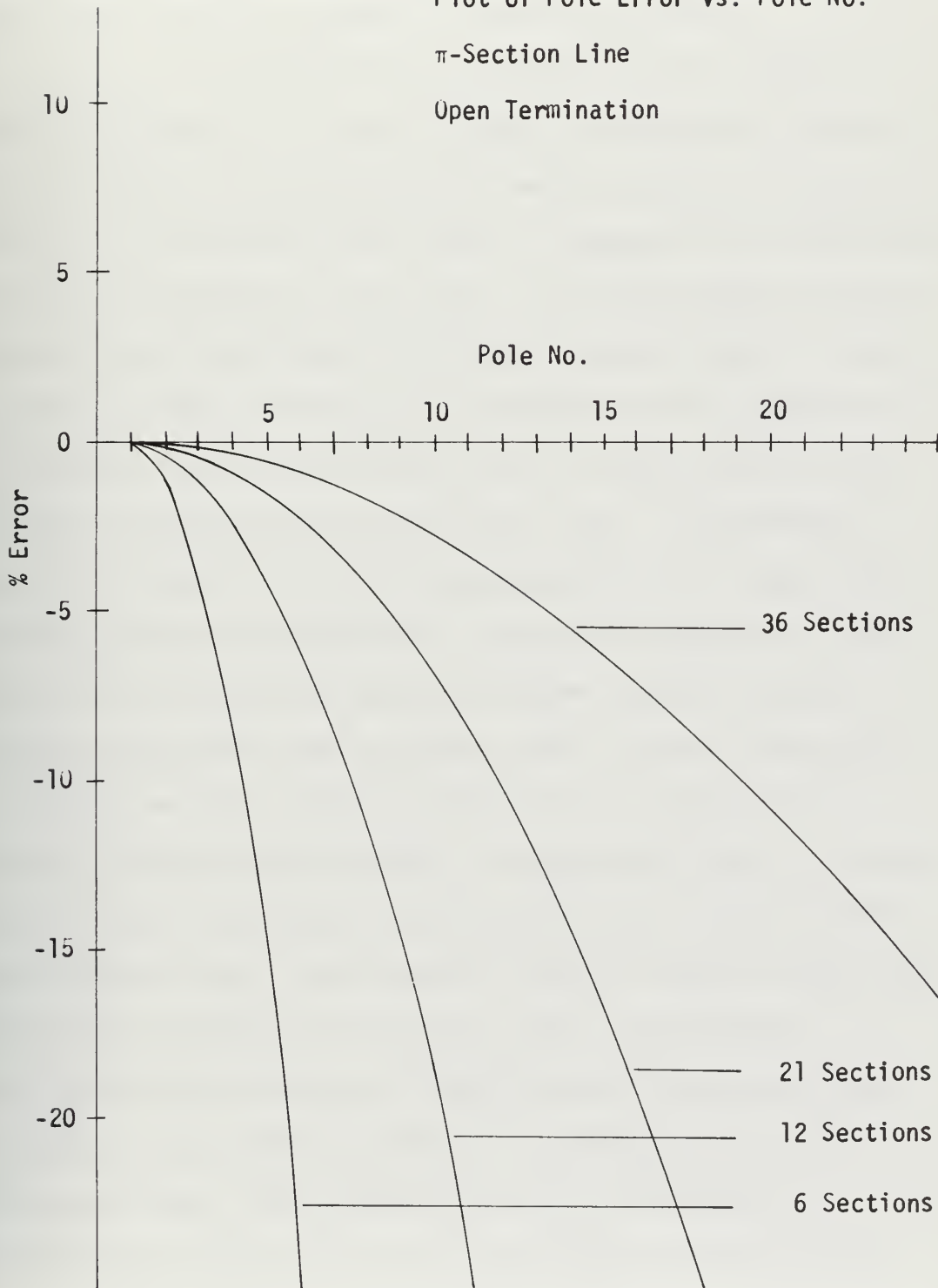
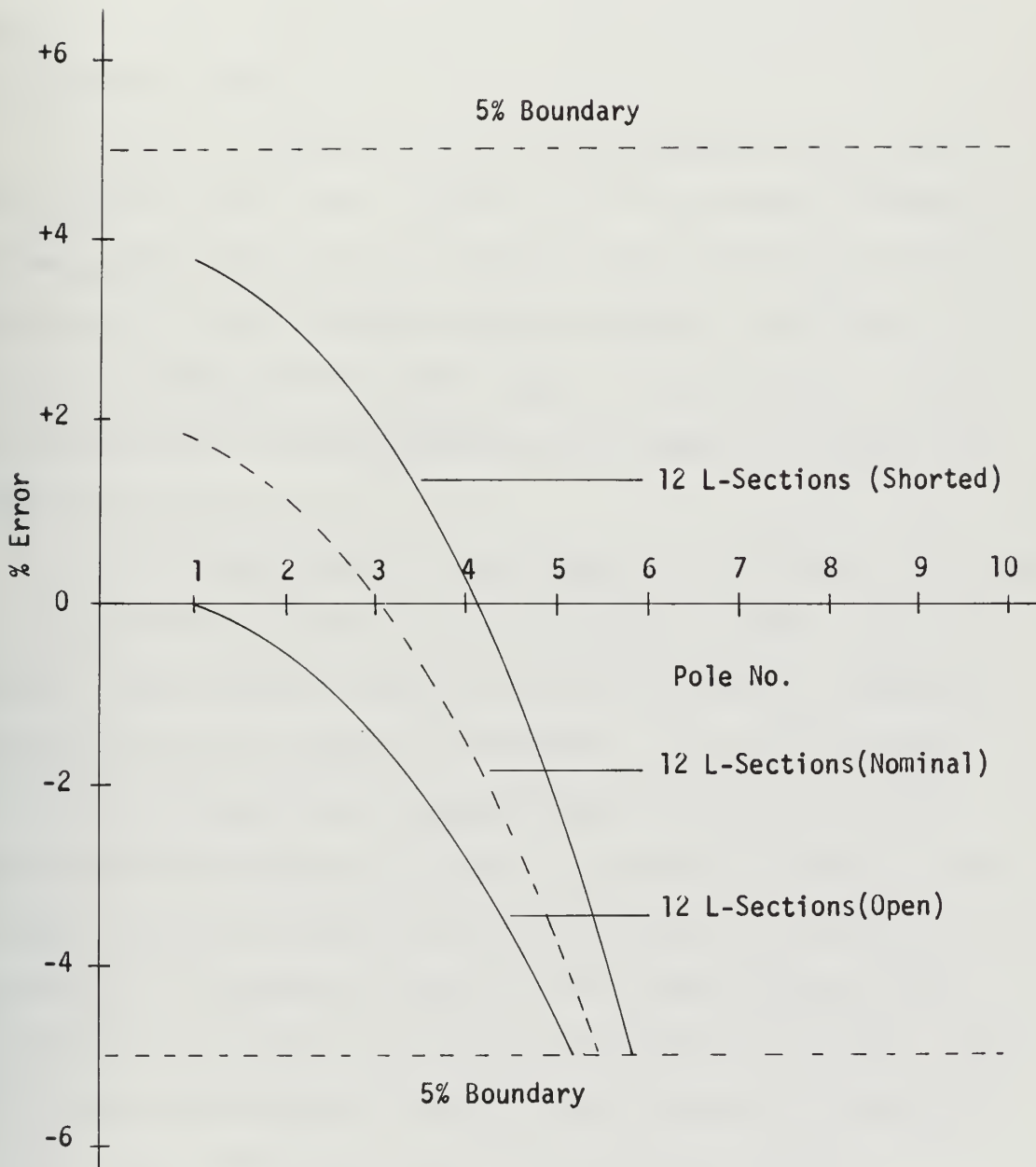


Figure 3.10

L-model.)

5. Any L-section model can be converted to either a π or T model by a simple change in the first and last sections to obtain any of the pole-error patterns of preceeding sections.

6. A suggested method of using the pole error plots is shown in Figure 3.11. Figure 3.11 shows, as an example, the pole error "curves" of a twelve section L-model as taken from Figures 3.4b and 3.8. A five percent error bound is suggested by the dotted lines at the top and bottom of the figure. The region between the solid curves is the "error band" of the twelve section L-model. If the terminals of the line appear as a predominantly high impedance to frequencies corresponding to the first five poles, the line error is given (approximately) by the "open" curve. A corresponding observation applies for the low impedance case. The dashed curve mid-way between the solid curves is meant to indicate the "nominal error" when the terminals appear as neither open nor shorted. If twelve sections were used to model a sixty mile line, Figure 3.11 shows that the error band lies within the five percent error bounds up to about the fifth pole. As seen from Tables 3.1 and 3.2 the fifth pole corresponds to about 6000 Hz for a sixty mile line. One could say then - "the 12-section L-model is good to within five percent up to 6000 Hz" (for a 765 kV line). An error plot similar to that of Figure 3.11 could be made for any model type composed of any number of sections. In particular, if it is desired to model a 400 mile line to "within five percent" an inspection of Figures 3.4b, and 3.8 shows that a model of about



Example of an "Error Band-Error Bound"
Plot for a Twelve Section L-Model

Figure 3.11

forty sections will ensure that the line is "good to within five percent" up to the fifteenth pole. Tables 3.1 and 3.2 show that the fifteenth pole corresponds to a frequency of about 3100 Hz (for a typical 765 kV line). Thus, a minimum of forty ten-mile sections would be required to model a 400 mile line to within the five percent criteria.

Tables 3.1 and 3.2 give the pole frequencies, specifically, for a typical 765 kV line. Actually, as will be shown in Chapter 4, corresponding tables for most other EHV lines would be very similar to Tables 3.1 and 3.2 (within about ten percent). With Tables 3.1 and 3.2 as representative of EHV lines, it is now possible to make some quantitative decisions concerning the number of sections to be built for the t.l.m.

7. As stated earlier in this report - as a minimum - the t.l.m. is to model EHV lines from sixty to 400 miles in length. The five percent "specification" referred to earlier is actually a result of observations such as those in Conclusion 6. It was noted earlier that forty sections is the minimum number which will just ensure that a 400 mile line-model is within five percent to 3060 Hz. This in turn, implies at least forty ten-mile sections for the model. In addition, it is proposed to model all line lengths between sixty and 400 miles by changing the number of sections in the model. Thus, if a line to be modeled is 396 miles long, it would be desirable to set up a model "396 miles long". This adjustment could be accomplished with the ten-mile sections by using "taps" to adjust length. However, this t.l.m. design must model, horizontal or

vertical, non-transposed lines - this too requires taps. To avoid having to tap the sections for length, it is proposed to make the sections "fine" enough (i.e. short enough) so as to make tapping unnecessary for length adjustments. Line lengths to 400 miles can be reached to within one percent by making the largest sections have only eight-mile length. Thus, the 396 mile line, e.g., could be reached (to one percent) by either forty nine or fifty eight-mile sections. But eight-mile sections are not "fine" enough to model short lines, etc., etc. Finally then, with considerations such as those above, it was decided that the t.l.m. design should consist of thirty four-mile sections and thirty-five eight-mile sections. This selection is seen to be quite conservative (by the chosen criteria) and provides a model somewhat "finer" than some other t.l.m.'s.¹⁻⁴

8. The pole error analysis is seen to provide a means of quantitatively comparing proposed models, and is useful in indicating the relative merit of, say, doubling the number of sections - or halving them, etc.

3.6 Applications and Recommendations

The solution technique employed to solve the impedance functions of this chapter can have application in other fields of study. The denominator of each of the impedance functions of this chapter corresponds to the "frequency polynomial" of mechanical vibrations problems. If the frequency polynomial is set equal to zero, it becomes the "frequency equation" for determining the natural frequencies of mechanical systems. Even in systems with

only two degrees of freedom the frequency equation is of fourth degree (quadratic in ω^2) so that, in continuous systems or systems having more than two degrees of freedom, complicated solution techniques must be employed or approximations made. The technique suggested in this chapter and employed in Appendices C and D is a means of having the computer generate the frequency equation and then solve it for the natural frequencies of the system. A detailed investigation into the exact class of problems for which this solution technique may have validity has not been conducted by the author, but it is suggested that such an investigation could be worthwhile.

CHAPTER 4

PARAMETERS OF EHV LINES AND MODELS

4.1 Parameters of Representative EHV Lines

In order to determine the parameters or component values for a t.l.m., it is first necessary to know the parameters of typical lines the t.l.m. would be expected to model. The t.l.m. should be capable of modeling not only lines already in existence but, in addition, it should be capable of modeling proposed and even hypothetical lines. For information pertaining to the parameters of existing lines use was made of Report No. 710, Electrical Characteristics of Transmission Lines, of the American Electric Power Service Corporation (AEP)¹⁰. Appendix IV of Report No. 710 describes in detail thirty-four different EHV transmission line configurations in use by the company. From the thirty-four configurations a sample of six was selected as representative of types of configurations. For example, AEP type "H" was taken as one representative of a 345 kV, single conductor per phase, single ground wire, vertical configuration. Type "H-Special" was selected since it is a common line and represents a form of triangular configuration. A hypothetical type "39F" was "constructed" by using two phase-conductors per bundle spaced eighteen inches apart - this was taken as representative of a two-conductor, "vertical", 345 kV line. A type "41A" line was selected to represent a 345 kV, two-conductor, horizontal configuration. The AEP "Typical Aluminum Tower" configuration was taken as representative of most 765 kV lines (horizontal). A hypothetical 765 kV "H-Special" was constructed by scaling the 345 kV "H-Special" conductor

distances in the ratios that exist between the type "41A" and the "Typical Aluminum Tower". Finally, two hypothetical 1500 kV configurations were taken from reference 11 - a horizontal configuration (Geometry No. 2 and Bundle Drawing No. 4), and a triangular line (Geometry No. 3 and Bundle Drawing No. 4).

Typical positive and zero-sequence parameters obtained for these representative lines are shown in Tables 4.1 and 4.2. The values shown in Tables 4.1 and 4.2 (except for X_C/X_L and Q) were obtained with the aid of a computer using the "Electric Power Systems Engineering Laboratory (EPSEL) Line Parameters Program".¹² This program requires as input the geometrical configuration of the conductors of a given line (along with conductor and earth properties) and computes the inductance, capacitance, and resistance matrices of the actual line as a function of frequency. In addition, as well as the parameters of Tables 4.1 and 4.2, the program computes and prints the values of the model parameters of Figure 2.2. The model parameters are printed on the basis of a one-mile long section and assumes a scale factor of one between impedances of the line and model. Model parameter values at sixty Hz, on the basis described above, for the eight representative line models are shown in Table 4.3 (earth resistivity is taken to be 100 ohms-meters). Referring to Table 4.2 note that, except for the 1500 kV lines, the positive-sequence (or average) Q at 60 Hz is about twenty or lower. The high Q values for the 1500 kV lines are questionable and would be difficult to duplicate in a practical model. Consequently, no attempt will be made to even approach the Q values suggested by the

	Pos. Seq. $1/X_C$	Pos. Seq. X_L	Pos. Seq. R	$\frac{X_C}{X_L}$
Type 39F	7.11 $\frac{\text{miles}}{\text{meg } \Omega}$	0.594 $\frac{\Omega}{\text{mile}}$	0.063 $\frac{\Omega}{\text{mile}}$	236,000 (mi.) ²
345 kV H-Spec.	5.25	0.810	0.087	263,000
Type H	5.65	0.751	0.087	236,000
765 kV H-Spec.	7.49	0.561	0.027	239,000
Type 41A	6.82	0.627	0.054	234,000
1500 kV Horizontal	8.08	0.522	0.005	237,000
1500 kV Triangular	8.41	0.494	0.005	240,000
765 kV Horizontal	7.78	0.548	0.028	236,000

Table of Positive Sequence Parameters for
Some Typical EHV Line Configurations (at 60 Hz).

Table 4.1

	Zero Seq. X_L	Zero Seq. R	Zero. Seq. $1/X_C$	Pos. Seq. Q
Type 39F	$1.59 \frac{\Omega}{mi}$	$0.329 \frac{\Omega}{mi}$	$3.92 \frac{mi}{meg \Omega}$	9
345 kV H-Spec.	1.85	0.395	3.63	9
Type H	1.97	0.395	3.30	9
765 kV H-Spec.	1.66	0.418	4.65	21
Type 41A	1.79	0.598	4.80	12
1500 kV Horizontal	1.10	0.131	5.83	104
1500 kV Triangular	1.23	0.133	4.81	99
765 kV Horizontal	1.64	0.522	5.31	20

Table of Positive Sequence Q and Zero Sequence
Parameters of some Typical EHV Line
Configurations (at 60 Hz).

Table 4.2

Parameter	Type 39F	345 kV H-Spec.	Type H	765 kV H-Spec.
L'_{11}	1.83	2.21	2.21	1.52
L'_{22}	1.76	2.16	2.16	1.49
L'_{33}	1.59	2.05	2.05	1.42
L'_{00}	0.736	0.928	0.928	0.975
L'_{12}	0.297	0.022	0.276	0.004
L'_{23}	0.147	-0.051	0.168	-0.038
C'_{12}	3.6	1.3	2.5	2.2
C'_{23}	3.5	1.5	2.6	2.7
C'_{13}	1.5	1.5	1.2	2.7
C'_{10}	11.2	10.0	9.5	13.2
C'_{20}	9.2	9.6	8.0	12.2
C'_{30}	10.8	9.7	8.9	11.5
R'_{11}	56.2	80.0	80.0	16.5
R'_{22}	60.4	84.6	84.6	24.0
R'_{32}	71.4	94.9	94.9	40.4
R'_{00}	89.0	103.	103.	130.

Table of Unscaled Parameters for Models
of Representative EHV Lines. (L' in mh/mi.,
 C' in nf/mi., and R' in m Ω /mi.)

Table 4.3

Parameter	Type 41A	1500 kV Horizontal	1500 kV Triangular	765 kV Horizontal
L'_{11}	1.81	1.52	1.30	1.60
L'_{22}	1.78	1.40	1.46	1.59
L'_{33}	1.81	1.52	1.30	1.60
L'_{00}	0.886	0.410	0.604	0.820
L'_{12}	0.212	0.147	0.066	0.214
L'_{23}	0.212	0.147	0.066	0.214
C'_{12}	2.4	2.7	3.1	2.95
C'_{23}	2.4	2.7	3.1	2.95
C'_{13}	0.7	0.7	3.3	0.76
C'_{10}	13.2	15.8	12.5	14.7
C'_{20}	11.9	14.8	13.3	13.1
C'_{30}	13.2	15.8	12.5	14.7
R'_{11}	51.5	6.2	4.7	26.0
R'_{22}	58.0	4.0	6.7	30.6
R'_{33}	51.5	6.2	4.7	26.0
R'_{00}	182.	41.5	42.3	165.

Table of Unscaled Parameters for Models
of Representative EHV Lines. (L' in mh/mi.,
 C' in nf/mi., and R in $m\Omega$ /mi.)

Table 4.3 (Cont.)

1500 kV line values. With a Q of twenty, the 765 kV horizontal line will be taken as the minimum standard (in Q) to be achieved by this t.l.m. This means (referring to Table 4.2) that each of the sixty-five sections of the t.l.m. must have a positive sequence Q of at least twenty at sixty Hz. The positive and zero-sequence Q of transmission lines is not constant with frequency and, in fact, increases with frequency. Graphs of the positive and zero-sequence Q of representative lines are shown in Figures 4.1 and 4.2. The positive-sequence Q is seen to increase steadily in the range to 3060 Hz while the zero-sequence Q becomes nominally constant in the range from 1500-3060 Hz. Each model section must provide a Q characteristic equivalent to those of Figures 4.1 and 4.2 in order to accurately model the actual line. If the model section is designed to meet the positive-sequence Q requirement of the typical 765 kV line, than it can be made to model lines of lower Q by simply inserting resistance in the phase conductors.

The positive-sequence inductance of EHV transmission lines is practically constant over the frequency range of interest, but the zero-sequence inductance is not. A graph of the variation of zero sequence inductance with frequency is shown in Figure 4.3 for the typical 765 kV line. The zero-sequence inductance is seen to drop markedly with increasing frequency-particularly in the low frequency region. Thus, in the model also, the zero-sequence inductance must correctly decrease with increasing frequency and produce (as nearly as possible) the scaled equivalent of Figure 4.3.

Graph of Positive Sequence Q vs. Frequency for Representative EHV Lines

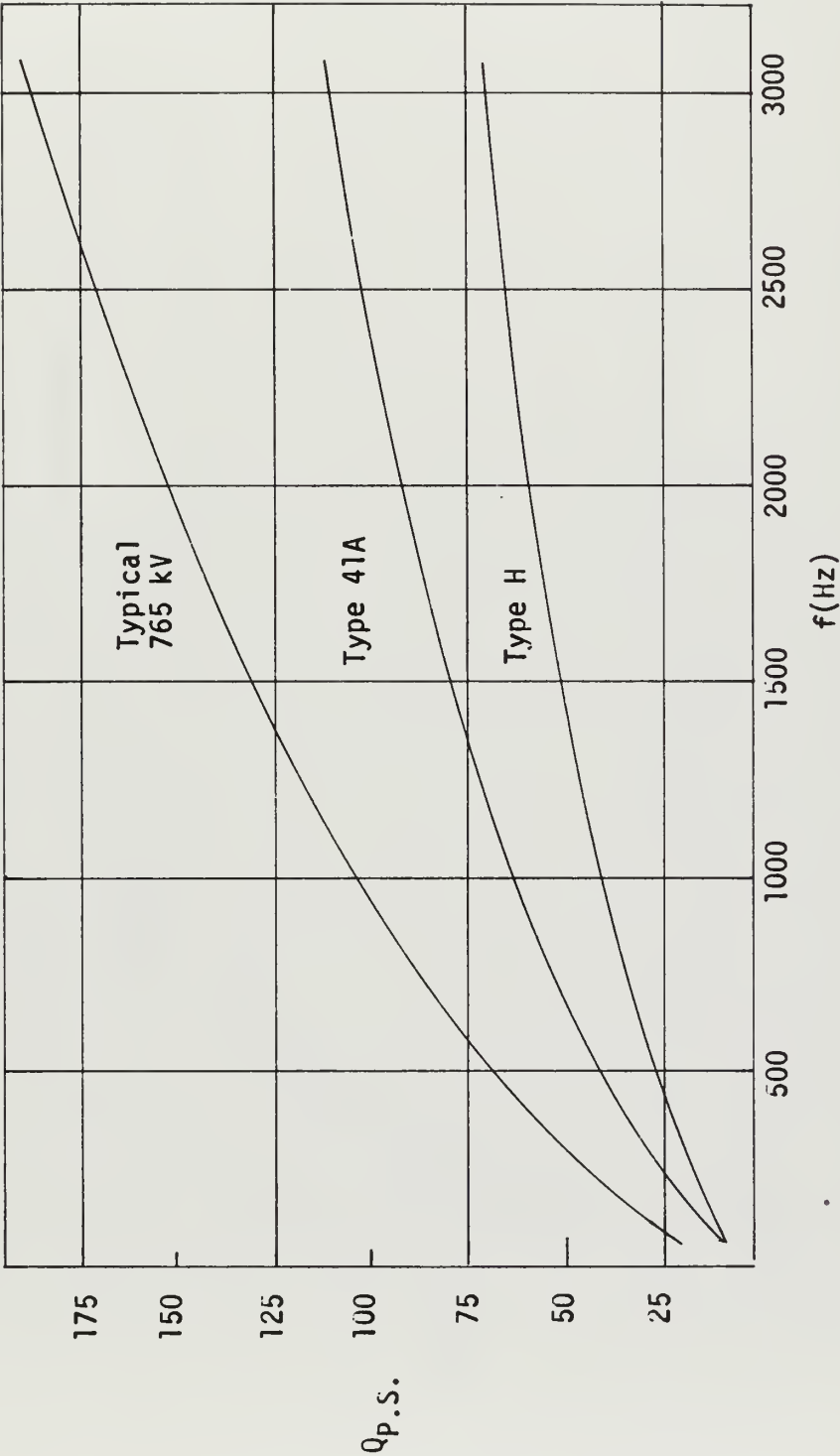


Figure 4.1

Graph of Zero-Sequence Q vs. Frequency for Representative EHV Lines

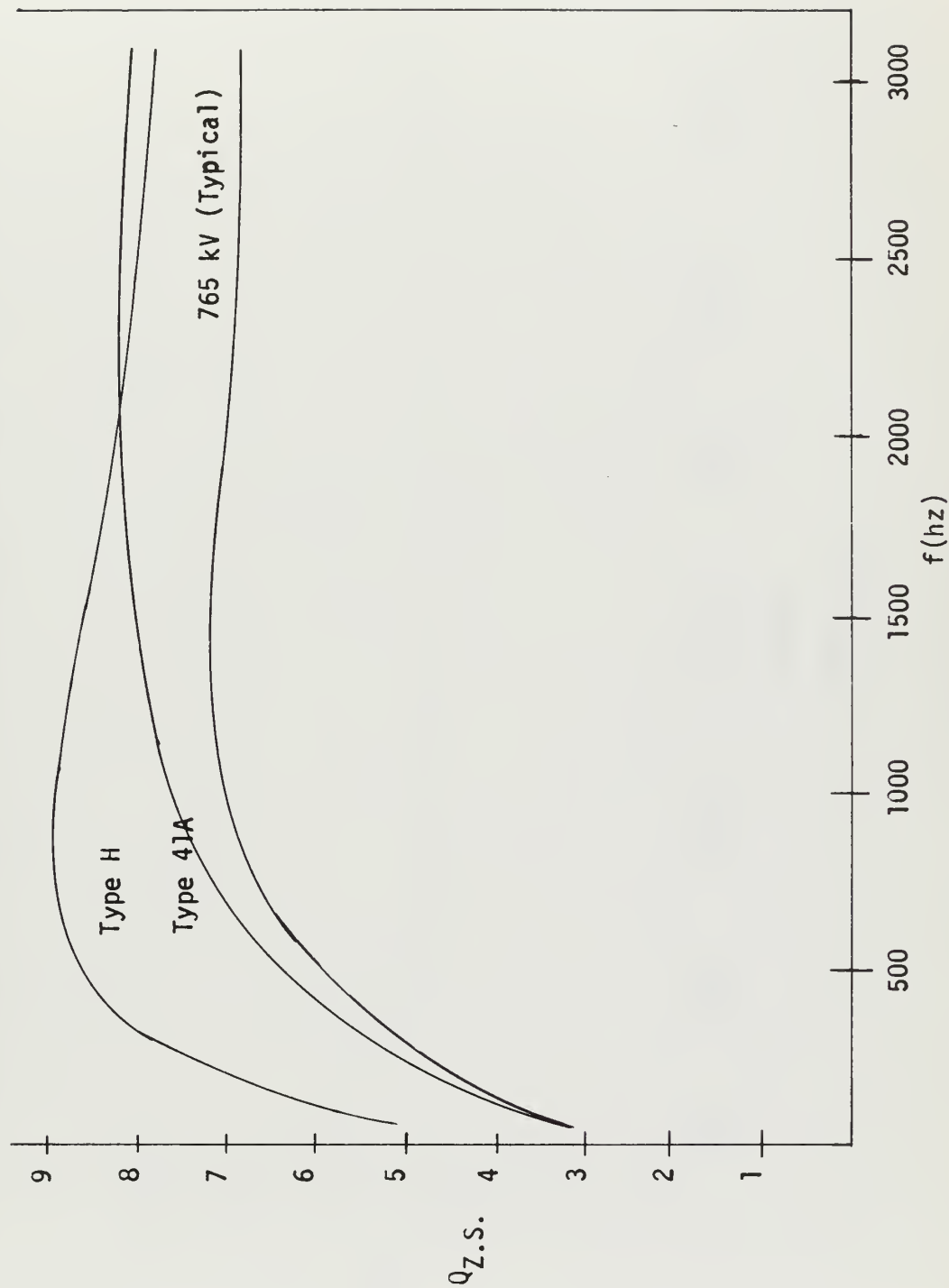


Figure 4.2

Graph of Zero-Sequence Inductance vs. Frequency for Typical 765 kV Line

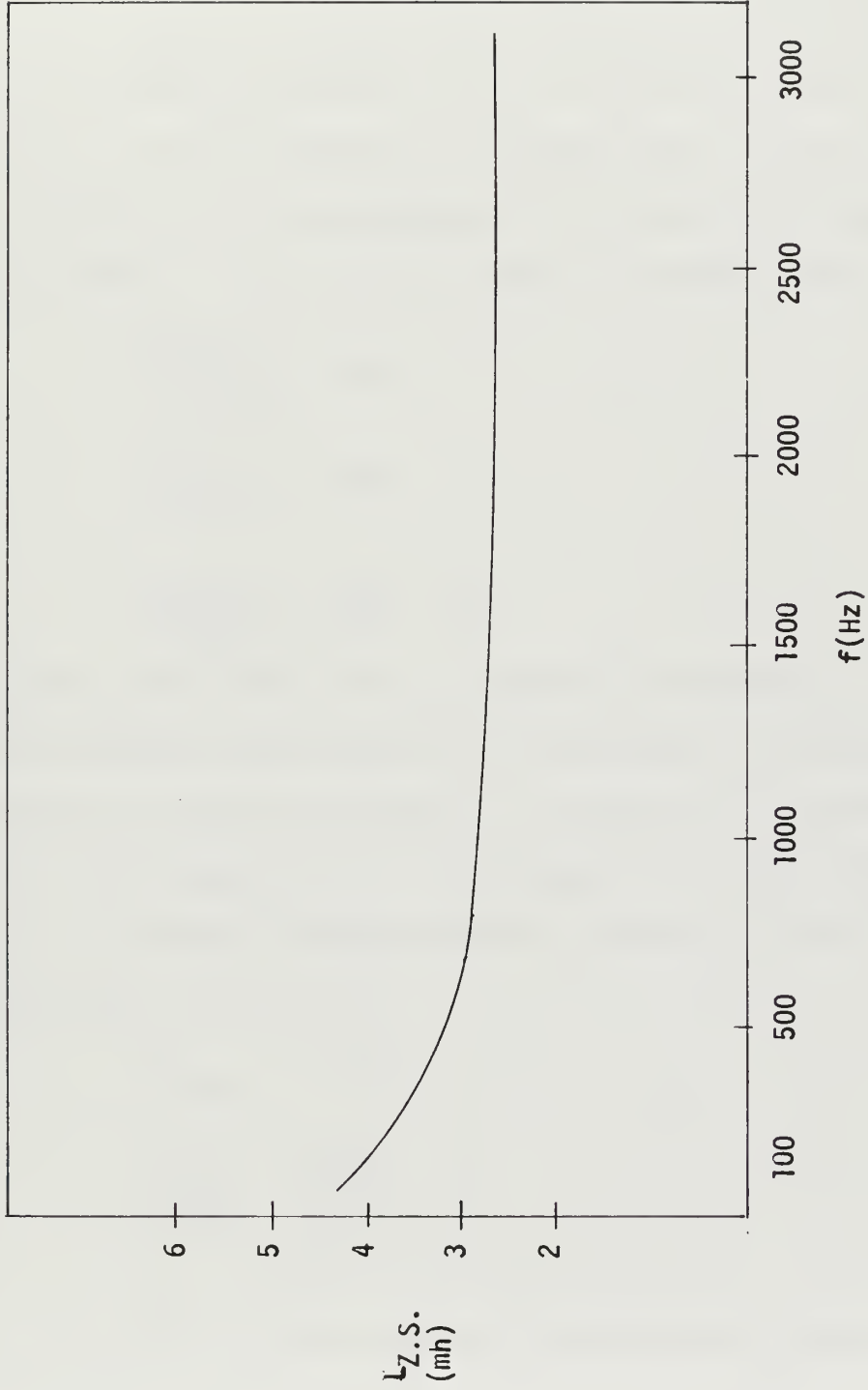


Figure 4.3

4.2.1 Line/Model Scale Factors and General Model Parameters

Due to the fact that the t.l.m. must be compatible with existing TSS transformer and compensating reactor models, the base voltage of the t.l.m. must be 138 V line-to-line, and the ratio of the base impedance of the model to that of a typical 765 kV line must be 0.355. This means that the base current and power of the t.l.m. are 38.6 ma and 9.2 watts respectively. The base impedance of a typical 765 kV line on a 100 MVA base is 5850 ohms. The base impedance of the model is 2078 ohms. With the above impedance ratio constraint between the model and 765 kV line,

$$\frac{L_{B \text{ model}}}{L_{B \text{ actual}}} = .355,$$

$$\frac{R_{B \text{ model}}}{R_{B \text{ actual}}} = .355,$$

and

$$\frac{C_{B \text{ model}}}{C_{B \text{ actual}}} = \frac{1}{.355} = 2.82 .$$

To model the typical 765 kV line, all the 765 kV parameters of Table 4.3 must be appropriately scaled by the ratios above. For example, L'_{22} of Table 4.3 becomes .564 mh/mi, or 2.26 mh/4 mi, or 4.52 mh/8 mi. Thus, the 4-mile section would be constructed with a basic 2.26 mh inductor. An identical procedure applied to the 345 kV type "41A" line gives (on a 100 MVA base):

$$(Z_B)_{345} = 1190\Omega$$

$$\frac{Z_{Bm}}{(Z_B)_{345}} = \frac{2078}{1190} = 1.74$$

$$L'_{22} = 3.1 \text{ mh/mi, or } 12.4 \text{ mh/4 mi, etc.}$$

To model the 765 kV line the inductor in the four mile section must be 2.26 mh and to model the 345 kV line it must be 12.4 mh. This implies a very wide range of taps on the model inductors. A wide

range of taps on an inductor is not only difficult and expensive to construct, but has the further disadvantage that the Q of the inductor gets "tapped" as the inductance. Thus, tapping the inductance down to one-sixth of the total inductance cuts the Q down to about one-sixth of what it was for the total inductor.

A procedure for solving this problem is to choose, for lines other than the typical 765 kV, a power base other than the commonly used 100 MVA. Again suppose that the 345 kV type "41A" line is to be modeled. The first step is to establish an impedance ratio between the actual line and model such that L'_{22} for the 345 kV model is the same as that already provided for the typical (horizontal) 765 kV line. In other words, using Table 4.3, seek a scale factor F ,

$$F = \frac{(Z_B)_{\text{model}}}{(Z_B)_{\text{line}}} , \quad (4-1)$$

such that

$$F(L'_{22})_{345} = (L'_{22})_{765 \text{ hor.}} . \quad (4-2)$$

So that

$$F = \frac{(L'_{22})_{765 \text{ hor.}}}{(L'_{22})_{345}} = \frac{.564}{1.78} = .316, \quad (4-3)$$

and

$$\frac{Z_{Bm}}{Z_{Bl}} = .316 .$$

But

$$Z_{Bl} = \frac{V_{Bl}^2}{P_{Bl}} , \quad (4-4)$$

so that

$$P_{Bl} = \frac{(.316)^2 V_{Bl}^2}{Z_{Bm}} = 18.1 \text{ MVA} . \quad (4-5)$$

Thus, when modeling a 345 kV type "41A" line, it is necessary to use

a power base in the line of 18.1 MVA instead of the usual 100 MVA. The resulting parameters required of a four-mile model section are shown in Tables 4.4a and 4.4b respectively. Note in Table 4.4a that the inductors corresponding to phases "a" and "c" are equal - reflecting the symmetry of the horizontal lines. This is not the case for the "vertical" lines of Table 4.4b. With the inductances of the 765 kV horizontal model as a base, note that all the L_a 's of Table 4.4b are larger than 2.28 and all the L_c 's are smaller. In fact, all the L_a 's of Table 4.4b are larger than 2.28 by the same amount (Δ) that all the L_c 's of Table 4.4b are smaller than 2.28. The scale factor to achieve this "balance" for vertical configurations is not given by equation (4-3) but is determined as follows:

Using Table 4.3, seek a scale factor F such that

$$\begin{aligned} F(L'_{11})_{\text{vert.}} - (L'_{11})_{765 \text{ hor.}} &= \Delta \\ F(L'_{33})_{\text{vert.}} - (L'_{33})_{765 \text{ hor.}} &= -\Delta. \end{aligned}$$

Solving for F [using the fact that $(L'_{11})_{765 \text{ hor.}} = (L'_{33})_{765 \text{ hor.}}$],

$$F = \frac{2(L'_{11})_{765 \text{ hor.}}}{(L'_{11} - L'_{33})_{\text{vert.}}} \quad (4-6)$$

The use of equation (4-6) ensures that the unbalance inherent in vertical lines is shared equally by both phases "a" and "b" in the model. A "balanced sharing" is desirable since a factor determined as in equation (4-3) gives the result that the phase "c" model inductor would be required to span a larger range than the phase "a" inductor - thus requiring more taps. Use of equation (4-6) ensures that the phase "a" and "c" inductors will have the same number of taps. Referring again to Table 4.4a, note that L_b for the two

Parameter	Type 41A	1500 kV Horizontal	1500 kV Triangular	765 kV Horizontal
L_a	2.29	2.34	2.16	2.28
L_b	2.26	2.16	2.41	2.26
L_c	2.29	2.34	2.16	2.28
L_n	1.12	0.630	1.0	1.16
L_{ab}	0.27	0.23	0.11	0.30
L_{bc}	0.27	0.23	0.11	0.30
C_{ab}	30.4	28.1	30	33.2
C_{bc}	30.4	28.1	30	33.2
C_{ac}	8.8	7.0	32	8.6
C_{an}	166	164	121	166
C_{bn}	149	154	129	148
C_{cn}	166	164	121	166
R_a	65	10	7.85	37
R_b	73	6.5	10.8	43
R_c	65	10	7.85	37
R_n	230	67	70	235

Table of Scaled Parameters Implied for a
4-mile Model Section. (L in mh/4 mi.,
 C in nf/4 mi., R in m Ω /4 mi.)

Table 4.4a

Parameter	Type 39	345 kV H-Spec.	Type H	765 kV H-Spec.
L_a	2.44	2.36	2.36	2.34
L_b	2.34	2.31	2.31	2.29
L_c	2.12	2.20	2.20	2.2
L_n	0.98	0.99	0.99	1.50
L_{ab}	0.40	0.24	0.30	0.006
L_{bc}	0.20	-0.05	0.18	-0.06
C_{ab}	43.2	19.4	37.3	22.8
C_{bc}	42.0	22.4	38.8	28.1
C_{ac}	18.0	22.4	17.9	28.1
C_{an}	135	149	142	137
C_{bm}	111	143	119	127
C_{cn}	129	145	131	119
R_a	75	86	86	20
R_b	80	91	91	37
R_c	95	102	102	62
R_n	117	110	110	201

Table of Scaled Parameters Implied for a 4-Mile
Model Section. (L in mh/4 mi., C in nf/4 mi., R in m Ω /4 mi.)

Table 4.4b

1500 kV lines is not 2.26 mh as would be found had equation (4-3) been used to determine the scale factor. In fact, still another technique has been employed to determine the scale factor of these two lines. This third technique will be discussed later in this chapter.

Some remarks are in order at this point concerning the model zero-sequence inductance, $L_{Z.S.}$, and the inductor L_n of Table 4.4a. To obtain the zero-sequence characteristic required of a 4-mile model section for modeling a 765 kV line, for example, the graph of Figure 4.3 is simply scaled by the factor $(0.355)(4.0) = 1.42$; the result is shown in Figure 4.4. The model zero-sequence inductance is required to fall from 6.2 mh at 60 Hz to about 4.0 mh at 1000 Hz. The point to note is that L_n of Tables 4.4a-b is not the zero-sequence inductance of the model per se, but L_n is the component which must be designed to produce the characteristic shown in Figure 4.4 if a transposed 765 kV horizontal line is to be modeled. The detailed design of a suitable L_n for this t.l.m. is being carried out by Mr. William Feero as part of his thesis to be completed in September, 1971. Thus, the design of L_n is being carried out in parallel with (but slightly behind) the design of the remainder of the t.l.m.

In preparation for the design of the model inductors, excluding consideration of the 1500 kV lines of Tables 4.4a and 4.4b, it was decided that the inductance values shown in Table 4.5 should be provided in the 4-mile sections in order to model most EHV lines.

Graph of Zero Sequence Inductance of a 4-Mile Model Section When
Modeling a Typical 765 kV Line

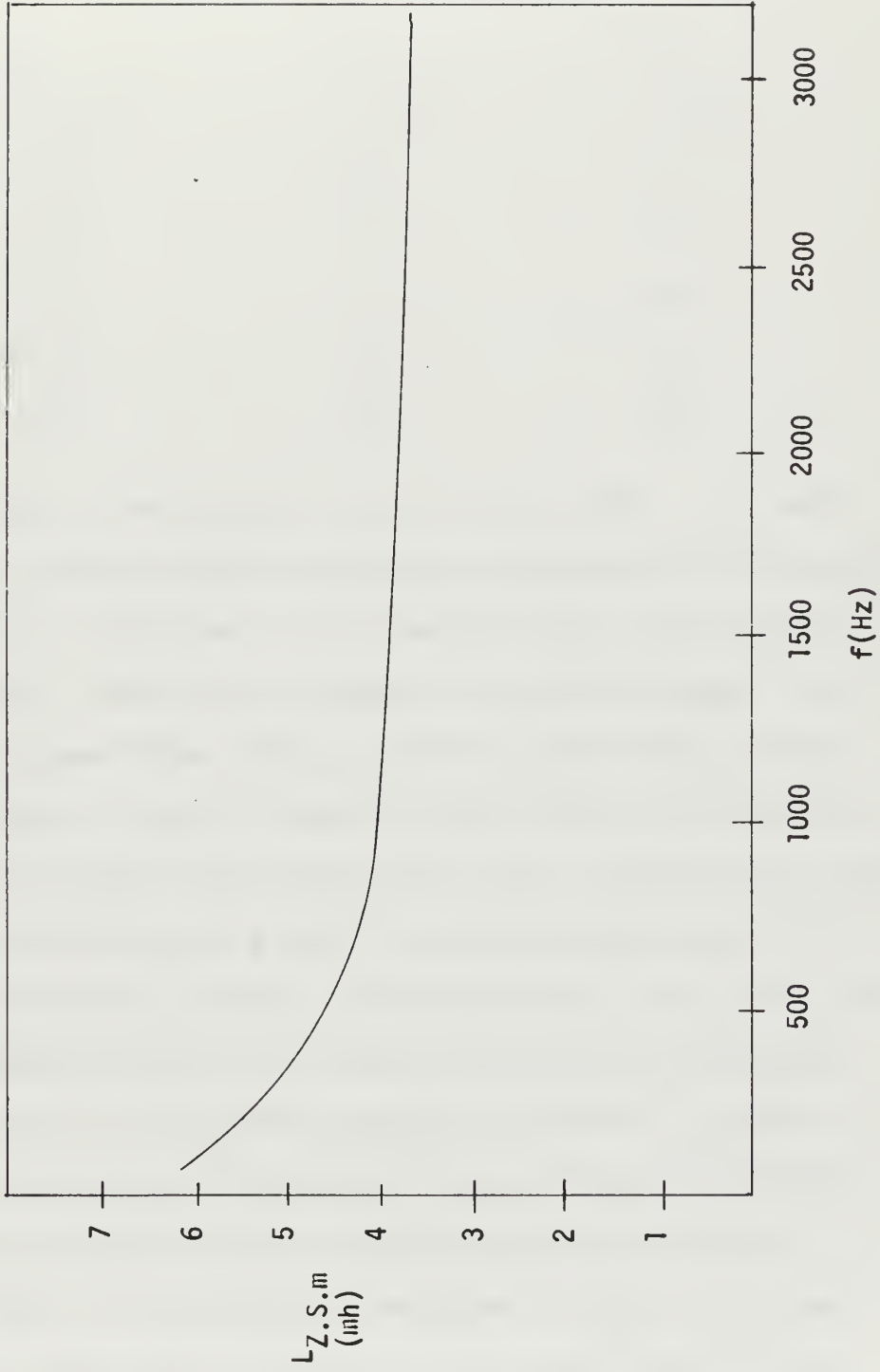


Figure 4.4

Table 4.5

Self Inductance Designed Into the 4-Mile Sections

$\underline{L_a}$	$\underline{L_b}$	$\underline{L_c}$
2.24 mh	2.16 mh	2.08 mh
2.29	2.21	2.13
2.34	2.26	2.18
2.39	2.31	2.23
2.44	2.36	2.28
2.49	2.41	2.33

Early in the design of the t.l.m. the 1500 kV lines were generally ignored as beyond the modeling capabilities attainable by this design. With respect to the quality factor, the preceeding statement is, indeed, true. However, in all other respects it is possible to model these lines also-with a proper choice of scale factor. Note in Table 4.5, under $\underline{L_b}$, the value 2.26 mh originally provided for modeling the typical 765 kV line. Equation (4-3) shows the L'_{22} (unscaled $\underline{L_b}$) of a 345 kV line being scaled to the 2.26 mh inductor previously provided. The 2.26 mh value is not unique, and any inductance parameter of a line to be modeled could be scaled to any one of the inductances provided in Table 4.5. In fact, to properly fit the two 1500 kV lines, the $\underline{L_b}$ of the horizontal 1500 kV line was scaled to 2.16 mh and the triangular to 2.41 mh. (The extremes of the existing $\underline{L_b}$ were used in order to keep the resulting values of $(\underline{L_c})_{1500}$ and $(\underline{L_a})_{1500}$ within "reach" of the ranges provided in Table 4.5.) The above procedure resulted in an impedance scale ratio of 0.414 for the triangular line and 0.384

for the horizontal. The resulting power bases to be applied to the actual lines are 448 MVA for the triangular, and 417 MVA for the horizontal. Thus, the three scaling examples provided in this section illustrate the considerable flexibility of the "Floating Power Base" technique. The values of self inductance to be designed into the 8-mile sections are obtained by simply doubling the values in Table 4.5.

4.2.2 Selection of Model Mutual Inductance Parameters

Tables 4.4a and 4.4b indicate that typical values of L_{ab} range from 0.006 mh/4 mi to 0.4 mh/4 mi, and those for L_{bc} from -0.06 mh/4 mi to 0.27 mh/4 mi. Providing this wide range of values is neither practical nor necessary for the following reasons:

1. To cover the range implied above would require too many taps on the mutual windings and too many values brought to the front panel of the section. As few as six "tap values" per component in Table 4.4 means that 120 lines must be brought to the front panel. (It is proposed to limit the number of taps on any component to six.)
2. In those cases where the mutual inductance value is $1/20$ or less of the self inductance upon which it is wound, it would be nearly impossible to measure the effect of the mutual inductance. Therefore, those values of mutual inductance amounting to $1/20$ or less of the self inductance in the same line will simply be ignored. Note that this rule leaves the negative mutuals ignored.

3. Discounting the extremes mentioned above, most mutual values appear to be in the range of from 0.17 mh to about 0.27 mh - the single exception being the far removed 0.40 mh of the hypothetical type "39F" line. Mutual taps actually provided in the model section should reflect this "crowding" in the mid-band by the provision of relatively more taps in this band.

4. Horizontal lines are common, and it is seen that for horizontal lines the mutual inductances are equal. The selection of taps to be provided in the model section should preserve this balance if possible.

Based upon the arguments above, the values of mutual inductance to be designed into the 4-mile model sections are shown in Table 4.6 - those for the 8-mile sections are shown in Table 5.5.

Table 4.6

<u>L_{ab} (mh)</u>	<u>L_{bc} (mh)</u>
.15	.15
.18	.18
.20	.20
.23	.23
.25	.25
.33	.32

Table of Mutual Inductance Values
Designed into the 4-Mile Sections

4.2.3 Selection of Model Resistance Parameters

The resistance ranges implied for a 4-mile model section are shown in Tables 4.4a and 4.4b in which the figures represent the total resistance required of a section from input terminal to output terminal. Thus, the resistance indicated includes the resistance of the self and mutual inductance windings discussed above. The amount provided for operator adjustment is the difference between winding and connection resistance and the values indicated in the tables. The resistance of the self and mutual windings must obviously be less than the resistance values in Tables 4.4 if the 4-mile model section is to provide a correct modeling of line Q. The exact value of the resistances to be designed into the 4-mile section cannot be determined until the resistance of the self and mutual windings is known. The setting of the operator adjusted resistance parameters to be provided is deferred to Chapter 7.

4.2.4 Selection of Model Capacitance Parameters

The capacitance parameters implied for a 4-mile section are also indicated in Tables 4.4a and 4.4b. With a wide range of capacitor sizes readily available from manufacturers, a bank of six capacitors will be provided for each capacitance parameter for a total of 36 capacitors in each section. The capacitors of each bank are to be sized so as to span the ranges indicated with "room" on either side. With six capacitors per capacitance parameter, about 4¹ values can be presented to cover the range of the parameter. Tables of the actual capacitor banks purchased for each parameter are presented in Chapter 6.

4.3 Summary Remarks

1. The parameters of the six non-1500 kV lines indicated in Tables 4.1, 4.2, and 4.3 are taken to "span" the range of typical EHV lines (including 500 kV lines).
2. No attempt is made to model positive sequence line Q's greater than 20.
3. Six model values spanning the range of EHV line configuration "types" are provided for each parameter.
4. Only three scaling techniques were illustrated, but any line to be modeled could be scaled to any one of the existing model values in an effort to make diverse lines fit the model.
5. A scale factor, F , obtained for inductance and resistance scaling is used as $1/F$ for capacitance scaling.
6. Values of mutual inductance less than five percent of the self inductance in the same line are ignored.
7. Parameters indicated in Tables 4.4a and 4.4b for a 4-mile model section are simply doubled to obtain the values for an 8-mile section.
8. The details of the return path inductor design, L_n , will appear in a subsequent report (by a different author) due in September, 1971.

CHAPTER 5

INDUCTOR DESIGN

5.1 Model Inductor Requirements

The model inductance values required of a 4-mile section are shown in Tables 4.5 and 4.6. The inductance values for an eight-mile section are simply double those of Tables 4.5 and 4.6. In addition to simply providing the inductance, the inductors in the model sections must have Q_s considerably greater than the Q characteristic for the "best" line to be modeled. The Q characteristic of the 765 kV horizontal line shown in Figure 4.1 is taken as the minimum standard to be met by the model sections. The Q characteristics of the individual model inductances must exceed the requirements of the overall section. While the line and section require a Q of twenty at 60 Hz, the inductors should have a Q of perhaps 40 at 60Hz - and a similar excess over the entire frequency range. The characteristic shown in Figure 4.1 is the "average" Q of the three phases so that it is not the exact characteristic to be tracked by any of the three self inductors of the model even if this tracking were possible. The solution of the "Q Tracking Problem" in this design is to design or select an inductor whose Q characteristic has the general shape shown in Figure 4.1 but whose Q value is approximately fifteen to twenty-five points higher along the range. Any excess Q of the model can be handled by simply inserting an additional small resistance in series with the model inductors.

In addition to the Q characteristic per se, the model inductors must produce the required Q at the very low values of base

current selected for the model, and must have an inductance that remains essentially constant up to at least 25 p.u. fault current. The inductance of all the phase and mutual inductors must also remain constant with frequency - only the return path inductor, L_n , is to vary with frequency to provide the zero sequence inductance characteristic.

5.2 Inductor Core Selection and Core Properties

The inductor characteristics described in section 5.1 are determined, to a very large extent, by the core material of the inductor. The theory leading to the final relations describing inductor behavior is rather involved and will not be included in this report - only the more significant relations will be presented to indicate the overall procedure. Readers interested in a more complete background leading to the relations presented herein should consult references 13-19.

A number of core materials and configurations were investigated to meet the specifications described above, but most were readily found to be unsuitable and rejected early in the design. A potted ferrite core, for example, meeting all other requirements, was rejected as too expensive (Ferroxcube series 6656). Two alternatives were considered in some detail - oriented silicon steel "C" cores and molybdenum-nickel-iron powdered toroids. The oriented silicon was rejected when the model base current was finally set at the relatively low value of 38.6 ma. At this low current the oriented silicon could not produce the desired Q characteristic at a sufficiently low cost or weight. Basically, the Q of oriented Fe-Si inductors increases with increasing current (up to saturation), whereas with molybdenum-nickel, Q decreases with increasing current. Thus, the Mo-Ni cores have their highest Q's at low currents and the Fe-Si cores have their lowest Q's

at low currents. The basic relation governing the Q of an inductor can be written as (for the frequencies of interest here)

$$Q = \frac{\omega L I^2}{R_{dc} I^2 + R_{ac} I^2} \quad (5-1)$$

Where

L = Inductance in henries

$\omega = 2\pi \times \text{frequency}$

R_{dc} = dc resistance of the winding (Ω)

R_{ac} = equivalent core loss resistance (Ω)

With these definitions it is seen that $R_{ac} I^2$ corresponds to both the hysteresis and eddy current losses (See reference 17 p.p. 58ff.) and thus represents the total core loss. R_{ac} , the core loss coefficient, is itself a function of current. For powdered cores the manufacturer¹⁸ provides data on R_{ac} explicitly, whereas for Fe-Si the entire term $R_{ac} I^2$ is provided. If the data provided by the manufacturer is converted to the terms of equation (5-1), it is found that for Fe-Si the core loss, W , is given by (approximately)

$$W = k_1(\omega) I^{1.7}, \quad (5-2)$$

whereas for the powdered Mo-Ni the loss is given by (approximately)

$$W = R_{ac} I^2 = k_2(\omega) I^{2.4} \quad (5-3)$$

In equations (5-2) and (5-3), $k_1(\omega)$ and $k_2(\omega)$ are core loss constants and are a function of frequency. If equations (5-2) and (5-3) are substituted in equation (5-1) there results, respectively,

$$Q_{\text{Fe-Si}} = \frac{\omega L I^2}{R_{dc} I^2 + k_1(\omega) I^{1.7}} \quad (5-4)$$

and

$$Q_{\text{Mo-Ni}} = \frac{\omega L I^2}{R_{\text{dc}} I^2 + k_2(\omega) I^{2.4}} \quad (5-5)$$

Equations (5-4) and (5-5) apply only in the region below saturation and suggest the reason why the Q of the Fe-Si core increases with current, whereas in the Mo-Ni core Q decreases. The Q calculations were conducted for a number of oriented Fe-Si cores (Arnold-AH-393, AH-34, AL-59, AH-95, AH-86, AH-31), maximized with respect to air gap, with the result that cores up to eight pounds each, costing up to \$39.00 each, could not produce the required Q characteristic at the base current levels required.

Several Mo-Ni cores could meet the characteristic, but the smallest (in terms of those offered by the Arnold Engineering Co. or Magnetics Corp.) and least expensive unit which could be made to produce the desired characteristic with a Q of 40 at 60 Hz was Arnold part no. A-218259-2. The Q characteristic of this small (2.25 inches O.D.) toroid when full wound is shown in Figure 5.1. The curve above 100 Hz is the manufacturers specification which was verified for a typical full wound core using a GR 1650A inductance bridge down to 300 Hz. The curve below 100 Hz is the extrapolation of the author. The Q at 59 Hz was checked using the circuit shown in Figure 5.2. R_c was determined by measuring the dissipation factor, D , of the 870 μf capacitor bank and using the relation

$$R_c = \frac{D}{\omega C} \quad (5-6)$$

D was measured at 60 Hz using a GR 1611-A capacitor bridge and found to be .0045. Five copper lug connections are included in the tank circuit along with thirteen feet of No. 10 AWG solid copper magnet

Quality Factor vs. Frequency for T.L.M. Inductors and 4-Mile Sections

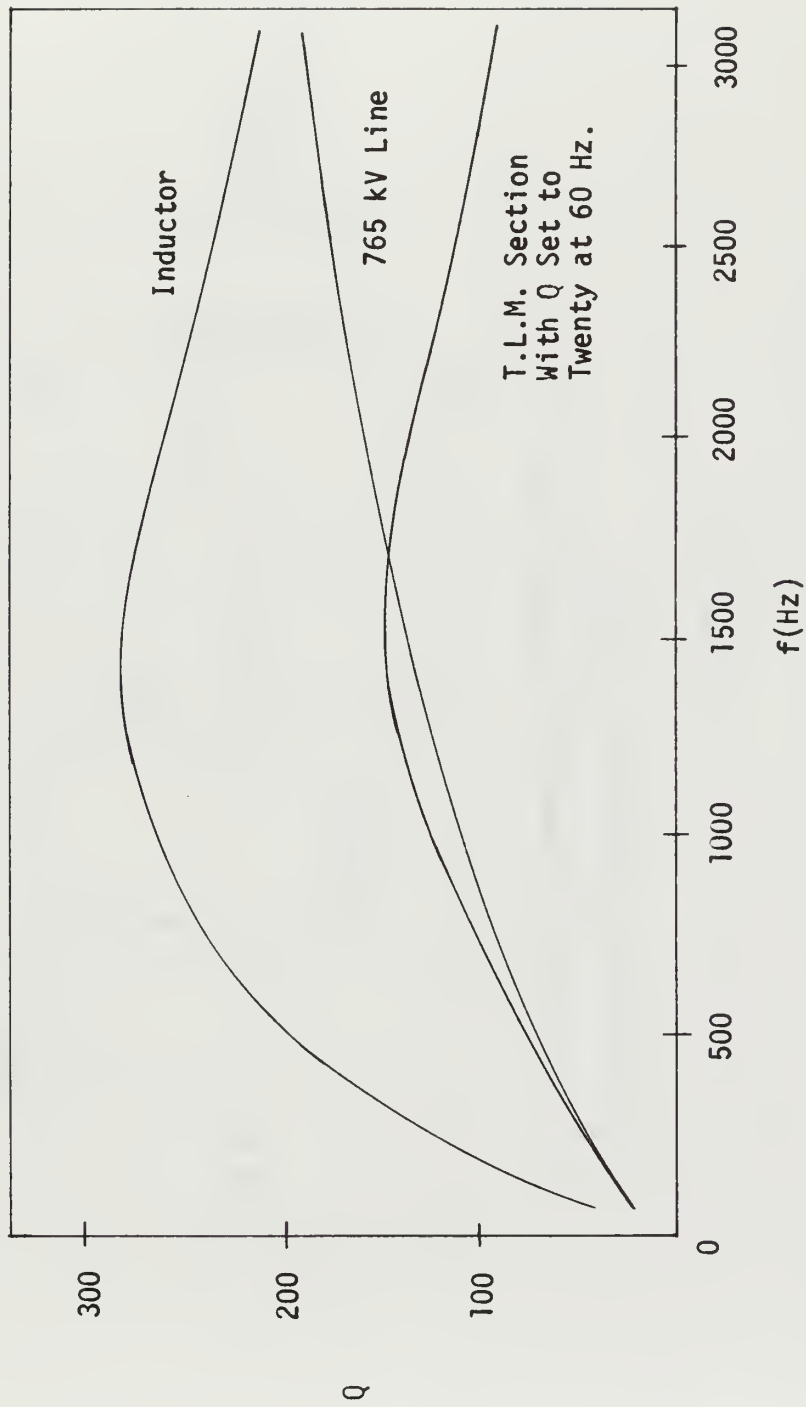


Figure 5.1

Circuit for Measuring T.L.M. Inductor Q at 59 Hz

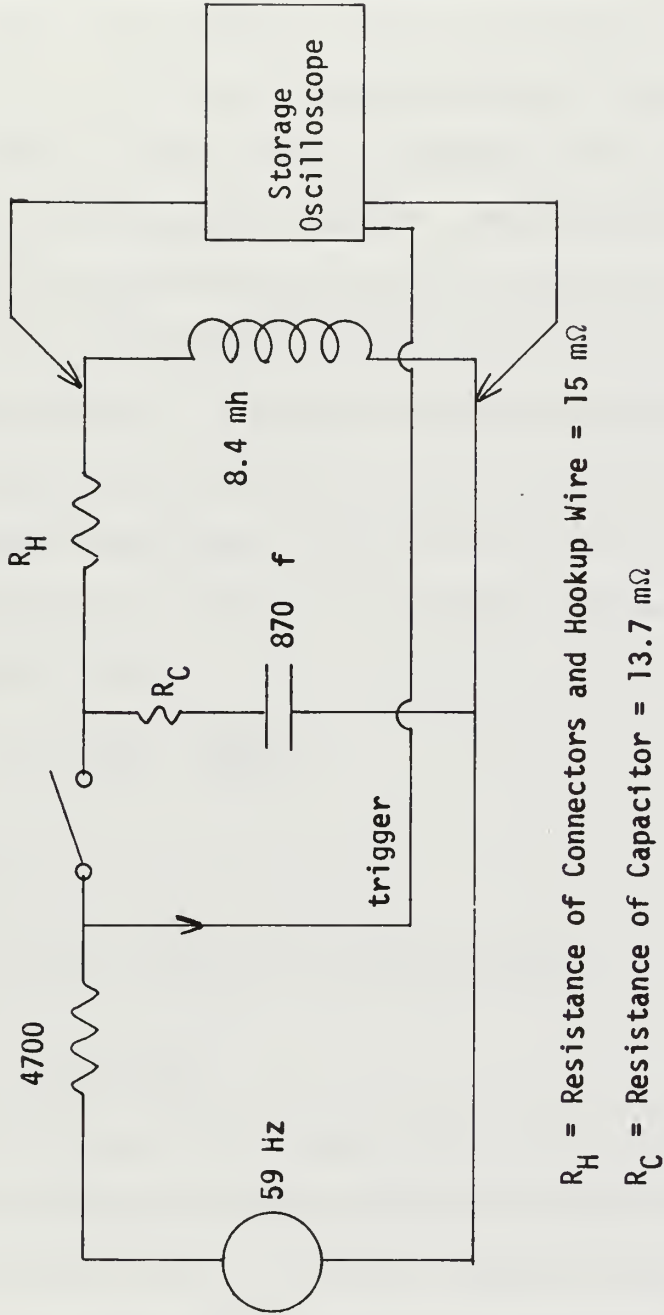


Figure 5.2

wire for a total measured resistance of 15 m Ω using a GR 1650-A resistance bridge. The voltage waveform across the inductors was observed with a Tektronix 549 storage oscilloscope. The 8.4 mh inductor shown in the figure is four 2.1 mh inductors wound on the t.l.m. cores. The tank circuit was "pumped up" using the oscillator at 59 Hz after which the switch was opened and the decay waveform observed on the storage oscilloscope. Twelve separate measurements were made covering the range of initial voltages from 0.02 v peak to 0.4 v peak - corresponding to peak initial currents in the range from 7 ma to 129 ma. In each case the time was measured for the voltage across the tank to fall to 1/e of its initial value. The times measured ranged from a low of 141 m sec at 0.4 v peak to 157 m sec below 0.1 v volt peak. The total resistance in the tank was determined from

$$R_T = \frac{2L}{\text{time}} = \frac{16.8 \text{ mh}}{\text{time}} . \quad (5-7)$$

Where

$$R_T = R_C + R_H + R_{dc} + R_{ac} . \quad (5-8)$$

Finally, Q of the inductors was determined from

$$Q = \frac{\omega L}{R_{dc} + R_{ac}} . \quad (5-9)$$

The twelve Q values at 59 Hz ranged from a low of 34.6 at .4 v peak (initial I = 129 ma), to a high of 40 for initial voltage values below 0.1 v peak (32 ma). A similar "pumping" technique was used to measure the inter-winding capacitance of a single t.l.m. inductor of 2.1 mh. A series circuit was formed of an H.P. 4204A variable frequency oscillator, a 4.7 meg Ω resistor, and a single 2.1 mh

t.l.m. inductor. The voltage across the coil was observed while the frequency was increased. The voltage peaked sharply at 300.0 KHz implying an inter-winding capacitance of 134 p.f.

The maximum inductor Q shown in Figure 5.1 occurs when the losses in the core of the inductor equal the losses in the resistance of the windings. At low frequencies the winding losses predominate; at maximum Q the two losses are equal, and for frequencies above Q_{\max} , the core losses predominate. The initial slope of the inductor Q curve is determined by winding losses which remain essentially constant in this frequency range.¹⁷ In other words - at low frequencies, the Q is determined by winding resistance alone. In fact, a t.l.m. inductor of 2.1 mh at 60 Hz has $\omega L = 800 \text{ m}\Omega$ and a winding resistance of $20\text{-m}\Omega$ indicating a Q of 40. To bring the Q of the t.l.m. section down to 20, for example, $20 \text{ m}\Omega$ of resistance is to be inserted into the inductor winding - sufficient to bring the overall Q of the section at 60 Hz down to about 20. Other, larger values of resistance would have to be added to produce Q 's less than 20 for modeling lower Q lines. The second curve in Figure 5.1 represents a typical Q characteristic of a section. Note that the section characteristic is lower, and the maximum is shifted to the right - reflecting the fact that core losses must reach a higher value before they can equal the winding losses thus producing the Q_{\max} condition. Note also that having shown a case in which the winding resistance was doubled, the initial slope of the section Q curve is about one-half of that of the inductor alone. The third curve in Figure 5.1 is that of the typical 765 kV line transferred from Figure 4.1; this curve

represents the highest Q which must be achieved by a section. It is seen that setting the Q of the section at 60 Hz to twenty results in the section Q falling below that of the line above 1700 Hz. Thus, if Q is a critical factor above 1700 Hz in a particular test on a typical 765 kV line, it will be necessary to accept higher Q at sixty Hz by setting less than 20 mΩ in series with the model inductors.

5.3 Design of Model Self Inductors

The inductance of a toroid is given by

$$L = \frac{4N^2 \mu_r A \times 10^{-9}}{D} \text{ henries,} \quad (5-10)$$

where

N = number of turns

μ_r = relative permeability

A = core cross sectional area (cm)²

D = mean core diameter (cm) .

For the Arnold core A-218259-2 used in this design, $\mu_r = 205$, so that L = 259 mh per 1000 turns on any full wound core. A full wound core is defined as one in which the winding occupies three-fourths of the available window area with a packing factor of 0.7. For any other full wound coil on the A-218259-2,

$$N = 1000 \sqrt{\frac{L}{259}} ; \quad (5-11)$$

where "L" is the desired inductance in mh. The inductances shown in Table 4.5 require the turns shown in Table 5.1. The listing of turns required in the 8-mile sections is shown in Table 5.2. To achieve the Q characteristic shown in Figure 5.1, it is necessary to have the

Table 5.1

Turns Required in 4-Mile t.l.m. Inductors

$\underline{N_a}$	$\underline{N_b}$	$\underline{N_c}$
93	91	90
94	92	91
95	93	92
96	94	93
97	95	94
98	96	95

Table 5.2

Turns Required in 8-Mile t.l.m. Inductors

$\underline{N_a}$	$\underline{N_b}$	$\underline{N_c}$
131	129	127
133	130	129
134	131	130
136	133	131
137	134	133
139	136	134

core full wound. In the case of the 4-mile inductors this works out to be No. 10 AWG, and for the 8-mile sections - No. 11 AWG. For the 4-mile sections, a nominal twenty feet of No. 10 is required at 1.0 mΩ/ft for 20 mΩ per inductor. For the 8 mile sections, a nominal twenty-eight feet of No. 11 is required at 1.26 mΩ/ft for 35 mΩ per 8-mile inductor. In Tables 5.1 and 5.2, the first five numbers

in each column are the turn numbers at which a tap must be provided.

Referring to equation (5-10) it is seen that the inductance of a toroid is independent of current if μ_r is independent of current. A graph of μ_r vs. a-c flux density taken from reference 18 is reproduced in Figure 5.3. It is seen that μ_r remains within five percent of nominal up to 4000 gauss. From basic inductor theory:

$$L = \frac{\lambda}{I} = \frac{N\phi}{I} = \frac{NBA}{I} = \frac{N\mu HA}{I} \quad (5-12)$$

$$\oint H \cdot d\ell = NI \quad (5-13)$$

$$\pi DH = NI \quad (5-14)$$

$$H = NI/\pi D \quad (5-15)$$

Substitute (5-15) into (5-12):

$$\frac{NBA}{I} = \frac{N^2 \mu A}{\pi D} \quad (5-16)$$

$$\frac{B}{I} = \frac{N\mu}{\pi D} \quad (5-17)$$

$$I = \frac{\pi DB}{N\mu} \quad (5-18)$$

In equation (5-18)

I = complex amplitude of current (amperes)

N = no. of turns in winding

D = mean diameter of core in meters = .0463 m

B = peak flux density (wb/m²)

μ = normal permeability = $\mu_r \mu_0$.

For the t.l.m. inductors at 4000 gauss:

$$B = .4 \text{ wb/m}^2$$

$$\mu = 205(4\pi \times 10^{-7}) \frac{\text{H}}{\text{m}} = 2.58 \times 10^{-4}$$

$$D = 0.0463 \text{ m}$$

$$N = 93 \text{ or } 133$$

Graph of Permeability vs. AC Flux Density for T.L.M. Inductors (Arnold PC-104D p. 60)

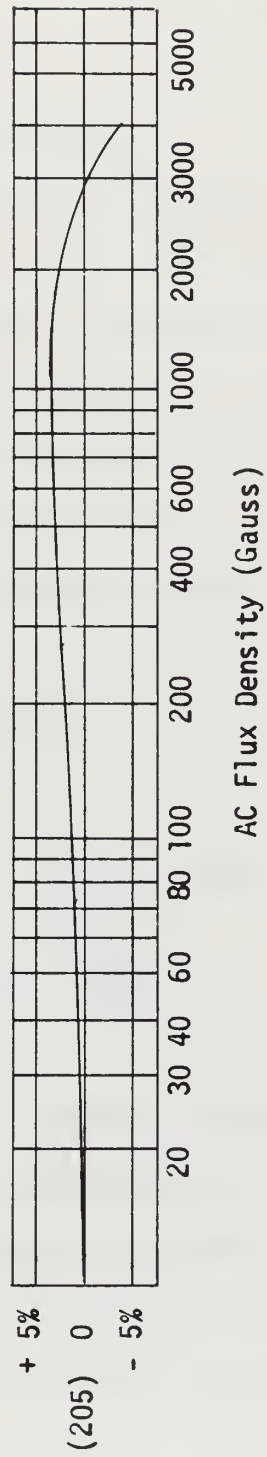


Figure 5.3

$$\begin{aligned}\text{So that } I_{\text{peak}} &= \frac{\pi DB}{133\mu} \text{ amperes} \\ &= 1.70 \text{ amperes,}\end{aligned}$$

and the inductance of the t.l.m. inductors remains within five percent of nominal up to 1.70 amperes r.m.s., or 31 p.u.

5.4 Design of Model Mutual Inductors

Figure 2.2 shows the mutual inductors $L'_{12}(L_{ab})$ and $L'_{23}(L_{bc})$ as transformers between the phases. Since the mutual inductances are small, and since there is sufficient space remaining in the windows of the self inductors, L_{ab} is wound over L_a , and L_{bc} is wound over L_b . The mutual inductances to be provided in the 4-mile sections are shown in Table 4.6; those for the 8-mile sections are simply double the values in Table 4.6. From basic mutual inductor theory (See e.g. reference 15 p.p. 178 ff) it is known that, for example,

$$L_{ab} = k \sqrt{(L_{ab})_s L_a} \quad (5-19)$$

$$L_{ab} = \frac{L'' - L'}{4}, \quad (5-20)$$

and from equation (5-11) for the model core,

$$(N_{ab})_s = 1000 \sqrt{\frac{(L_{ab})_s}{259}}. \quad (5-21)$$

Where (all in mh):

L_{ab} = mutual inductance between phases "a" and "b"

$(L_{ab})_s$ = self inductance of L_{ab}

k = coefficient of coupling between L_a and L_{ab}

L'' = measured mutual inductance when L_a and L_{ab}
are connected to reinforce.

L' = measured mutual inductance when L_a and L_{ab}
are connected to oppose.

$$(N_{ab})_s = \text{No. of turns to obtain } (L_{ab})_s, \text{ (or } L_{ab}).$$

Several tests were performed to determine k by winding six, seven, and eight turns of $(L_{ab})_s$ over an L_a inductor of 2.49 mh. Knowing the number of turns, $(L_{ab})_s$ was obtained from (5-21), and L_{ab} was obtained as indicated by (5-20). $(L_{ab})_s$ and L_{ab} were then substituted into (5-19) to determine k . Under these conditions, k for the t.l.m. inductors was found to be 0.986. Solving (5-19) for $(L_{ab})_s$ and substituting into (5-21),

$$(N_{ab})_s = 63 L_{ab} \frac{1}{L_a} . \quad (5-21)$$

With L_a taken as 2.49 mh,

$$(N_{ab})_s = 39.8 L_{ab}, \quad (5-22)$$

and the number of turns to achieve the mutual inductance values, L_{ab} , of Table 4.6 are 6, 7, 8, 9, 10, and 13, so that taps must be provided at 6, 7, 8, 9, and 10 turns. With the taps set, the self inductance corresponding to each tap can be found using equation (5-21) and then the values of L_{ab} with other values of L_a can be found using (5-19); the results are shown in Table 5.3. A similar procedure applied to L_{bc} yields,

$$(N_{bc})_s = 40.5 L_{bc}$$

and still the taps are at 6, 7, 8, 9, and 10 turns, with the 13th turn providing $L_{bc} = 0.32$ mh. A list of L_{bc} values for a 4-mile section is given in Table 5.4. In order to wind L_{ab} and L_{bc} over L_a and L_b respectively, it is necessary to use four feet of No. 12 AWG magnet wire at 1.59 mΩ/ft for an additional resistance of 6.4 mΩ in series with the phase "b" and "c" lines. A list of mutual inductance values to be built into the 8-mile sections is shown in

Tap Turns	$(L_{ab})_s$	L_{ab} with $L_a=2.49$	L_{ab} with $L_a=2.44$	L_{ab} with $L_a=2.39$	L_{ab} with $L_a=2.34$	L_{ab} with $L_a=2.29$	L_{ab} with $L_a=2.24$
6	0.0093	0.150	0.15	0.147	0.146	0.144	0.143
7	0.0127	0.176	0.175	0.173	0.171	0.169	0.167
8	0.0166	0.202	0.199	0.196	0.194	0.193	0.191
9	0.021	0.226	0.224	0.221	0.219	0.216	0.215
10	0.026	0.252	0.250	0.246	0.244	0.241	0.239
13	0.044	0.328	0.324	0.320	0.317	0.314	0.310

Table of L_{ab} and $(L_{ab})_s$ For T.L.M. 4-Mile Sections

Table 5.3

Tap Turns	$(L_{bc})_s$	L_{bc} with $L_b=2.41$	L_{bc} with $L_b=2.36$	L_{bc} with $L_b=2.31$	L_{bc} with $L_b=2.26$	L_{bc} with $L_b=2.21$	L_{bc} with $L_b=2.16$
6	0.0093	0.148	0.147	0.145	0.144	0.142	0.140
7	0.0127	0.174	0.172	0.170	0.168	0.166	0.164
8	0.0166	0.197	0.195	0.194	0.192	0.190	0.187
9	0.021	0.222	0.220	0.218	0.216	0.213	0.210
10	0.026	0.248	0.245	0.243	0.241	0.238	0.234
13	0.044	0.322	0.319	0.316	0.312	0.308	0.304

Table of L_{bc} and $(L_{bc})_s$ For T.L.M. 4-Mile Sections

Table 5.4

Table 5.5.

Table 5.5

<u>L_{ab} (mh)</u>	<u>L_{bc} (mh)</u>
0.30	0.30
0.36	0.36
0.40	0.40
0.46	0.46
0.50	0.50
0.66	0.56

Table of Mutual Inductance Values

Designed into the 8-Mile Sections

The taps to yield $(L_{ab})_g$ (using $L_a = 4.98$) are 8, 10, 11, 13, 14, and 18; taps for $(L_{bc})_g$ (using $L_b = 4.82$) are 8, 10, 11, 13, 14, and 17. The corresponding values of $(L_{ab})_s$ for the 8-mile sections are (in mh): 0.0166, 0.0259, 0.0312, 0.0435, 0.0505, and 0.0834. For $(L_{bc})_s$: 0.0166, 0.0259, 0.0312, 0.0435, 0.0505, and 0.0745. These tabulations, along with those of Tables 5.3 and 5.4 show that the self inductance of a mutual winding is negligible when compared to the self inductance of the line. In addition, Tables 5.3 and 5.4 indicate that the change in L_{ab} or L_{bc} resulting from a change in L_a or L_b over their entire range is less than five percent and therefore negligible also. In order to wind L_{ab} and L_{bc} over L_a and L_b in the 8-mile sections, it is necessary to use approximately six feet of No. 12 AWG magnet wire at 1.59 m Ω /ft for an additional resistance of 9.5 m Ω in series with the phase "b" and "c" lines.

CHAPTER 6

CAPACITOR SELECTION

6.1 Factors Determining Capacitor Selection

As discussed in detail in Chapter 4, eight diverse transmission line types were analyzed in the EPSEL Line Parameters Program, and these eight types were taken to cover the range of Typical EHV lines. The model capacitance values implied by these lines for a 4-mile model section are shown in Tables 4.4a and 4.4b. A complete listing of the capacitance parameters to be covered by both the 4 and 8-mile model sections is shown in Table 6.1. Having scaled the eight representative lines to result in a minimum inductance range, the range of each capacitance is seen to be somewhat larger. It is proposed to cover the range of each parameter of Table 6.1 with a bank of six capacitors wired and brought to the operating panel so that any combination of the six capacitors in each bank can be arranged in parallel. Thus, with one or two capacitors to set the lowest value in a range, approximately five or four capacitors are available to cover the remainder of the range. Thus there are a maximum of 120 and minimum of 24 capacitance values available to cover the range of each capacitance parameter indicated in Table 6.1. With this "dense" provision of model values it is possible to set any value in the span within a very few percent ($\sim 3\%$) if the tolerance of the capacitors is less than a few percent. It is proposed to provide a two to three percent tolerance on any capacitance selected by the operator so that the over-all capacitance provision of the model is within about 5% of the value required to model any given line. With expected transient overvoltage maxima

	C_{ab}		C_{ac}		C_{bc}		C_{an}		C_{bn}		C_{cn}	
	4 mi	8 mi	4 mi	8 mi	4 mi	8 mi	4 mi	8 mi	4 mi	8 mi	4 mi	8 mi
765 kV Horizontal	33.2	66.4	8.6	17.2	33.2	66.4	166	332	148	296	166	332
345 kV Type 41A	30.4	60.8	8.8	17.6	30.4	60.8	166	332	149	298	166	332
345 kV Type 39F	43.2	86.4	18	36	42	84	135	270	111	222	129	258
765 kV H-Special	22.8	45.6	28	56	28	56	137	274	127	254	119	238
345 kV Type H	37.3	74.6	18	36	39	78	142	284	119	238	131	262
345 kV H-Special	19.4	38.8	22	44	22.4	45	149	294	143	286	145	290
1500 kV Triangular	30.0	60.0	32.0	64.0	30.0	60.0	121	242	129	258	121	242
1500 kV Horizontal	28.1	56.2	7.3	14.6	27.7	55.4	164	328	154	308	164	328

Table of Capacitance Parameters to be Spanned by
4 and 8-Mile Model Sections (C in nf)

Table 6.1

of about four p.u., all capacitors must be capable of withstanding short duration peaks up to 500 or 600 volts. In addition to tolerance and voltage requirements the capacitors must have extremely low losses.

An indication of the dissipation factor required of the model capacitors can be obtained by a simple analysis of the "dissipation factor" of a typical line. Considering the positive sequence parameters of a type 41A line using the values given in Table 4.1,

$$C_{p.s.} = \frac{B_{p.s.}}{\omega} = .0181 \mu\text{f/mi.}$$

$$C_{p.s.} = .0725 \mu\text{f/4 mi.}$$

$$R_{p.s.} = .216 \Omega/4 \text{ mi.}$$

Using the "series model" for a lossy capacitor:

$$D_{p.s./4 \text{ mi}} = \omega R_{p.s.} C_{p.s.} \quad (6-1)$$

$$D_{p.s.} = 0.0000059/4 \text{ mi.} \quad @ 60 \text{ Hz} \quad (6-2)$$

$$D_{p.s.} = 0.0000985/4 \text{ mi.} \quad @ 1000 \text{ Hz} \quad (6-3)$$

That the values given by equations (6-2) and (6-3) are the values required of a 4-mile model section can be seen by a corresponding calculation for the model. Using Table 4.4a for the type 41A model:

$$C_{p.s.} = C_0^T + 3C_M^T = \frac{C_{an} + C_{bn} + C_{cn}}{3} + C_{ab} + C_{ac} + C_{bc}$$

$$C_{p.s.} = .230 \mu\text{f/4 mi.}$$

$$R_{p.s.} = R_S^T = \frac{R_a + R_b + R_c}{3} = .068 \Omega/4\text{mi.}$$

$$D_{p.s.} = 0.0000059/4 \text{ mi.} \quad @ 60 \text{ Hz} \quad (6-4)$$

$$D_{p.s.} = 0.0000985/4 \text{ mi.} \quad @ 1000 \text{ Hz.} \quad (6-5)$$

at low currents. The basic relation governing the Q of an inductor can be written as (for the frequencies of interest here)

$$Q = \frac{\omega L I^2}{R_{dc} I^2 + R_{ac} I^2} \quad (5-1)$$

Where

L = Inductance in henries

$\omega = 2\pi \times \text{frequency}$

R_{dc} = dc resistance of the winding (Ω)

R_{ac} = equivalent core loss resistance (Ω)

With these definitions it is seen that $R_{ac} I^2$ corresponds to both the hysteresis and eddy current losses (See reference 17 p.p. 58ff.) and thus represents the total core loss. R_{ac} , the core loss coefficient, is itself a function of current. For powdered cores the manufacturer¹⁸ provides data on R_{ac} explicitly, whereas for Fe-Si the entire term $R_{ac} I^2$ is provided. If the data provided by the manufacturer is converted to the terms of equation (5-1), it is found that for Fe-Si the core loss, W , is given by (approximately)

$$W = k_1(\omega) I^{1.7}, \quad (5-2)$$

whereas for the powdered Mo-Ni the loss is given by (approximately)

$$W = R_{ac} I^2 = k_2(\omega) I^{2.4}. \quad (5-3)$$

In equations (5-2) and (5-3), $k_1(\omega)$ and $k_2(\omega)$ are core loss constants and are a function of frequency. If equations (5-2) and (5-3) are substituted in equation (5-1) there results, respectively,

$$Q_{\text{Fe-Si}} = \frac{\omega L I^2}{R_{dc} I^2 + k_1(\omega) I^{1.7}}, \quad (5-4)$$

and

occurs primarily at low frequencies in connection with switching operations which connect the terminals of a charged line to large inductive reactances. Natural frequencies of the order of 40 Hz are known to occur under these conditions with over-all Q approaching 300.

Most capacitor manufacturers specify or test dissipation factor at 1000 Hz, so that at 1000 Hz it is possible to measure capacitance and compute resistance using either the parallel or series model of a lossy capacitor:

$$D = \omega R_s C_s = \frac{1}{\omega R_p C_p} \quad (6-6)$$

The values of R_s or R_p so obtained, however, are true only for a limited range of frequencies and cannot be used at 40 Hz. As frequency decreases toward zero the value of R_p (resistance in the parallel model) approaches the insulation resistance of the dielectric - which for polystyrene is of the order of ten million megohms for a 0.15 μf capacitor.²⁰ The dissipation factor, D, of a typical .15 μf polystyrene capacitor at 1000 Hz is given as 0.0001.²⁰ This value of D implies $R_p = 10.6$ megohms at 1000 Hz. Few materials other than Teflon or a modified polystyrene can equal this low value of D or high value of R_p at 1000 Hz. If equation (6-6) is solved for R_p in terms of ω , R_s , C_p , and C_s ($C_s \approx C_p$), and R_s set equal to 1.0 m Ω , $C_s = 0.15$ μf , and $f = 40$ Hz the value of R_p obtained is 4.4 million megohms. Thus in order to obtain R_s as low as .001 Ω , it is necessary to have R_p as high as 4.4 million megohms at 40 Hz. Little data exists on any dielectric material below 100 Hz - standard reference works²¹ supply no data below 100 Hz on any material and give no information vs. frequency on polystyrene. In an effort to obtain an estimate of R_p for the 0.15 μf polystyrene capacitor

at 40 Hz, it was assumed that R_p remains constant at the 10.6 megohm value down to 100 Hz and then rises linearly to 10 million megohms at d.c. This procedure gives R_p as 6 million megohms at 40 Hz. (This is a conservative estimate in the opinion of the author.) No material less costly than polystyrene can approach within an order of magnitude of this value. Polystyrene capacitors are therefore selected to form the "base" capacitance of each capacitor bank in the model.

6.2 Capacitors Selected for Model Sections

Since the polystyrene capacitors conservatively (but not by orders of magnitude) meet all line requirements, a compromise in favor of lower cost is made in selecting the trimming capacitors in each bank. Thus, while polystyrene capacitors will be made to provide 80 percent (approximately) of any capacitor value selectable by the operator, the remaining 20 percent (approximately) is to be made up of lower cost mylar or silvered mica capacitors. The latter capacitors have losses ten to fifty times higher than the polystyrene but they constitute only ten to twenty percent of a selected capacitor value and so should not appreciably lower the high quality provided by the polystyrene base capacitors. The severe low-loss constraint applies mainly to the 765 kV line, so that the polystyrene capacitors in each bank are selected so that for the 765 kV case they will constitute no less than 90% of the required capacitance of a 4-mile section. The polystyrene capacitors selected for the t.l.m. are Arco Manufacturing Co., type PJ, 400 VDC, $\pm 2\%$, tubular capacitors. The 400 V units were judged adequate since each capacitor receives a minimum of two sixteen hour burn-in periods with 300 percent of rated voltage applied at 85°C.²⁰ The mylar capacitors are Cornell Dubilier Co., type WMF6,

Capacitor Type	C _{ab}		C _{ac}		C _{bc}		C _{an}		C _{bn}		C _{cn}	
	4 mi	8 mi	4 mi	8 mi	4 mi	8 mi	4 mi	8 mi	4 mi	8 mi	4 mi	8 mi
Polystyrene	22	33	15	27	22	33	120	220	100	220	120	220
Polystyrene	15	22	8.2	15	15	22	33	82	47	68	33	82
Polystyrene	8.2	22	4.7	8.2	8.2	22	*	47	22	33	*	47
Mylar	4.7	6.8	2.2	4.7	4.7	6.8	22	33	10	22	22	33
Mylar	2.2	3.3	*	2.2	2.2	3.3	10	22	4.7	10	10	22
Mylar	1.0	2.2	*	1.0	1.0	2.2	4.7	10	2.2	5	4.7	10
Mylar	*	*	*	*	*	*	2.2	*	*	*	2.2	*
Silvered Mica	*	*	.68	*	*	*	*	*	*	*	*	*
Silvered Mica	*	*	.33	*	*	*	*	*	*	*	*	*

Table of Capacitor Values Provided in T.L.M. Capacitor Banks
(Capacitances in nf)

Table 6.2

600 VDC, ± 10 percent, tubular capacitors. Two small capacitance values below the range of standard mylar sizes (330 pf and 680 pf) are Cornell Dubilier Co., type CD19FD, silvered mica, 500 VDC, $\pm 5\%$. The capacitor types and sizes selected to span each capacitance parameter (the capacitor banks) are shown in Table 6.2.

CHAPTER 7

RESISTANCE AND LOSS CONSIDERATIONS

7.1 Over-all Q Considerations

As discussed in Chapters 4 and 5, the Q requirements of this t.l.m. are dictated by the need to model the 765 kV line. This constraint is particularly severe in the 4-mile model sections since connection resistance is expected to take up any margin provided by designing the inductors with double the required Q at 60 Hz. In Chapter 4 it is indicated that the positive sequence Q of a typical 765 kV line is twenty. The resistance required in each phase to achieve this result is shown in Table 4.4a - 37 m Ω in phases "a" and "c" and 43 m Ω in phase "b". As discussed in Chapter 5, 20 m Ω is "provided" in each phase by the resistance of the wire to wind the self inductors L_a , L_b , and L_c . An additional 6 m Ω is provided in phases "b" and "c" due to the fact that these phases contain the resistance of the windings for L_{ab} and L_{bc} respectively. (Actually, L_{ab} and L_{ac} for the typical 765 kV line are provided by the 7-turn-tap so that the resistance added by the L_{ab} and L_{bc} windings will be approximately 4 m Ω in the 4-mile sections. The operating panel resistance to be provided at this point in the accounting is 17 m Ω in phase "a", 19 m Ω in phase "b", and 13 m Ω in phase "c". But connection resistance has not yet been accounted for in these figures.

In a typical model set up (See Chapter 8), six to eight banana jack connections will be made in series in each section from input to output, so that the resistance of these must be accounted for. The jacks selected for this design are E.F. Johnson Co., standard banana

jack, cadmium plated insert, catalog no. 108-0900-001. The corresponding plug is E.F. Johnson Co., standard plug, catalog no. 108-0300-001. Six of these jacks and plugs were connected in series as shown in Figure 7.1. Sixteen inches of solid, no. 14 AWG, copper bus bar wire was used, and all connections were heavily soldered. The total resistance was measured at $12 \text{ m}\Omega$ with the GR 1650A resistance bridge. The resistance of the no. 14 wire is $3.3 \text{ m}\Omega$ so that the resistance of each connection averages to about $1.5 \text{ m}\Omega$. All plugs and jacks were new, clean, tight fitting, and all connections were made and remade several times - always with the same result. The resistance accounting to this point is:

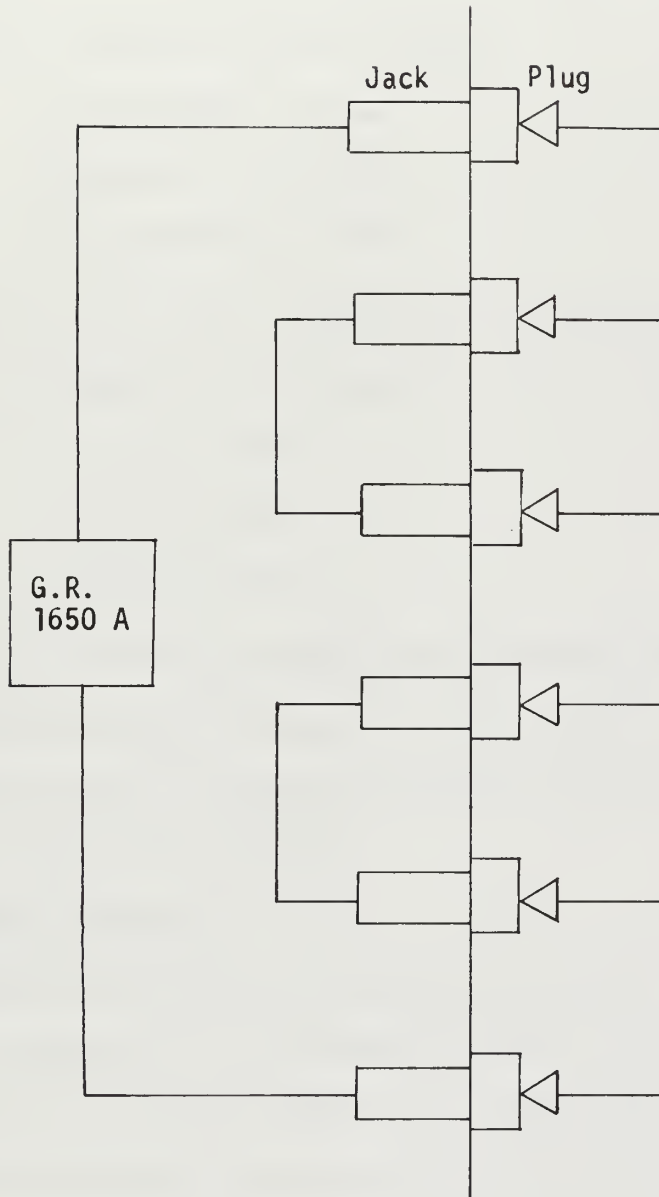
$R_a = 8 \text{ m}\Omega$, $R_b = 5 \text{ m}\Omega$, $R_c = 1 \text{ m}\Omega$. In other words, at this point the resistance values required at the front panel to bring the section positive sequence Q down to twenty at 60 Hz are the values cited just above. Each 4-mile section; exclusive of external hookup wire, but including operator panel connector resistance is seen to have built into it,

$$R_a(\text{intrinsic})_4 \approx 29 \text{ m}\Omega \quad (7-1)$$

$$R_b(\text{intrinsic})_4 \approx 38 \text{ m}\Omega \quad (7-2)$$

$$R_c(\text{intrinsic})_4 \approx 38 \text{ m}\Omega \quad (7-3)$$

To provide an exact positive sequence Q of twenty at 60 Hz, it is necessary to provide for operator selection; $R_a = 8 \text{ m}\Omega$, $R_b = 5 \text{ m}\Omega$, and $R_c = 1 \text{ m}\Omega$. As pointed out in Chapter 5 in connection with Figure 5.1 however; setting the Q to twenty at 60 Hz for a 765 kV line model will result in the model Q falling below line Q above about 1700 Hz. Thus, it may be desirable under certain circumstances to set



Test Circuit for Measuring Resistance
of Banana Jacks and Plugs

Figure 7.1

Q at 60 Hz slightly above twenty to ensure that the model Q remains above line Q up to 3060 Hz.

An accounting procedure identical to that above applied to the 8-mile model sections gives the results,

$$R_a(\text{intrinsic})_8 \approx 44 \text{ m}\Omega \quad (7-4)$$

$$R_b(\text{intrinsic})_8 \approx 57 \text{ m}\Omega \quad (7-5)$$

$$R_c(\text{intrinsic})_8 \approx 57 \text{ m}\Omega \quad (7-6)$$

The values of R_a , R_b , and R_c required in the 8-mile sections to model a 765 kV line are (doubling the appropriate values in Table 4.4a):

$$(R_a)_{765} \approx 74 \text{ m}\Omega \quad (7-7)$$

$$(R_b)_{765} \approx 86 \text{ m}\Omega \quad (7-8)$$

$$(R_c)_{765} \approx 74 \text{ m}\Omega \quad (7-9)$$

It is seen that the 8-mile sections have considerably more margin than the 4-mile sections and, in fact, using the intrinsic values of equations (7-4)-(7-6), the positive sequence Q of the 8-mile sections can be set as high as 31 at 60 Hz.

7.2 Resistance Selection

Referring to Table 4.2 (excluding the 1500 kV lines) the values of positive sequence Q to be provided are seen to range from about eight to twenty. To achieve the Q values lower than twenty, resistance values must be provided at the operating panel for insertion with the intrinsic resistance of the section. For the 4-mile sections, the lowest resistance value to be made available is clearly zero since this is the required value to ensure positive-sequence Q's just over twenty. For the 8-mile sections a similar zero base will be provided since it would simply not make sense to deny the operator the selection

of positive sequences Q's to thirty should the occasion arise. A listing of Q values to be provided for each phase is shown in Table 7-1.

Table 7.1

4-Mile Section			8-Mile Section		
Q_a	Q_b	Q_c	Q_a	Q_b	Q_c
30	22	21	40	30	28
25	19	18	34	25	24
20	16	15	28	20	20
15	13	12	22	16	16
12	11	10	16	12	11
10	9	8	11	9	8

Table of Q Values Provided
in the T.L.M. Sections

The operating panel resistance values to achieve the Q's shown in Table 7.1 are shown in Table 7.2.

Table 7.2

4-Mile Sections			8-Mile Sections		
R_a	R_b	R_c	R_a	R_b	R_c
0	0	0	0	0	0
6	7	8	8	11	12
15	15	17	19	28	25
30	27	30	36	49	46
44	40	43	66	85	92
59	67	64	116	132	147

Table of Operating Panel Resistance Values
Corresponding to Q's of Table 7.1 (R in $m\Omega$)

The resistance values indicated in Table 7.2 were obtained using

$$R_i = \frac{\omega(L_i)_{4,8}}{Q_j} - R_i(\text{intrinsic}) \quad (7-10)$$

$$(L_a)_4 = 2.34 \text{ mh}, (L_b)_4 = 2.26 \text{ mh}, (L_c)_4 = 2.18 \text{ mh}$$

$$(L_a)_8 = 4.68 \text{ mh}, (L_b)_8 = 4.52 \text{ mh}, (L_c)_8 = 4.36 \text{ mh}$$

$i = a, b, c$ for each section length

Q_j is the corresponding Q value from Table 7.1.

It is seen in practice, rather than setting positive sequence Q per se, the Q of each phase is set individually using Tables 4.4, 7.1, and 7.2.

The resistance indicated in Table 7.2 is achieved by connecting resistances in series so that each indicated value is the sum of the resistances required to form each of the preceeding resistors. The actual resistors required to obtain the operating panel values indicated in Table 7.2 are shown in Table 7.3.

Table 7.3

4-Mile Sections			8-Mile Sections		
R_a 's	R_b 's	R_c 's	R_a 's	R_b 's	R_c 's
6	7	8	8	11	12
9	8	9	11	17	13
15	12	13	17	21	21
14	13	13	30	36	46
15	27	21	50	47	55

Table of Resistors in the T.L.M. Sections

The resistors indicated in Table 7.3 are to be "manufactured" by cutting appropriate lengths of nickel or copper-nickel alloy ("cupron")

resistance wire. A very large selection of resistance wire sizes and types are available from the Driver Harris Co. of Newark, N.J., a type particularly suited to the smaller resistors above is the company's 0.035" diameter nickel wire of 0.045 ohms per foot. For the larger resistors no. 20 AWG "Cupron" (copper-nickel) wire with a nominal resistance of 0.287 ohms per foot can be used. The latter wire can safely carry a direct current of three amperes indefinitely but is hot to touch at this current level. Three rms amperes is far in excess of that required to simulate the most severe faults, so that no. 20 AWG resistance wire should be adequate for this t.l.m.

CHAPTER 8

MODEL PHYSICAL CONSTRUCTION

8.1 Electrical Construction of a Typical Section

As discussed in Chapter 4, this t.l.m. consists of thirty 4-mile sections and thirty-five eight mile sections. A simplified schematic diagram of the wiring of a typical section is shown in Figure 8.1 and is the same for both the 4-mile and 8-mile sections. The component values are not indicated since they are different for the two section types, but the required values can be taken from the tables of Chapters 5, 6, and 7. In wiring each section, all hookup wire in a direct path from input to output is No. 10-stranded, tinned, copper wire. Capacitor hookup is effected with No. 16 stranded copper wire. All connections are soldered.

8.2 T.L.M. Physical Construction

Each t.l.m. section is constructed on the chassis shown in Figure 8.2. The sixty-five chassis are made of plexiglass of the sizes indicated - the operator's panel is of black plexiglass. The layout of the operator's panel is shown in Figure 8.3. The jacks are color coded by "phase" and the circuit diagram is painted by a silkscreen stenciling process. Each of the sixty five chassis is assembled in a larger console as shown in Figure 8.4. The chassis slide into the console on rails and are secured with screws through the operating panel. The chassis are inserted into the console from both "front" and "rear", so that twenty-four sections are accommodated per console. Three consoles such as that shown in Figure 8.4 are required with a fourth "half-console" for the output section and terminal equipment.

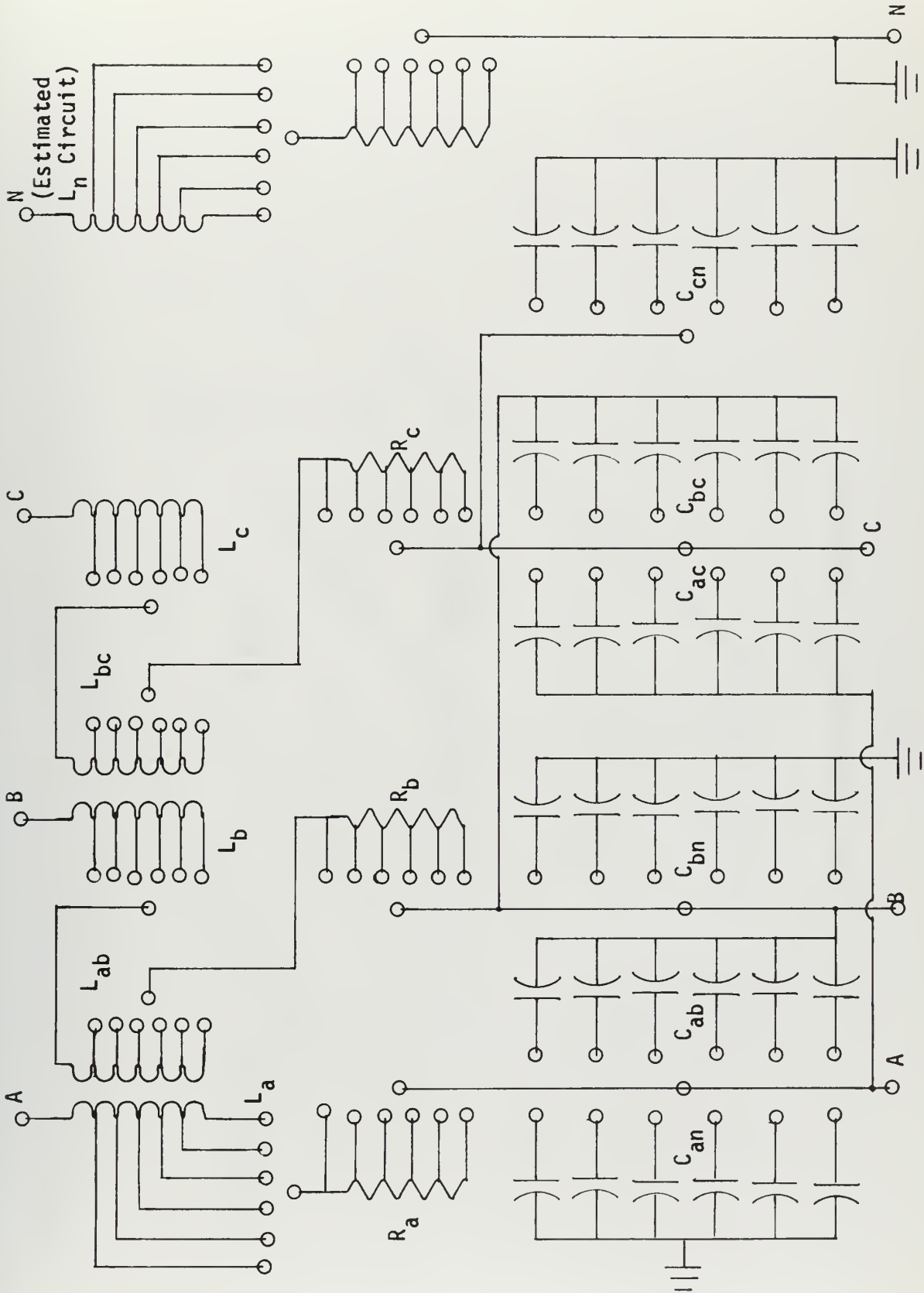
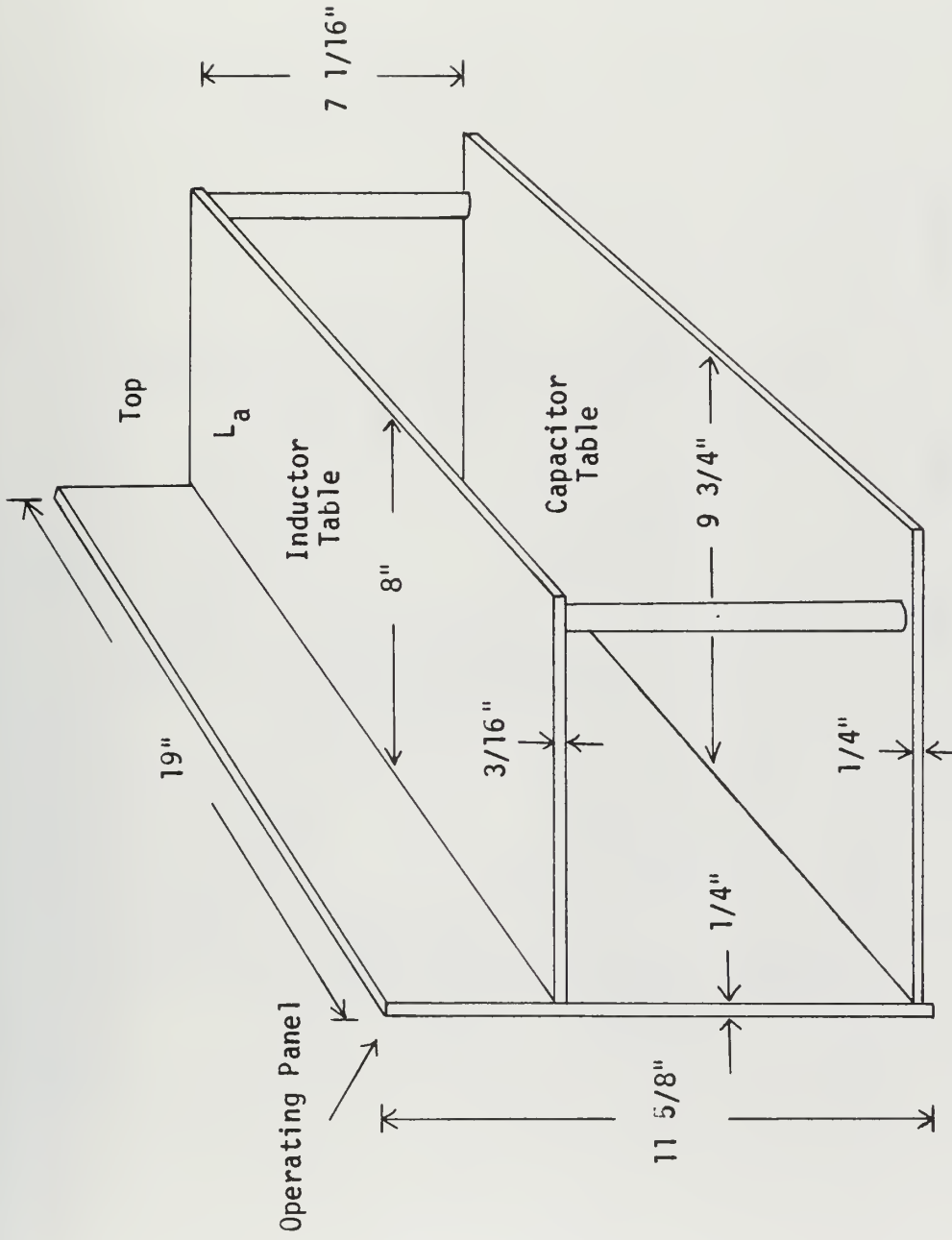
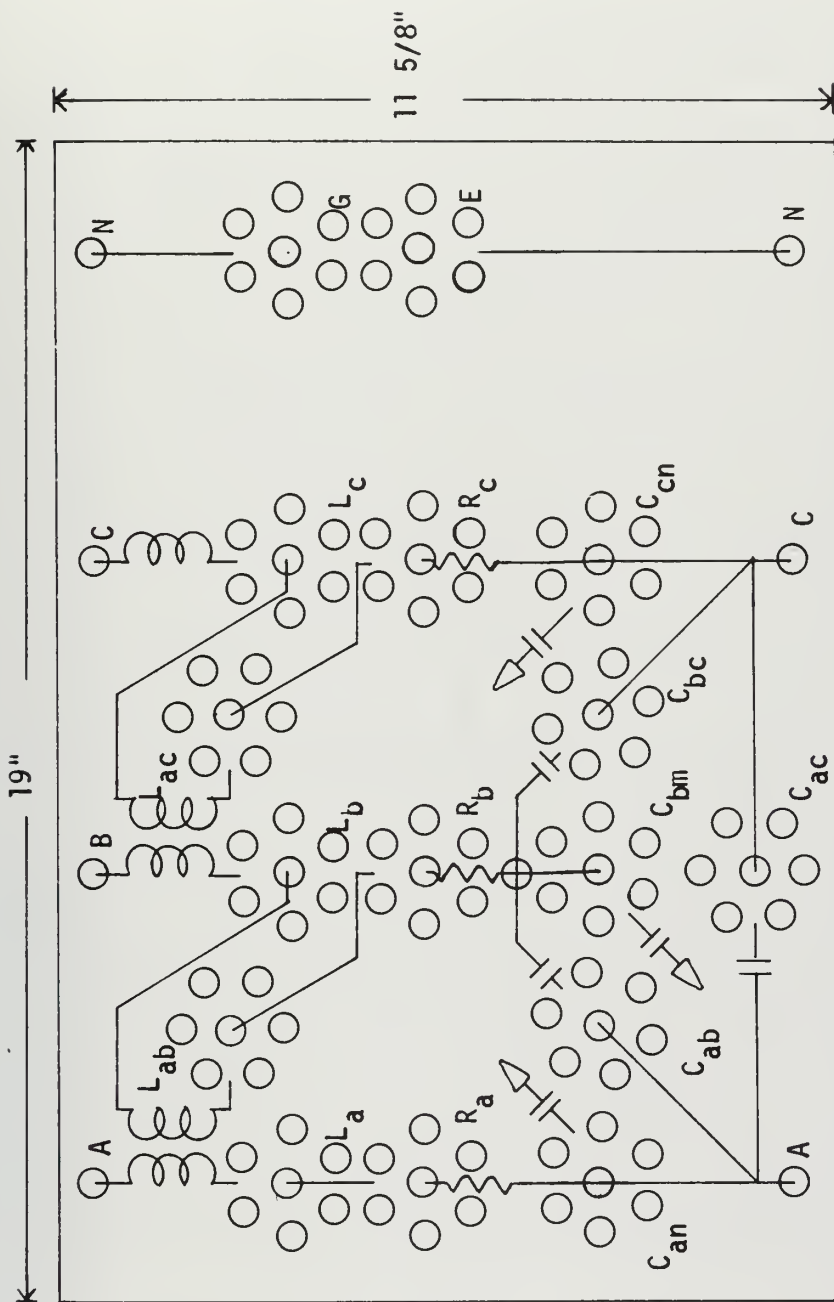


Figure 8.1



Typical Section Chassis Construction

Figure 8.2



Operating Panel of Typical T.L.M. Section

Figure 8.3

T.L.M. Console

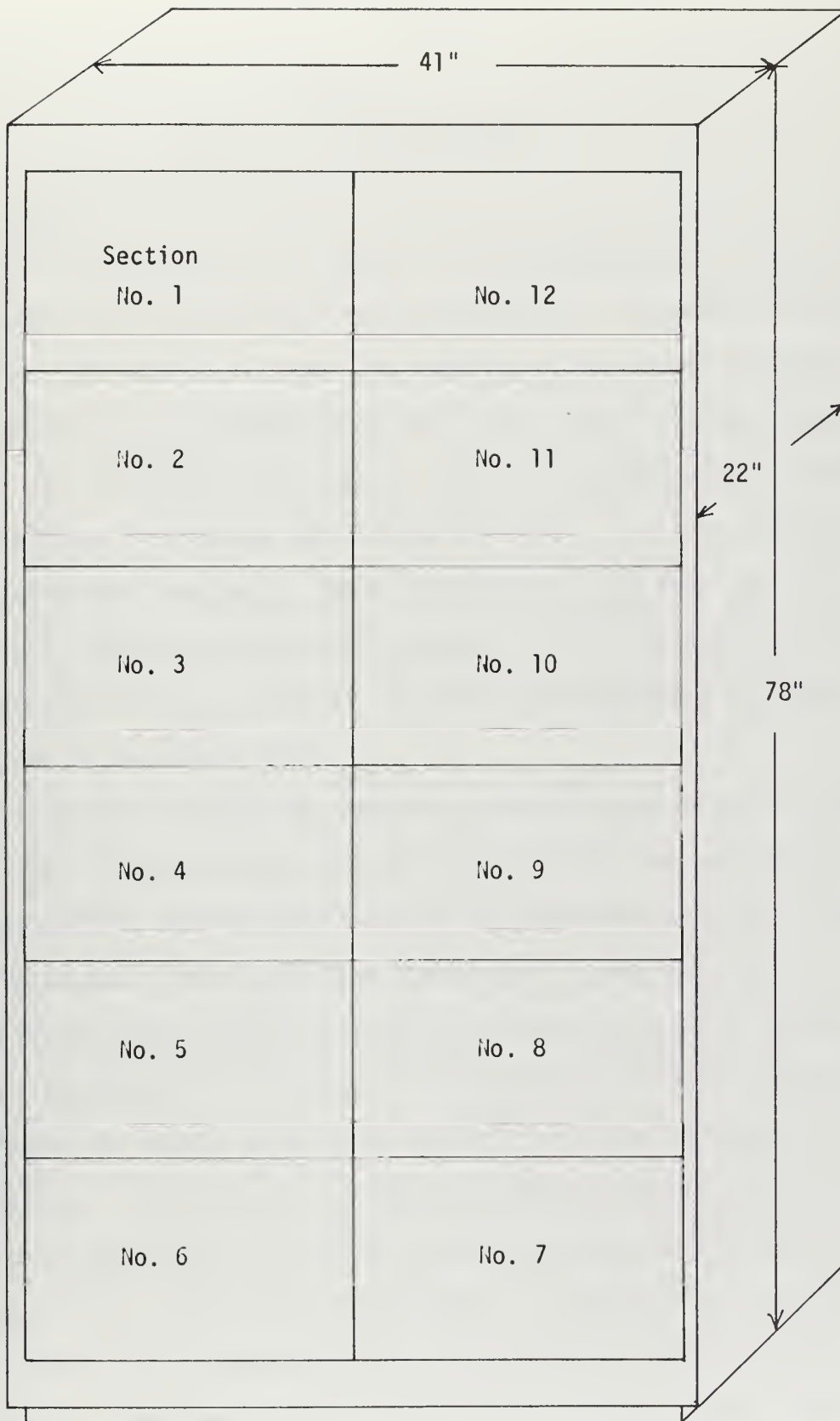


Figure 8.4

CHAPTER 9

SUMMARY AND RECOMMENDATIONS

9.1 Summary

This report presents in detail the considerations in the design of a transmission line model for use in the M.I.T. Transmission System Simulator. The design includes the modeling of the inductive effects of non-transposition by incorporating two linear mutual inductors between phases. The inter-phase resistance effects are approximated by assuming that the three inter-phase resistances are equal. A circuit diagram of one three-phase L-section is shown in Figures 2.2 and 8.1. Note that the mutual inductors are physically wound on the respective self inductor core and that the return circuit is provisional pending a complete design due in September, 1971.

In order to deduce the number of sections required for the model and establish a quantitative measure for predicting the performance of model types with various terminations, the pole error analysis of Chapter 3 was developed. This analysis is based upon a comparison of the poles of the driving point impedance of actual lines with those of proposed models. Solutions for the poles of π and L-section models were obtained by computer for models up to forty sections with open and short circuited terminations. The pole error curves of Chapter 3 show in quantitative terms the convergence of the poles of various models toward those of continuous lines with similar terminations. A technique is outlined (See Figure 3.11) in which the pole error curves are used to deduce the number of sections required to meet any arbitrary accuracy specification. The specification set for the M.I.T. model is that the

error in the pole frequency of the model shall be within five percent of the frequency of the corresponding actual pole over the range from sixty to 3060 Hz for line lengths of sixty to four hundred miles for both open and short circuited terminations. This criteria led to the decision to construct thirty four-mile model sections and thirty-five eight-mile sections ("L" configuration).

In Chapter 4 parameter data for eight representative EHV line configuration types are presented in order to deduce the parameter values required in the four and eight-mile model sections. Several scaling techniques are suggested for scaling the parameters of the diverse line types to the parameters provided in the model. Careful scaling suggests that only a **narrow** range of component values need be provided for each parameter in the model. In the M.I.T. design, six values are provided for each of the sixteen parameters to be modeled.

The quality factor (Q) of typical EHV lines are seen (Figure 4.1) to vary markedly with frequency in the range from sixty to 3060 Hz. Positive sequence Q increases monotonically to over 175 for the highest Q lines studied, and zero-sequence Q maximizes near 1000 Hz and generally remains constant up to 3060 Hz. The requirement to model these Q characteristics is a major factor in the design of all model inductors and in the selection of all model capacitors. The positive sequence Q characteristics is achieved by the use of molybdenum-nickel toroids for all phase inductors. In fact, the model inductors have an intrinsic Q characteristic approximately double the value required to model the highest Q EHV lines in operation. Preliminary plans for modeling the return path or zero-sequence inductance and

Q suggest a separate modeling of the ground wire path and earth return path - the final design is to be completed by September, 1971.

A careful account of wire and connector resistance shows that for the section lengths chosen, every milliohm significantly reduces the intrinsic Q provided by the model inductors. To avoid excessive losses and provide for operator adjustment of Q, all connections are soldered, and all wire on a direct path from input to output is no. 10 AWG hook up wire. To avoid further losses, and to model the condition of a charged line isolated with a high Q reactor at its terminals, extremely low loss polystyrene capacitors are incorporated into each t.l.m. capacitor bank. Approximately eighty-five percent of any model capacitance parameter selectable by the operator is low loss polystyrene in parallel with approximately fifteen percent additional "trimming" capacity provided by mylar units. Overall capacitance tolerance in the t.l.m. is within five percent of any value selected. Six capacitors are provided for each capacitance parameter and all capacitors are available for operator connection into any desired configuration.

The final result for the M.I.T. t.l.m. is a total of sixty-five L-sections for modeling line lengths to 400 miles. Average Q in the four-mile model sections is a maximum of 24 at 60 Hz; the maximum average in the eight mile sections is 32. All capacitance and inductance selection within the range of a parameter is within five percent of any desired value. A similar five percent tolerance is planned for the return path inductance and Q. Q values less than the

maxima given above are obtained by the insertion of appropriate resistors provided in each section.

9.2 Recommendations

The design of this t.l.m. has progressed in parallel with its actual construction and component procurement. This was attempted in view of a master's thesis time constraint. The basic scale factor between the model and lines was selected in order to make the t.l.m. compatible with existing laboratory equipment. In fact, the t.l.m. ultimately will represent an investment several times the cost of the TSS transformer which dictated the scale ratio. This scale ratio (the 0.355 for the 765 kV line) was selected and found acceptable primarily on the basis that it resulted in a feasible, low cost inductor core without scaling the capacitors out of the range of economical values provided "off the shelf" by manufacturers. Not until after the cores had been purchased was the significance of capacitor dissipation factor fully appreciated. Although the required capacitor values are well within the range of normal capacitors, they are among the highest and most costly polystyrene units. The result was the requirement to purchase capacitors nearly three times the cost of inductor cores. Polystyrene capacitors are required regardless of what reasonable scale ratio is selected, but it is suggested that perhaps a better cost trade off could have been achieved had the TSS transformers been redesigned to permit a scale ratio closer to unity. This would require larger, more expensive, cores for the t.l.m. inductors but would significantly reduce the size of capacitors required. The larger polystyrene units are very expensive, so that even a small reduction in values required could result

in considerable savings. This savings could be directed toward purchasing a better (larger) inductor core permitting even more margin in Q by making the connector resistance a smaller fraction of the total resistance of the section. It is recommended that, should a similar project be undertaken in the future, the entire design should be completed in every detail, a prototype section constructed, and a cost analysis completed before a single large scale purchase is made. With a better cost trade off between t.l.m. components and a more complete view of overall t.l.m. investment compared to other TSS components, a more informed decision can be made as to what part of the TSS should be scaled to achieve compatibility between them all.

Concerning the pole error analysis of Chapter 3, several comments seem appropriate. It should be noted that none of the pole error analysis was carried to more than 39 sections. This is due to the fact that none of the root subroutines available was able to generate stable solutions beyond this point. Several algebraic root finding methods were used in an effort to obtain solutions above the 40th degree, but none succeeded. This is believed due to the fact that all the roots are in the region between minus one and plus one, and as the degree of the polynomial gets higher the roots tend to crowd near the extremes. Scaling of the coefficients of the polynomials was attempted but this technique resulted in instabilities at even lower degree. Three of the four subroutines used in this problem are available in the IBM System/360 Scientific Subroutine Package (360-CM-03X version III) using three different (but algebraic) techniques. The subroutine POLRT uses the

Newton-Raphson iterative technique and is explicitly limited to polynomials of degree thirty-six or less. The subroutine DPRQD uses the quotient-difference-displacement method - this routine generally became unstable at about the 30th degree for this problem. The DPRBM subroutine uses the Bairstow iterative method of quadratic factorization; this routine was the most stable of the four methods - giving stable solutions through degree thirty-nine. A fourth subroutine, ROOT 1, using Muller's method (written by the computation group at M.I.T.) became unstable at about degree twenty-four. The Bairstow method is the routine selected for all the programs of Appendix D. No extensive effort was made to determine exactly why the subroutines became unstable, nor were more elegant matrix methods attempted. It was felt that solutions to degree forty gave information sufficient for the purposes of this design, so that no further effort was expended in this direction. Nevertheless the instability problem is at least of academic value and worth further study.

APPENDICES

APPENDIX A

MODEL TRANSFORMATIONS

A.1 Equations of the General Non-Transposed Model

In the general, non-transposed model of Figure 2.1 Chapter 2, the differential equations relating the line to ground voltages and the currents are given by Kirchoff's Voltage Law (The Voltage Law):

$$-\frac{\partial V_a}{\partial z} = (R_{11}+R_{00})I_a + (L_{11}+L_{00})\frac{\partial I_a}{\partial t} + R_{00}I_b + (L_{12}+L_{00})\frac{\partial I_b}{\partial t} + R_{00}I_c + (L_{13}+L_{00})\frac{\partial I_c}{\partial t} \quad (A-1a)$$

$$-\frac{\partial V_b}{\partial z} = R_{00}I_a + (L_{12}+L_{00})\frac{\partial I_a}{\partial t} + (R_{22}+R_{00})I_b + (L_{22}+L_{00})\frac{\partial I_b}{\partial t} + R_{00}I_c + (L_{23}+L_{00})\frac{\partial I_c}{\partial t} \quad (A-1b)$$

$$-\frac{\partial V_c}{\partial z} = R_{00}I_a + (L_{13}+L_{00})\frac{\partial I_a}{\partial t} + R_{00}I_b + (L_{23}+L_{00})\frac{\partial I_b}{\partial t} + (R_{33}+R_{00})I_c + (L_{33}+L_{00})\frac{\partial I_c}{\partial t} \quad (A-1c)$$

Similarly, the currents can be related to the line to ground voltages by Kirchoff's Current Law (The Current Law):

$$-\frac{\partial I_a}{\partial z} = (C_{10}+C_{12}+C_{13})\frac{\partial V_a}{\partial t} - C_{12}\frac{\partial V_b}{\partial t} - C_{13}\frac{\partial V_c}{\partial t} \quad (A-2a)$$

$$-\frac{\partial I_b}{\partial z} = -C_{12}\frac{\partial V_a}{\partial t} + (C_{20}+C_{12}+C_{23})\frac{\partial V_b}{\partial t} - C_{23}\frac{\partial V_c}{\partial t} \quad (A-2b)$$

$$-\frac{\partial I_c}{\partial z} = -C_{13}\frac{\partial V_a}{\partial t} - C_{23}\frac{\partial V_b}{\partial t} + (C_{30}+C_{13}+C_{23})\frac{\partial V_c}{\partial t} \quad (A-2c)$$

A.2 Transformation of the General Non-Transposed Model to a "Balanced Mutual" Model

Equations (A-1) describing Figure 2.1 can be transformed to a set describing Figure 2.2 using simple algebra. Let $I_a+I_b+I_c = 3I_0$ and add and subtract

$$L_{13} \frac{\partial I_a}{\partial t} + L_{13} \frac{\partial I_b}{\partial t} \quad \text{from eq. (A-1a)}$$

$$L_{13} \frac{\partial I_a}{\partial t} + L_{13} \frac{\partial I_b}{\partial t} + L_{13} \frac{\partial I_c}{\partial t} \quad \text{from eq. (A-1b)}$$

$$\text{and} \quad L_{13} \frac{\partial I_b}{\partial t} + L_{13} \frac{\partial I_c}{\partial t} \quad \text{from eq. (A-1c).}$$

The result is

$$-\frac{\partial V_a}{\partial z} = R_{11}I_a + (L_{11}-L_{13}) \frac{\partial I_a}{\partial t} + (L_{12}-L_{13}) \frac{\partial I_b}{\partial t} + 3R_{00}I_0 + 3(L_{00}+L_{13}) \frac{\partial I_0}{\partial t} \quad (\text{A-3a})$$

$$-\frac{\partial V_b}{\partial z} = (L_{12}-L_{13}) \frac{\partial I_a}{\partial t} + R_{22}I_b + (L_{22}-L_{13}) \frac{\partial I_b}{\partial t} + (L_{23}-L_{13}) \frac{\partial I_c}{\partial t} + 3R_{00}I_0 + 3(L_{00}+L_{13}) \frac{\partial I_0}{\partial t} \quad (\text{A-3b})$$

$$-\frac{\partial V_c}{\partial z} = (L_{23}-L_{13}) \frac{\partial I_a}{\partial t} + R_{33}I_c + (L_{33}+L_{13}) \frac{\partial I_c}{\partial t} + 3R_{00}I_0 + 3(L_{00}+L_{13}) \frac{\partial I_0}{\partial t} \quad (\text{A-3c})$$

Equations (A-2) and (A-3) are the relations describing the "balanced mutual" model of Figure 2.2 with:

$$\begin{array}{lll} L'_{11} = L_{11} - L_{13} & L'_{12} = L_{12} - L_{13} & C'_{10} = C_{10} \\ L'_{22} = L_{22} - L_{13} & L'_{23} = L_{23} - L_{13} & C'_{20} = C_{20} \\ L'_{33} = L_{33} - L_{13} & L'_{00} = L_{00} + L_{13} & C'_{30} = C_{30} \\ C'_{12} = C_{12} & R'_{11} = R_{11} & R'_{00} = R_{00} \\ C'_{13} = C_{13} & R'_{22} = R_{22} & \\ C'_{23} = C_{23} & R'_{33} = R_{33} & \end{array} \quad (\text{A-4})$$

A.3 Transformation of the General Non-Transposed Model to a Transposed Model

One transposition cycle of a transposed three-phase transmission line can be visualized physically as shown in Figure A.1. In the

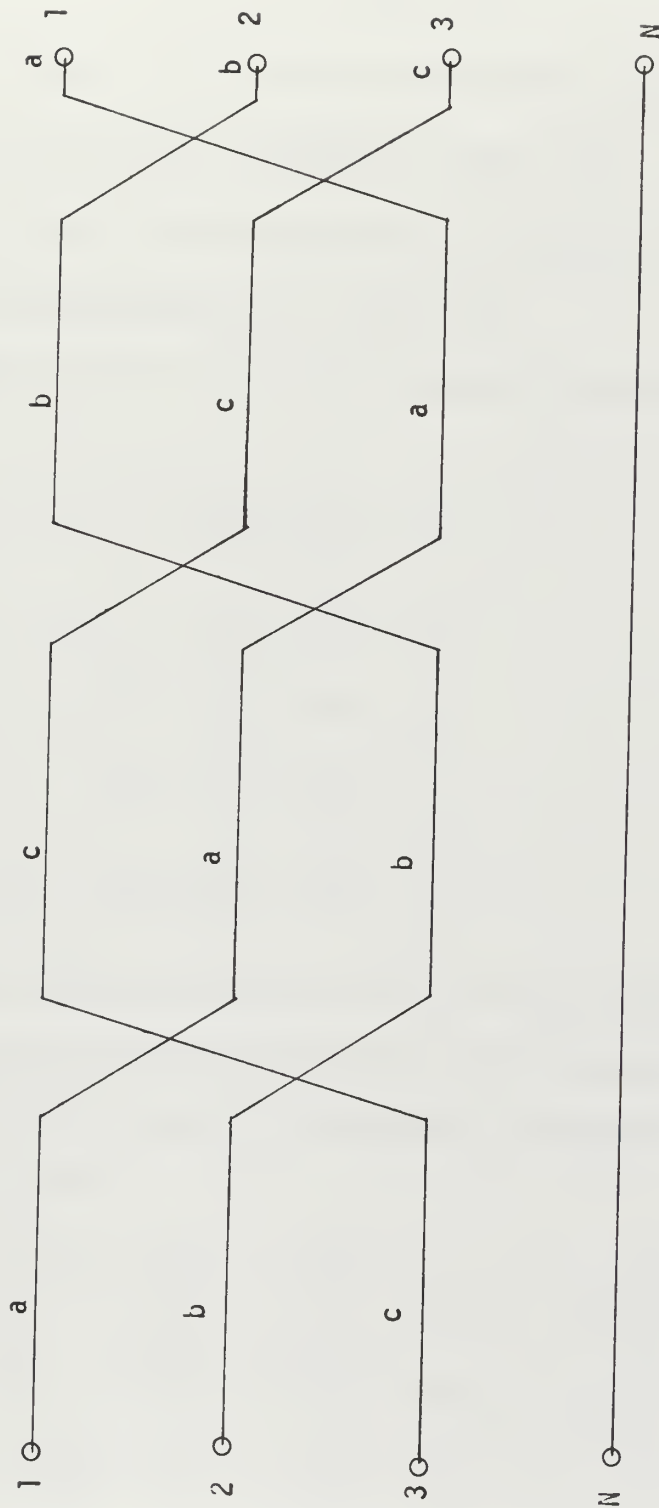


Illustration of One Cycle of Transposed Line

Figure A.1

transposed line let:

$$L_{ii}^T = \text{self inductance of a phase} = L_S^T$$

$$L_{ij}^T = \text{mutual inductance between two phases} = L_M^T$$

$$C_{i0}^T = \text{capacitance to ground of a phase} = C_0^T$$

$$C_{ij}^T = \text{mutual capacitance between two phases} = C_M^T$$

$$R_{ii}^T = \text{self resistance of a phase} = R_S^T$$

Then from figure (A-1) it is seen that in terms of the parameters of Figure 2.1:

$$L_{11}^T = L_{22}^T = L_{33}^T = \frac{L_{11} + L_{22} + L_{33}}{3} = L_S^T \quad (\text{A-5a})$$

$$L_{12}^T = L_{13}^T = L_{23}^T = \frac{L_{12} + L_{13} + L_{23}}{3} = L_M^T \quad (\text{A-5b})$$

$$C_{10}^T = C_{20}^T = C_{30}^T = \frac{C_{10} + C_{20} + C_{30}}{3} = C_0^T \quad (\text{A-5c})$$

$$C_{12}^T = C_{13}^T = C_{23}^T = \frac{C_{12} + C_{13} + C_{23}}{3} = C_M^T \quad (\text{A-5d})$$

$$R_{11}^T = R_{22}^T = R_{33}^T = \frac{R_{11} + R_{22} + R_{33}}{3} = R_S^T \quad (\text{A-5e})$$

The significance of these relations can be seen more clearly by modeling a transposition cycle of the transposed line with the model of Figure 2.1. The differential equations corresponding to equations (A-1) with $I_a + I_b + I_c = 3I_0$ are:

$$-\frac{\partial V_a}{\partial z} = R_S^T I_a + L_S^T \frac{\partial I_a}{\partial t} + L_M^T \frac{\partial I_b}{\partial t} + L_M^T \frac{\partial I_c}{\partial t} + 3R_{00} I_0 + 3L_{00} \frac{\partial I_0}{\partial t} \quad (\text{A-6a})$$

$$-\frac{\partial V_b}{\partial z} = L_M^T \frac{\partial I_a}{\partial t} + R_S^T I_b + L_S^T \frac{\partial I_b}{\partial t} + L_M^T \frac{\partial I_c}{\partial t} + 3R_{00} I_0 + 3L_{00} \frac{\partial I_0}{\partial t} \quad (\text{A-6b})$$

$$-\frac{\partial V_c}{\partial z} = L_M^T \frac{\partial I_a}{\partial t} + L_M^T \frac{\partial I_b}{\partial t} + R_S^T I_c + L_S^T \frac{\partial I_c}{\partial t} + 3R_{00} I_0 + 3L_{00} \frac{\partial I_0}{\partial t} . \quad (\text{A-6c})$$

Adding and subtracting $L_M^T \frac{\partial I_{a,b,c}}{\partial t}$ as appropriate in equations A-6 obtain:

$$-\frac{\partial V_a}{\partial z} = R_S^T I_a + (L_S^T - L_M^T) \frac{\partial I_a}{\partial t} + 3R_{00} I_0 + 3(L_M^T + L_{00}) \frac{\partial I_0}{\partial t} \quad (A-7a)$$

$$-\frac{\partial V_b}{\partial z} = R_S^T I_b + (L_S^T - L_M^T) \frac{\partial I_b}{\partial t} + 3R_{00} I_0 + 3(L_M^T + L_{00}) \frac{\partial I_0}{\partial t} \quad (A-7b)$$

$$-\frac{\partial V_c}{\partial z} = R_S^T I_c + (L_S^T - L_M^T) \frac{\partial I_c}{\partial t} + 3R_{00} I_0 + 3(L_M^T + L_{00}) \frac{\partial I_0}{\partial t} \quad (A-7c)$$

In the balanced steady-state $I_0 = 0$; the currents in the transposed line are positive sequence only, and equations (A-7) reduce still further to three decoupled "single-phase equivalent" equations. With $L_S^T - L_M^T = L_{P.S.}$ = positive-sequence inductance and $R_S^T = R_{P.S.}$ = positive-sequence resistance:

$$-\frac{\partial V_a}{\partial z} = R_{P.S.} I_a + L_{P.S.} \frac{\partial I_a}{\partial t} \quad (A-8a)$$

$$-\frac{\partial V_b}{\partial z} = R_{P.S.} I_b + L_{P.S.} \frac{\partial I_b}{\partial t} \quad (A-8b)$$

$$-\frac{\partial V_c}{\partial z} = R_{P.S.} I_c + L_{P.S.} \frac{\partial I_c}{\partial t} \quad (A-8c)$$

If only zero-sequence currents flow in the line, $I_a = I_b = I_c$, and equations (A-7) reduce to

$$-\frac{\partial V_a}{\partial z} = (R_S^T + 3R_{00}) I_a + (L_S^T + 2L_M^T + 3L_{00}) \frac{\partial I_a}{\partial t} \quad (A-9a)$$

$$-\frac{\partial V_b}{\partial z} = (R_S^T + 3R_{00}) I_b + (L_S^T + 2L_M^T + 3L_{00}) \frac{\partial I_b}{\partial t} \quad (A-9b)$$

$$-\frac{\partial V_c}{\partial z} = (R_S^T + 3R_{00}) I_c + (L_S^T + 2L_M^T + 3L_{00}) \frac{\partial I_c}{\partial t} \quad (A-9c)$$

Equations (A-8) and (A-9) describe (in terms of The Voltage Law) the symmetrical components equivalent circuits of the transposed line described by equations (A-7). The transposed line corresponding to equations (A-7) is shown in Figure 2.3.

The Current Law equations for the transposed line corresponding to equations (A-2) can be seen by inspection of Figures 2.1 and A-1:

$$-\frac{\partial I_a}{\partial z} = (C_0^T + 2C_{11}^T) \frac{\partial V_a}{\partial t} - C_{11}^T \frac{\partial V_b}{\partial t} - C_{11}^T \frac{\partial V_c}{\partial t} \quad (A-10a)$$

$$-\frac{\partial I_b}{\partial z} = -C_{11}^T \frac{\partial V_a}{\partial t} + (C_0^T + 2C_{11}^T) \frac{\partial V_b}{\partial t} - C_{11}^T \frac{\partial V_c}{\partial t} \quad (A-10b)$$

$$-\frac{\partial I_c}{\partial z} = -C_{11}^T \frac{\partial V_a}{\partial t} - C_{11}^T \frac{\partial V_b}{\partial t} + (C_0^T + 2C_{11}^T) \frac{\partial V_c}{\partial t} \quad (A-10c)$$

Setting $V_a + V_b + V_c = 3V_0$ and adding and subtracting $C_{11}^T \frac{\partial V_{a,b,c}}{\partial t}$ from equations (A-10) as appropriate:

$$-\frac{\partial I_a}{\partial z} = (C_0^T + 3C_{11}^T) \frac{\partial V_a}{\partial t} - 3C_{11}^T \frac{\partial V_0}{\partial t} \quad (A-11a)$$

$$-\frac{\partial I_b}{\partial z} = (C_0^T + 3C_{11}^T) \frac{\partial V_b}{\partial t} - 3C_{11}^T \frac{\partial V_0}{\partial t} \quad (A-11b)$$

$$-\frac{\partial I_c}{\partial z} = (C_0^T + 3C_{11}^T) \frac{\partial V_c}{\partial t} - 3C_{11}^T \frac{\partial V_0}{\partial t} \quad (A-11c)$$

In the balanced steady-state $V_0 = 0$; the voltages are positive sequence only, and equations (A-11) reduce to three decoupled "single-phase equivalent" equations. With $(C_0^T + 3C_{11}^T) = C_{P.S.}$ = positive sequence capacitance, equations (A-11) become:

$$-\frac{\partial I_a}{\partial z} = C_{P.S.} \frac{\partial V_a}{\partial t} \quad (A-12a)$$

$$-\frac{\partial I_b}{\partial z} = C_{P.S.} \frac{\partial V_b}{\partial t} \quad (A-12b)$$

$$-\frac{\partial I_c}{\partial z} = C_{P.S.} \frac{\partial V_c}{\partial t} \quad (A-12c)$$

If only zero-sequence voltages are applied to the transposed line, $V_a = V_b = V_c$. And with $C_0^T = C_{Z.S.}$ = zero sequence capacitance, equations (A-11) become:

$$-\frac{\partial I_a}{\partial z} = C_{Z.S.} \frac{\partial V_a}{\partial t} \quad (A-13a)$$

$$-\frac{\partial I_b}{\partial z} = C_{Z.S.} \frac{\partial V_b}{\partial t} \quad (A-13b)$$

$$-\frac{\partial I_c}{\partial z} = C_{Z.S.} \frac{\partial V_c}{\partial t} \quad (A-13c)$$

Equations (A-12) and (A-13) describe (in terms of The Current Law) the symmetrical components equivalent circuits of the transposed line described by equations (A-11). The transposed line model corresponding to equations (A-11) is shown in Figure 2.3.

APPENDIX B

MODEL IMPEDANCE DERIVATIONS

B.1.1 Derivation of L-Section Model Impedance-Inductor Input-Shorted Termination

Using the m section line shown in Figure 3.3, write difference equations near the nth section ($0 < n < m$):

$$V_n - V_{n-1} = L_s \frac{dI_n}{dt} + R_s I_n \quad (B-1)$$

$$I_{n+1} - I_n = C_s \frac{dV_n}{dt} \quad (B-2)$$

$$V_{n+1} - V_n = L_s \frac{dI_{n+1}}{dt} + R_s I_{n+1} \quad (B-3)$$

Subtracting (B-1) from (B-3):

$$V_{n-1} - 2V_n + V_{n+1} = L \frac{d}{dt} (I_{n+1} - I_n) + R_s (I_{n+1} - I_n) . \quad (B-4)$$

Substitute (B-2) into (B-4):

$$V_{n-1} - 2V_n + V_{n+1} = L_s C_s \frac{d^2 V_n}{dt^2} + R_s C_s \frac{dV_n}{dt} . \quad (B-5)$$

Assuming solutions of the form $V_n = \text{Re}[\hat{V}_n e^{st}]$:

$$\hat{V}_{n-1} - 2\hat{V}_n + \hat{V}_{n+1} = s^2 L_s C_s \hat{V}_n + s R_s C_s \hat{V}_n \quad (B-6)$$

Next assume $\hat{V}_n = K_{\pm} e^{\pm n\lambda}$ (where λ may be a complex constant, $\lambda = \lambda_r + j\lambda_i$) and substitute into equation (B-6):

$$e^{\pm(n-1)\lambda} - 2e^{\pm n\lambda} + e^{\pm(n+1)\lambda} = (s^2 L_s C_s + s R_s C_s) e^{\pm n\lambda}$$

$$e^{-\lambda} - 2 + e^{\lambda} = s^2 L_s C_s + s R_s C_s$$

$$\cosh \lambda = 1 + \frac{s^2 L_s C_s}{2} + \frac{s R_s C_s}{2} \quad (B-7)$$

Therefore, provided λ satisfies (B-7), the solutions to equation (B-5) take either of the forms:

$$V_n = \text{Re}[\hat{V}_n e^{st}] = \text{Re}[(K_+ e^{n\lambda} + K_- e^{-n\lambda})e^{st}] \quad (\text{B-8})$$

$$V_n = \text{Re}[(A \cosh n\lambda + B \sinh n\lambda)e^{st}] \quad (\text{B-9})$$

To obtain the current, I_n , use equation (B-1) assuming solutions of the form:

$$I_n = \text{Re}[\hat{I}_n e^{st}] \quad (\text{B-10})$$

$$V_n = \text{Re}[\hat{V}_n e^{st}] . \quad (\text{B-11})$$

Then (B-1) becomes:

$$\begin{aligned} \hat{I}_n (s L_s + R_s) &= \hat{V}_{n-1} - \hat{V}_n \\ I_n &= \frac{V_n - V_{n-1}}{R_s + s L_s} . \end{aligned} \quad (\text{B-12})$$

In terms of equation (B-9) equation (B-12) can be written as:

$$I_n = \frac{A(\cosh n\lambda - \cosh(n-1)\lambda) + B(\sinh n\lambda - \sinh(n-1)\lambda)}{R_s + s L_s} \quad (\text{B-13})$$

If the short is connected at the zeroth node, then $V_0 = 0$ and from equation (B-9) it is seen that $A = 0$, so that elsewhere on the line:

$$\hat{V}_n = B \sinh n\lambda . \quad (\text{B-14})$$

And from equation (B-13):

$$\hat{I}_n = \frac{B(\sinh n\lambda - \sinh(n-1)\lambda)}{R_s + s L_s} . \quad (\text{B-15})$$

Finally, the impedance looking into the m th node - or driving point terminals - is seen to be:

$$\hat{Z}_m(s) = \frac{(R_s + s L_s) \sinh m\lambda}{\sinh m\lambda - \sinh(m-1)\lambda} \quad (\text{B-16})$$

Where it is noted again that λ must satisfy

$$\cosh \lambda = 1 + \frac{s^2 L_s C_s}{2} + \frac{s R_s C_s}{2} . \quad (\text{B-7})$$

In the case that the model is lossless ($R_s = 0$), equations (B-16) and (B-7) reduce to:

$$Z_m(j\omega) = \frac{j\omega L_s \sinh m\lambda}{\sinh m\lambda - \sinh(m-1)\lambda} \quad (\text{B-17})$$

$$\cosh \lambda = 1 - \frac{\omega^2 L_s C_s}{2} . \quad (\text{B-18})$$

The solution for the poles of (B-17) is indicated in Appendices B.1.2, C.2.1, and D.1.

B.1.2 Solution for the Poles of the L-Section Model-Inductor Input-Shorted Termination

The solution for the poles of equation (B-16) or (B-17) rests upon recognition of the fact that the denominator of (B-16) and (B-17) is a polynomial in $\cosh \lambda$ of degree $(m-1)$ for all m . That this is true can be seen by expansion of the denominator for the first few values of m . The expansions of $\sinh m\lambda$ up to $m = 7$ are shown in Table B.1.

Table B.1

Expansions of $\sinh m\lambda$

$$\sinh \lambda = \sinh \lambda$$

$$\sinh 2\lambda = \sinh \lambda (2 \cosh \lambda)$$

$$\sinh 3\lambda = \sinh \lambda (4 \cosh^2 \lambda - 1)$$

$$\sinh 4\lambda = \sinh \lambda (8 \cosh^3 \lambda - 4 \cosh \lambda)$$

$$\sinh 5\lambda = \sinh \lambda (16 \cosh^4 \lambda - 12 \cosh^2 \lambda + 1)$$

$$\sinh 6\lambda = \sinh \lambda (32 \cosh^5 \lambda - 32 \cosh^3 \lambda + 6 \cosh \lambda)$$

$$\sinh 7\lambda = \sinh \lambda (64 \cosh^6 \lambda - 80 \cosh^4 \lambda + 24 \cosh^2 \lambda - 1)$$

The expansions listed in the table were obtained by repeated application of the identity $\sinh m\lambda = \sinh(m-1)\lambda \cosh \lambda + \cosh(m-1)\lambda \sinh \lambda$. The use of this identity to obtain $\sinh m\lambda$ requires the preceeding recursion terms $\sinh(m-1)\lambda$ and $\cosh(m-1)\lambda$. The term $\sinh(m-1)\lambda$ is simply the preceeding term in the table, but $\cosh(m-1)\lambda$ must be obtained from a separate process of expansions of $\cosh m\lambda$. Table B.2 shows the first few expansions of $\cosh m\lambda$ generated in the loop required to get $\sinh m\lambda$.

Table B.2

Expansions of $\cosh m\lambda$

$$\begin{aligned}\cosh \lambda &= \cosh \lambda \\ \cosh 2\lambda &= 2 \cosh^2 \lambda - 1 \\ \cosh 3\lambda &= 4 \cosh^3 \lambda - 3 \cosh \lambda \\ \cosh 4\lambda &= 8 \cosh^4 \lambda - 8 \cosh^2 \lambda + 1 \\ \cosh 5\lambda &= 16 \cosh^5 \lambda - 20 \cosh^3 \lambda + 5 \cosh \lambda \\ \cosh 6\lambda &= 32 \cosh^6 \lambda - 48 \cosh^4 \lambda + 18 \cosh^2 \lambda - 1 \\ \cosh 7\lambda &= 64 \cosh^7 \lambda - 112 \cosh^5 \lambda + 56 \cosh^3 \lambda - 7 \cosh \lambda\end{aligned}$$

Using Table B.1, the first seven polynomials set equal to zero in the denominator of equations (B-16) and (B-17) are listed in Table B.3.

Table B.3

Expansions of Impedance Function Denominator

$$\begin{aligned}0 &= 1 - \cosh \lambda = 0 & (m=1) \\ 0 &= 1 - 2 \cosh \lambda & (m=2) \\ 0 &= 1 + 2 \cosh \lambda - 4 \cosh^2 \lambda & (m=3) \\ 0 &= 1 - 4 \cosh \lambda - 4 \cosh^2 \lambda + 8 \cosh^3 \lambda & \text{etc.} \\ 0 &= 1 + 4 \cosh \lambda - 12 \cosh^2 \lambda - 8 \cosh^3 \lambda + 16 \cosh^4 \lambda \\ 0 &= 1 - 6 \cosh \lambda - 12 \cosh^2 \lambda + 32 \cosh^3 \lambda + 16 \cosh^4 \lambda - 32 \cosh^5 \lambda\end{aligned}$$

The equations listed in Table B.3 are the equations which must be solved to obtain the poles of L-section models of from one to seven sections. In obtaining the equations of Table B.3 the $\sinh \lambda$ term is divided out since $\sinh \lambda \neq 0$. A more thorough discussion of the constant λ is now in order. In general, $\lambda = \lambda_r + j\lambda_i$, so that in equation (B-18), for example,

$$\cosh \lambda = \cosh \lambda_r \cos \lambda_i + j \sinh \lambda_r \sin \lambda_i = 1 - \frac{\omega^2 L_s C_s}{2} . \quad (B-19)$$

Equation (B-19) implies:

$$\cosh \lambda_r \cos \lambda_i = 1 - \frac{\omega^2 L_s C_s}{2} \quad (B-20)$$

$$\sinh \lambda_r \sin \lambda_i = 0 \quad (B-21)$$

But, again,

$$\cosh \lambda = \cosh \lambda_r \cos \lambda_i = 1 - \frac{\omega^2 L_s C_s}{2} \quad (B-23)$$

and it is seen that $\cosh \lambda$ is real, and λ is pure imaginary ($= j\lambda_i$) if

$\frac{\omega^2 L_s C_s}{2} > 0$. With $\lambda = j\lambda_i$, $\lambda_r = 0$ so that finally,

$$\cosh \lambda = \cosh j\lambda_i = \cos \lambda_i = 1 - \frac{\omega^2 L_s C_s}{2} . \quad (B-24)$$

Equation (B-24) shows that all values of $\cosh \lambda$ must be real and lie between minus one and plus one. This, in turn implies that all solutions to the "equation" in the denominator of (B-17) must also be real and lie between minus one and plus one i.e.,

$$-1.0 \leq [\cosh \lambda]_{\text{root}} \leq 1.0 . \quad (B-25)$$

But the denominator of equation (B-17) is the same as that of equation (B-16), so equation (B-25) applies for the lossy line also.

Thus, the equations listed in Table B.3 are polynomial equations in the real variable $\cosh \lambda$ for which there are numerous "root-finding" sub-routines in any good computation facility. With the roots of equations like those in Table B.3 readily available, equations (B-7) or (B-16) can be solved for s or ω respectively to give the poles:

$$s_{s.c.} = -\frac{R}{2L} \pm \sqrt{\left(\frac{R}{2L}\right)^2 - \frac{2m^2}{\ell^2 LC} [1 - (\cosh \lambda)_{\text{root}}]} \quad (\text{B-26})$$

$$m = 1, 2, 3, \dots$$

$$\omega_{s.c.} = \frac{m}{\ell} \sqrt{\frac{2}{LC} [1 - (\cosh \lambda)_{\text{root}}]} \quad (\text{B-27})$$

$$m = 1, 2, 3, \dots$$

Where use has been made of the fact that:

$$R_s = \frac{R\ell}{m}, \quad L_s = \frac{L\ell}{m}, \quad \text{and} \quad C_s = \frac{C\ell}{m} \quad (\text{B-28})$$

Equations like those in Table B.3 are seen to be solved easily enough, but the problem of how to generate the equations up to fifty or more sections (m) remains. The details of the generation problem are left to Appendix C.

B.2 Derivation of L-Section Model Impedance, Capacitor Input, Shorted Termination

Using the m -section line shown in Figure 3.6, write difference equations near the n th section ($0 < n < m$):

$$V_{n+1} - V_n = L_s \frac{dI_n}{dt} \quad (\text{B-29})$$

$$V_n - V_{n-1} = L_s \frac{dI_{n-1}}{dt} \quad (\text{B-30})$$

$$I_n - I_{n-1} = C_s \frac{dV_n}{dt} \quad (\text{B-31})$$

Subtracting (B-30) from (B-29):

$$V_{n+1} - 2V_n + V_{n-1} = L_s \frac{d}{dt} (I_n - I_{n-1}). \quad (B-32)$$

Substitute (B-31) into (B-32):

$$V_{n+1} - 2V_n + V_{n-1} = L_s C_s \frac{d^2 V_n}{dt^2}$$

Similar to the development in Appendix B.1.1 assume,

$$V_n = \text{Re}[\hat{V}_n e^{\pm j\omega t}]$$

$$V_n = K_{\pm} e^{\pm n\lambda}$$

and obtain:

$$\cosh \lambda = 1 - \frac{\omega^2 L_s C_s}{2} \quad (B-33)$$

$$V_n = A \cosh n\lambda + B \sinh \lambda \quad (B-34)$$

To obtain the current, I_n , assume $I_n = \text{Re}[\hat{I}_n e^{j\omega t}]$ in equation (B-29):

$$j\omega L_s \hat{I}_n = \hat{V}_{n+1} - \hat{V}_n \quad (B-35)$$

$$\hat{I}_n = \frac{1}{j\omega L_s} [A \cosh(n+1)\lambda + B \sinh(n+1)\lambda - A \cosh n\lambda - B \sinh n\lambda] \quad (B-36)$$

With a short at the zeroth node $V_0 = 0$ implies $A = 0$, and

$$\hat{V}_n = B \sinh n\lambda \quad (B-37)$$

$$\hat{I}_n = \frac{B}{j\omega L_s} [\sinh(n+1)\lambda - \sinh n\lambda]. \quad (B-38)$$

Finally, for the driving point impedance at the m th node,

$$Z_{s.c.} = j\omega L_s \frac{\sinh m\lambda}{\sinh(m+1)\lambda - \sinh m\lambda} \quad m = 1, 2, 3, \dots \quad (B-39)$$

and using equation (B-33):

$$\omega_{s.c.} = \frac{m}{\ell} \sqrt{\frac{2}{LC} [1 - (\cosh \lambda)_{\text{root}}]} \quad m = 1, 2, 3, \dots \quad (\text{B-40})$$

The solution for the poles of equation (B-39) is indicated in Appendices C.2.2 and D.2.

B.3 Derivation of L-Section Model Impedance, Open Termination

Using the m section line shown in Figure 3.3, but with the short removed, $R_s = 0$, and $s = j\omega$, the derivation proceeds as in Appendix B.1.1 to obtain:

$$\hat{V}_n = A \cosh n\lambda + B \sinh n\lambda \quad (\text{B-41})$$

$$\hat{I}_n = \frac{1}{j\omega L_s} A [\cosh(n-1)\lambda - \cosh n\lambda] + B [\sinh(n-1)\lambda - \sinh n\lambda] \quad (\text{B-42})$$

But now, $I_0 = 0$, and equation (B-42) implies,

$$B = \frac{\cosh \lambda - 1}{\sinh \lambda} . \quad (\text{B-43})$$

Substituting (B-43) into (B-41) and (B-42):

$$\hat{V}_n = A \left[\frac{\sinh(n+1)\lambda - \sinh n\lambda}{\sinh \lambda} \right] \quad (\text{B-44})$$

$$I_n = \frac{A}{j\omega L_s} \left[\frac{2 \sinh n\lambda - \sinh(n+1)\lambda - \sinh(n-1)\lambda}{\sinh \lambda} \right] \quad (\text{B-45})$$

So that looking into the m th section:

$$Z_{o.c.} = j\omega L_s \left[\frac{\sinh(m+1)\lambda - \sinh m\lambda}{2 \sinh m\lambda - \sinh(m+1)\lambda - \sinh(m-1)\lambda} \right] \quad (\text{B-46})$$

As in Appendix B.1.1,

$$\cosh \lambda = 1 - \frac{\omega_s^2 L_s C_s}{2} \quad (\text{B-18})$$

from which

$$\omega_{o.c.} = \frac{m}{\ell} \sqrt{\frac{2}{LC} [1 - (\cosh \lambda)_{\text{root}}]} \quad (\text{B-47})$$

The solution for the poles of equation (B-46) is indicated in Appendices C.2.3 and D.3.

B.4 Derivation of π -Section Model Impedance, Shorted Termination

Using Figure B.1, write difference equations near the n th section:

$$V_n - V_{n+1} = L_s \frac{dI_{\star}}{dt} \quad (B-48)$$

$$I_n - I_{\star} = C_s \frac{dV_n}{dt} \quad (B-49)$$

$$I_{\star} - I_{n+1} = C_s \frac{dV_{n+1}}{dt} . \quad (B-50)$$

Substitute (B-50) into (B-48) to eliminate I_{\star} :

$$V_n - V_{n+1} = L_s \frac{d}{dt} \left[C_s \frac{dV_{n+1}}{dt} + I_{n+1} \right] . \quad (B-51)$$

Substitute (B-50) into (B-49) to eliminate I_{\star} :

$$I_n - C_s \frac{dV_{n+1}}{dt} - I_{n+1} = C_s \frac{dV_n}{dt} . \quad (B-52)$$

Write the equivalent to equation (B-51) for the next section toward the left:

$$V_{n-1} - V_n = L_s \frac{d}{dt} \left[C_s \frac{dV_n}{dt} + I_n \right] . \quad (B-53)$$

From equation (B-52) write:

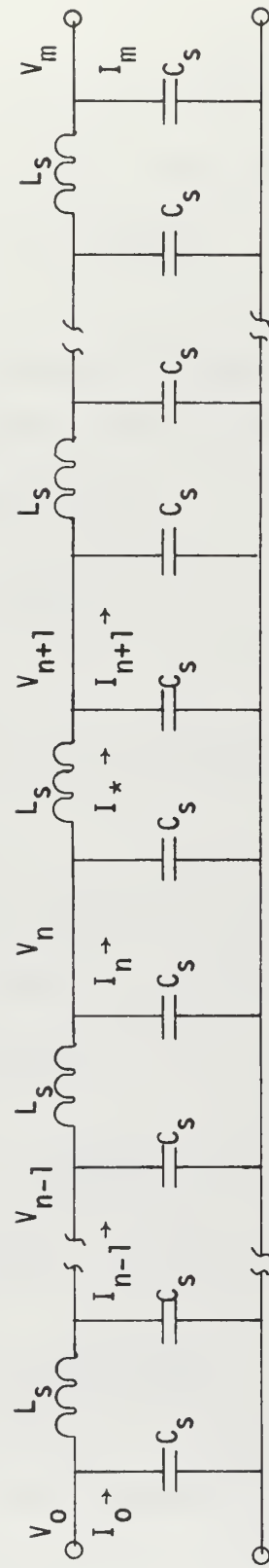
$$I_{n+1} = I_n - C_s \frac{d}{dt} [V_{n+1} + V_n] . \quad (B-54)$$

Substitute (B-54) into (B-51) to eliminate I_{n+1} :

$$V_n - V_{n+1} = L_s C_s \frac{d^2 V_{n+1}}{dt^2} + L_s \frac{dI_n}{dt} - L_s C_s \frac{d^2}{dt^2} (V_{n+1} + V_n) . \quad (B-55)$$

Rewrite equation (B-53):

$$V_{n-1} - V_n = L_s C_s \frac{d^2 V_n}{dt^2} + L_s \frac{dI_n}{dt} . \quad (B-56)$$



π -Section Model (Lossless)

Figure B.1

Substitute (B-56) into (B-55) to eliminate $L \frac{dI_n}{dt}$:

$$V_{n+1} - 2V_n + V_{n-1} = 2L_s C_s \frac{d^2 V_n}{dt^2} \quad (B-57)$$

Solve equation (B-57) as in earlier cases to obtain:

$$\cosh \lambda = 1 - \omega^2 L_s C_s \quad (B-58)$$

and

$$\hat{V}_n = A \cosh n\lambda + B \sinh n\lambda . \quad (B-59)$$

To find the current use equation (B-56) assuming solutions

$$I_n = \text{Re}[\hat{I}_n e^{j\omega t}]$$

$$V_n = \text{Re}[\hat{V}_n e^{j\omega t}]$$

to obtain:

$$\hat{I}_n = \frac{1}{j\omega L} [\hat{V}_{n-1} - \hat{V}_n + \omega^2 L_s C_s V_n] . \quad (B-60)$$

Expanding equation (B-60):

$$\hat{I}_n = - \frac{1}{j\omega L} [A \sinh \lambda \sinh n\lambda + B \cosh n\lambda \sinh \lambda] . \quad (B-61)$$

With a short at the zeroth node, $V_0 = 0$ implies $A = 0$ so that

$$\hat{V}_n = B \sinh n\lambda \quad (B-62)$$

and

$$Z_n = - j\omega L_s \frac{\sinh n\lambda}{\cosh n\lambda \sinh \lambda} . \quad (B-63)$$

At the m th node or driving point terminals :

$$Z_m = - j\omega L_s \frac{\sinh m\lambda}{\cosh m\lambda \sinh \lambda} . \quad (B-64)$$

The solution of equation (B-64) for the poles is discussed in Appendices C.2.4 and D.4. The results of the solution are the values of $[\cosh \lambda]_{\text{root}}$ which give the poles of (B-64). Also, using

equation (B-58),

$$\omega_{s.c.} = \sqrt{\frac{1 - (\cosh \lambda)_{\text{root}}}{L_s C_s}} \quad (\text{B-65})$$

or

$$\omega_{s.c.} = \frac{m}{\ell} \sqrt{\frac{2[1 - (\cosh \lambda)_{\text{root}}]}{LC}} \quad (\text{B-66})$$

Equation (B-66) follows from (B-65) since

$$L_s = \frac{L\ell}{m} \quad \text{and} \quad C_s = \frac{C\ell}{2m} \quad (\text{B-67})$$

B.5 Derivation of π -Section Model Impedance Open Termination

The derivation of the open circuit case is the same as that of the short circuit case through equation (B-61). Now, at the "0"th node, $I_0 = 0$, and equation (B-61) implies $B = 0$. Thus

$$\hat{I}_n = -\frac{1}{j\omega L} [A \sinh \lambda \sinh n\lambda] \quad (\text{B-68})$$

$$\hat{V}_n = A \cosh n\lambda \quad (\text{B-69})$$

$$Z_m = \frac{V_m}{I_m} = -j\omega L \frac{\cosh m\lambda}{\sinh \lambda \sinh m\lambda} \quad (\text{B-70})$$

Again,

$$\omega_{o.c.} = \frac{m}{\ell} \sqrt{\frac{2[1 - (\cosh \lambda)_{\text{root}}]}{LC}} \quad (\text{B-71})$$

The solution of equations (B-70), (B-71), and (3-1) is discussed in Appendices C.2.5 and D.5.

APPENDIX C

SOLUTIONS FOR THE POLES OF THE MODEL IMPEDANCE FUNCTIONS

C.1 Model Impedance Functions

The model impedance functions obtained in Appendix B for which solutions are sought are shown in Table C.1. For the purposes of Appendix C, "solutions" refers to those values of $\cosh \lambda$ in the denominator of the impedance function which result in the poles of the function. In Appendix B.1.2 it was shown that the denominator of equation (B-17) is a polynomial in the real variable $\cosh \lambda$. In addition it was shown that the polynomial had real coefficients and that all solutions for $[\cosh \lambda]_{\text{root}}$ should be such that

$$-1.0 \leq [\cosh \lambda]_{\text{root}} \leq 1.0 .$$

Since the denominator of equation (B-17) is a polynomial in $\cosh \lambda$, it follows that the denominator of all the impedance functions is a polynomial in $\cosh \lambda$ with all the properties of the polynomial in equation (B-17). It is the denominator polynomial set equal to zero which results in the poles of the respective impedance function. If the denominator polynomials $[D(\cosh \lambda)]$ can be generated for any number of sections, m , then it is a simple matter to call upon root routines in the computer library to solve for the roots of the denominator equation, $D = 0$. An inspection of Table C.1 and reference to Appendix B.1.2 shows that the "generation" of D involves first the generation of $\sinh m\lambda$ and $\cosh m\lambda$ for any m . In Appendix B.1.2 it was shown that

$$\sinh m\lambda = \sinh \lambda [\text{Polynomial in } \cosh \lambda] \quad (\text{C-1})$$

<u>Model</u>	<u>Driving Pt. Impedance Function</u>	
L-Section Inductor Input Shorted Termination	$Z_m = \frac{j\omega L_s \sinh m\lambda}{\sinh m\lambda - \sinh(m-1)\lambda}$	(B-17)
	$\omega = \frac{m}{\ell} \sqrt{\frac{2}{LC} [1 - (\cosh \lambda)_{\text{root}}]}$	(B-27)
L-Section Capacitor Input Shorted Termination	$Z_m = \frac{j\omega L_s \sinh m\lambda}{\sinh(m+1)\lambda - \sinh m\lambda}$	(B-39)
	$\omega = \frac{m}{\ell} \sqrt{\frac{2}{LC} [1 - (\cosh \lambda)_{\text{root}}]}$	(B-40)
L-Section Open Termination	$Z_m = \frac{j\omega L_s [\sinh(m+1)\lambda - \sinh \lambda]}{2 \sinh m\lambda - \sinh(m+1)\lambda - \sinh(m-1)\lambda}$	(B-46)
	$\omega = \frac{m}{\ell} \sqrt{\frac{2}{LC} [1 - (\cosh \lambda)_{\text{root}}]}$	(B-47)
π -Section Shorted Termination	$Z_m = \frac{-j\omega L_s \sinh m\lambda}{\cosh m\lambda \sinh \lambda}$	(B-64)
	$\omega = \frac{m}{\ell} \sqrt{\frac{2}{LC} [1 - (\cosh \lambda)_{\text{root}}]}$	(B-66)
π -Section Open Termination	$Z_m = \frac{-j\omega L_s \cosh m\lambda}{\sinh \lambda \sinh m\lambda}$	(B-70)
	$\omega = \frac{m}{\ell} \sqrt{\frac{2}{LC} [1 - (\cosh \lambda)_{\text{root}}]}$	(B-71)

Table of Impedance Functions for Which
Poles are Sought

Table C.1

and

$$\cosh m\lambda = [\text{Polynomial in } \cosh \lambda] . \quad (\text{C-2})$$

Denote the polynomial in equation (C-1) by $B = B(\cosh \lambda)$ and that in equation (C-2) by $A = A(\cosh \lambda)$ so that

$$\sinh m\lambda = \sinh \lambda B_m(\cosh \lambda) \quad (\text{C-3})$$

$$\cosh m\lambda = A_m(\cosh \lambda). \quad (\text{C-4})$$

Then it follows that in all the impedance functions of Table C.1 the denominator has the form

$$D(\cosh \lambda) = \text{Linear Combination of } A(\cosh \lambda) \text{ and } B(\cosh \lambda). \quad (\text{C-5})$$

A routine must be found which will enable the computer to generate A_m and B_m , combine them to form $D_m = 0$, and then solve for the values of $[\cosh \lambda]_{\text{root}}$ for use in

$$\omega = \frac{m}{\ell} \sqrt{\frac{2}{LC} [1 - (\cosh \lambda)_{\text{root}}]} . \quad (\text{C-6})$$

C.2 Generation of Impedance Function Denominator Polynomial

In general

$$\sinh m\lambda = \sinh(m-1)\lambda \cosh \lambda + \cosh(m-1)\lambda \sinh \lambda,$$

so that in the terminology of Appendix C.1,

$$\sinh \lambda B_m = \sinh \lambda B_{m-1} \cosh \lambda + A_{m-1} \sinh \lambda,$$

and

$$B_m = B_{m-1} \cosh \lambda + A_{m-1} . \quad (\text{C-7})$$

Similarly

$$\cosh m\lambda = \cosh(m-1)\lambda \cosh \lambda + \sinh(m-1)\lambda \sinh \lambda,$$

so that

$$A_m = A_{m-1} \cosh \lambda + B_{m-1} \sinh^2 \lambda,$$

or

$$A_m = A_{m-1} \cosh \lambda + (\cosh^2 \lambda - 1) B_{m-1} . \quad (C-8)$$

Throughout the remainder of this appendix denote

$\cosh \lambda$ by "C"

and

$\sinh \lambda$ by "S"

so that equations (C-7) and (C-8) become:

$$B_m = C B_{m-1} + A_{m-1} \quad m = 1, 2, \dots \quad (C-9)$$

$$A_m = C A_{m-1} + (C^2 - 1) B_{m-1} \quad m = 1, 2, \dots \quad (C-10)$$

With $m = 1, 2, \dots$, comparison of equations (C-9) and (C-10) with Tables B.1 and B.2 indicates that with $A_0 = 1$ and $B_0 = 0$ equations (C-9) and (C-10) form a recursion loop for generating all B_m and A_m . In equations (C-9) and (C-10) it is the coefficients of the powers of $\cosh \lambda$ which are needed to solve for the roots of the "D" polynomial, so that in B_m and A_m it is the coefficients which are of interest.

In their most general form the polynomials $A(m)$ and $B(m)$ take the form (for $m = 1, 2, \dots$):

$$A(m) = a_{m+1}(m)C^m + a_m(m)C^{m-1} + \dots + a_1(m) \quad (C-11)$$

$$B(m) = b_m(m)C^{m-1} + b_{m-1}(m)C^{m-2} + \dots + b_1(m) . \quad (C-12)$$

Where

m = number of sections in the model

C = $\cosh \lambda$

$A(m)$ = "A" polynomial when model has m sections

$B(m)$ = "B" polynomial when model has m sections

$a_i(m)$ = coefficient of C^{i-1} when model has m sections

$b_i(m)$ = coefficient of C^{i-1} when model has m sections

The subscripts of the coefficients begin at "1" in order to be compatible with the subscripting convention in the Fortran IV language. Note from Tables B.1 and B.2 that

$$B(1) = 1 \text{ implies } b_1(1) = 1,$$

$$A(1) = C \text{ implies } a_2(1) = 1, \quad (C-13)$$

$$\text{and } a_1(1) = 0.$$

To compute B_2 , for example, use equations (C-9), (C-10), and (C-11):

$$B_2 = B(2) = C B(1) + A(1)$$

$$B(2) = C[b_1(1)] + [a_2(1) C + a_1(1)]$$

$$B(2) = [a_2(1) + b_1(1)] C + a_1(1)$$

Where

$$[a_2(1) + b_1(1)] = b_2(2)$$

and

$$a_1(1) = b_1(2)$$

In general:

$$B(m) = C B(m-1) + A(m-1)$$

$$= C[b_{m-1}(m-1)C^{m-2} + b_{m-2}(m-1)C^{m-3} \dots b_1(m-1)]$$

$$+ [a_m(m-1)C^{m-1} + a_{m-1}(m-1)C^{m-2} \dots a_1(m-1)] .$$

Combining coefficients of like powers:

$$\begin{aligned} B(m) = & + [b_{m-1}(m-1) + a_m(m-1)]C^{m-1} \\ & + [b_{m-2}(m-1) + a_{m-1}(m-1)]C^{m-2} \\ & + \dots \end{aligned}$$

$$\begin{aligned}
 &+ [b_1(m-1) + a_2(m-1)]C \\
 &+ [a_1(m-1)] .
 \end{aligned} \tag{C-14}$$

Inspection of equation (C-14) shows that

$$b_i(m) = [b_{i-1}(m-1) + a_i(m-1)] \quad 2 \leq i \leq m \tag{C-15}$$

$$b_i(m) = a_1(m-1) . \quad i = 1 \tag{C-16}$$

A similar procedure applied for $A(m)$ gives:

$$a_i(m) = [a_{i-1}(m-1) + b_{i-2}(m-1)] \quad i=m, m+1 \tag{C-17}$$

$$a_i(m) = [a_{i-1}(m-1) + b_{i-2}(m-1) - b_i(m-1)] \quad i=2,3,\dots,m-1 \tag{C-18}$$

$$a_2(m) = [a_1(m-1) - b_2(m-1)] \quad i=2 \tag{C-19}$$

$$a_1(m) = [-b_1(m-1)] . \quad i=1 \tag{C-20}$$

Given the initial values for $A(1)$ and $B(1)$, equations (C-15) through (C-20) can be implemented in Fortran IV, and the computer made to generate and store the coefficients of the "A" and "B" polynomials. Having the coefficients of "A" and "B" up to, say, fifty sections ($m=50$), the "D" polynomial can be generated by simple algebra.

C.2.1 Polynomial for L-Section Model, Inductor Input, Shorted

For the case of the L-Section, inductor input model with a shorted termination, the equation for which the roots are sought is (from equation B-17)

$$\sinh m\lambda - \sinh(m-1)\lambda = 0$$

$$\sinh \lambda [B(m) - B(m-1)] = 0.$$

The case $\lambda = 0$ has no meaning for this model and so

$$B(m) - B(m-1) = 0, \quad (C-21)$$

and equation (C-21) is seen to be the relation which gives the poles of equation (B-17). Thus

$$D(m) = B(m) - B(m-1) = 0. \quad (C-22)$$

Equation (C-22) must also be written for implementation into Fortran IV in the same way that $A(m)$ and $B(m)$ were implemented. Thus:

$$\begin{aligned} D(m) &= d_m(m)C^{m-1} + d_{m-1}(m)C^{m-2} + \dots + d_2(m)C + d_1(m) \\ &= B(m) - B(m-1) \\ &= [b_m(m)C^{m-1} + b_{m-1}(m)C^{m-2} + \dots + b_2(m)C + b_1(m)] \\ &\quad - [b_{m-1}(m-1)C^{m-2} + b_{m-2}(m-1)C^{m-3} + \dots + b_2(m-1)C + b_1(m-1)]. \end{aligned}$$

Combining coefficients of like powers:

$$\begin{aligned} D(m) &= b_m(m)C^{m-1} + [b_{m-1}(m) - b_{m-1}(m-1)]C^{m-2} + \\ &\quad [b_{m-2}(m) - b_{m-2}(m-1)]C^{m-3} + \dots \\ &\quad \dots [b_2(m) - b_2(m-1)]C + [b_1(m) - b_1(m-1)]. \end{aligned}$$

So that identifying coefficients of $D(m)$:

$$d_i(m) = b_i(m) - b_i(m-1) \quad i = 1 \dots m-1 \quad (C-23)$$

$$d_m(m) = b_m(m). \quad (C-24)$$

Thus the computer can be made to generate the coefficients of the "D" polynomial. The form of the coefficients given in equations (C-24) and (C-25) are explicitly suited for several "root" subroutines available in the IBM-360 Scientific Subroutine Package (SSP) at the Computation Center of M.I.T. Equations (C-15) through (C-20) and (C-23) and (C-24)

were implemented in Fortran and solved with the IBM-360 as shown in Appendix D.1. In Appendix C.1 the roots of D are put into equation (B-26) to obtain the poles of a 100 mile long typical 765 kV line. The poles of the model thus obtained are compared to the poles of the actual line to obtain the pole error plots of Chapter 3.

C.2.2 Polynomial for L-Section Model, Capacitor Input, Shorted

For the case of the L-section, capacitor input model with a shorted termination, the equation for which the roots are sought is (from equations B-39):

$$\sinh(m+1)\lambda - \sinh m\lambda = 0$$

$$\sinh \lambda [B(m+1) - B(m)] = 0.$$

The case $\lambda = 0$ has no meaning for this model and so

$$D(m) = B(m+1) - B(m) = 0.$$

Following a procedure identical to that in Appendix C.2.1, the coefficients of the "D" polynomial are found to be

$$d_m(m) = b_m(m) \quad (C-25)$$

$$d_i(m) = [b_i(m) - b_i(m-1)], \quad i=1,2,\dots,m-1 \quad (C-26)$$

Note that equations (C-25) and (C-26) appear identical to equations (C-24) and (C-23) respectively, but that in the case of equations (C-25) and (C-26) the coefficients pertain to a higher power of the variable C . Equations (C-15) through (C-20) and equations (C-25) and (C-26) were implemented in Fortran and solved with the computer as shown in Appendix D.2.

C.2.3 Polynomial for L-Section Model, Open Termination

For the case of the open circuited L-section model, the equations for which the roots are sought is (from equation B-46):

$$2 \sinh m\lambda - \sinh(m+1)\lambda - \sinh(m-1)\lambda = 0$$

$$\sinh m\lambda(1 - \cosh \lambda) = 0$$

$$\sinh \lambda B(m)[1-C] = 0.$$

Again the case $\lambda = 0$ adds no solutions, so that division by $\sinh \lambda$ can be performed assuming $\lambda \neq 0$. Finally then

$$D(m) = B(m)(1-C) = 0$$

$$D(m) = [b_m(m)C^{m-1} + b_{m-1}(m)C^{m-2} + \dots + b_2(m) + b_1(m)](1-C).$$

Collecting coefficients of like powers of C:

$$D(m) = -b_m(m)C^m + [b_m(m) - b_{m-1}(m)]C^{m-1} + \dots + [b_2(m) - b_1(m)]C + b_1(m).$$

The coefficients, d_i , are then seen to be

$$d_1(m) = b_1(m) \tag{C-27}$$

$$d_i(m) = [b_i(m) - b_{i-1}(m)] \quad i=2,3,\dots,m \tag{C-28}$$

$$d_{m+1}(m) = -b_m(m) \quad \text{when } i=m+1 \tag{C-29}$$

Equations (C-15) through (C-20) and (C-27) through (C-29) were implemented in Fortran and solved with the computer as shown in Appendix D.3.

C.2.3 Polynomial for π -Section Model, Shorted

For the case of the shorted π -section model, the equation for which roots are sought is (from equation B-64):

$$\cosh m\lambda \sinh \lambda = 0.$$

The case $\lambda = 0$ has no meaning for this model so that

$$D(m) = \cosh m\lambda,$$

$$D(m) = A(m),$$

$$d_i(m) = a_i(m) \quad i = 1, 2, \dots, m+1$$

This case is particularly simple and is shown implemented in Appendix D.4.

C.2.4 Polynomial for π -Section Model, Open

For the case of the open π -section model, the equation for which roots are sought is (from equation B-70):

$$\sinh \lambda \sinh m\lambda = 0$$

$$\sinh^2 \lambda B(m) = 0$$

$$(1 - \cosh^2) B(m) = 0$$

$$D(m) = (1 - C^2) B(m) = 0 \quad . \quad (C-30)$$

Expanding equation (C-30) and collecting like powers of C :

$$\begin{aligned} D(m) = & b_m(m)C^{m+1} + B_{m-1}(m)C^m + [b_{m-2}(m) - b_m(m)]C^{m-1} + \dots \\ & \dots [b_2(m) - b_4(m)]C^3 + [b_1(m) - b_3(m)]C^2 - b_2(m)C - b_1(m). \end{aligned}$$

The coefficients d_i are then identified as

$$d_i(m) = -b_i(m) \quad \text{if } i = 1, 2 \quad (C-31)$$

$$d_i(m) = [b_{i-2}(m) - b_i(m)] \quad i = 3, 4, \dots, m \quad (C-32)$$

$$d_i(m) = b_{m-1}(m) \quad i = m+1 \quad (C-33)$$

$$d_i(m) = b_m(m) \quad i = m+2 \quad (C-34)$$

Equations (C-15) through (C-20) and (C-31) through (C-34) were implemented in Fortran and solved with the computer as shown in Appendix D.5.

APPENDIX D.1


```

C      K. SCHMIDT PROGRAM TO CCMPUTE POLES OF LUMPED LINE MODEL
C      LUMPED MODEL OF LOSSY LINE
C      "L" SECTION LINE
C      SHORT CIRCUITED TERMINATION
C      VIEWED FROM INDUCTOR AT INPUT
C      CONSTANT R,L,AND C ASSUMED (PCS. SEQUENCE)
C      TYPICAL 765KV LINE PARAMETERS
C      LENGTH=100 MILES, R=0.0251 OHMS/MILE, L=0.00145HENRYS/MILE
C      C=2.1*10**(-8) FARADS/MILE
C      W=CCOMPLEX PCLES OF THE MODEL
C      F=CCOMPLEX PCLES OF THE ACTUAL LINE 100 MILES LONG
C      D(I)"DENOMINATOR OF DRIVING PT. IMPEDANCE POLYNOMIAL
C
C      CCOMPLEX*8 F(100)/100*(C.0,C.0)/
C      CCOMPLEX*8 G,Q,S,T,W(60)/60*(0.0,0.0)/,CC,GG,DD
C      REAL*4 H(60)/60*0.0/
C      REAL*8 A(60,60)/3600*0.0/,B(60,60)/3600*0.0/
C      REAL*8 C(60)/60*0.0/,R(60)/60*0.0/,E(60)/60*0.0/,P(60)/60*0.0/
C      "INC" IS THE INCREMENT IN GENERATING THE "D" POLYNOMIAL AND IN
C      OBTAINING ITS PCCTS
C      "M" IS THE MAX. NO. OF SECTIONS IN THE MODEL
C      READ(5,100)M,INC
C      FCNMT(213)
C      TO GENERATE "D" IT'S NECESSARY TO GEN.A AND B POLYS
C      A(2,1)=1.0
C      B(1,1)=1.0
C      THE ABOVE ARE THE COEFFICIENTS OF THE FIRST A AND B POLYS
C      THE FOLLOWING DOUBLE LOOP GENERATES THE A AND B POLYS
C      DO 40 K=2,M
C      L=K+1
C      N=K+1
C      DO 30 I=1,N
C      IF(I.EQ.1) GO TO 11
C      GO TO 25
C      11 A(1,K)=-E(1,K-1)

```

```

E.0*0001
E.0*0002
E.0*0003
E.0*0004
E.0*0005
E.0*0006
E.0*0007
E.0*0008
E.0*0009
E.0*0010
E.0*0011
E.0*0012
E.0*0013
E.0*0014
E.0*0015
E.0*0016
E.0*0017
E.0*0018
E.0*0019
E.0*0020
E.0*0021
E.0*0022
E.0*0023
E.0*0024
E.0*0025
E.0*0026
E.0*0027
E.0*0028
E.0*0029
E.0*0030
E.0*0031
E.0*0032
E.0*0033
E.0*0034
E.0*0035
E.0*0036

```



```

      P(I,K)=A(I,K-1)
      GO TO 30
25 IF(I.EQ.2) GO TO 12
      GL TO 26
12 A(2,K)=A(1,K-1)-B(2,K-1)
      P(2,K)=B(1,K-1)+A(2,K-1)
      GO TO 30
26 IF(I.EQ.K) GC TO 13
      GO TO 27
13 A(I,K)=A(I-1,K-1)+B(I-2,K-1)
      P(I,K)=B(I-1,K-1)+A(I,K-1)
      GO TO 30
27 IF(I.EQ.L) GC TO 13
      A(I,K)=A(I-1,K-1)+B(I-2,K-1)-B(I,K-1)
      P(I,K)=B(I-1,K-1)+A(I,K-1)
30 CONTINUE
40 CCNTINUE
      C THE FOLLOWING LOOPS GENERATE THE "D" POLY AND CALL DPRBM
      DO 70 K=1,M,INC
      DO 60 I=1,K
      IF(I.EQ.K) GC TO 61
      GO TO 65
61 D(I)=B(K,K)
      GO TO 60
65 D(I)=B(I,K)-E(I,K-1)
60 CONTINUE
      J=K-1
      CALL DPRBM(C,6C,R,E,P,J,IER)
      DO 601 IP=1,50
      H(IP)=R(IP)
601 CCNTINUE
      DO 66 IN=1,J
      G=(75.0,C.0)
      C=(656000C.C,C.0)
      S=(1.0,0.0)
      T=(-8.66,0.0)

```

```

E.0*0037
E.0*0038
E.0*0039
E.0*0040
E.0*0041
E.0*0042
E.0*0043
E.0*0044
E.0*0045
E.0*0046
E.0*0047
E.0*0048
E.0*0049
E.0*0050
E.0*0051
E.0*0052
E.0*0053
E.0*0054
E.0*0055
E.0*0056
E.0*0057
E.0*0058
E.0*0059
E.0*0060
E.0*0061
E.0*0062
E.0*0063
E.0*0064
E.0*0065
E.0*0066
E.0*0067
E.0*0068
E.0*0069
E.0*0070
E.0*0071
E.0*0072

```


E.0*0073
 E.0*0074
 E.0*0075
 E.0*0076
 E.0*0077
 E.0*0078
 E.0*0079
 E.0*0080
 E.0*0081
 E.0*0082
 E.0*0083
 E.0*0084
 E.0*0085
 E.0*0086
 E.0*0087
 E.0*0088
 E.0*0089
 E.0*0090
 E.0*0091
 E.0*0092
 E.0*0093

```

KSQD=K**2
W(IN)=T+CSQRT(G-C*KSQD*(S-H(IN)))
  66 CONTINUE
  WRITE(6,800)K,IER
  800 FORMAT('CFOR',I3,'SEC. THE ERROR CODE FROM SUBROUTINE IS',I3)
  WRITE(6,500)K
  500 FORMAT('CFOR',I3,'SEC. THE COEFS,ROOTS(RE),ROOTS(IM),POLES ARE')
  DO 80 I=1,K
    WRITE(6,700)D(I),R(I),E(I),W(I)
  700 FORMAT(/1X,5D23.12)
  80 CONTINUE
  70 CONTINUE
  DO 90 N=1,100,2
    F(N)=(-8.66,0.0)+CDSQRT((75.0,0.0)-809CC0).0*(N**2))
  90 CONTINUE
  WRITE(6,701)
  701 FORMAT('1 THE 1ST 50 POLES OF THE REAL SHORTED LINE ARE')
  WRITE(6,500) (F(N),N=1,100,2)
  900 FORMAT(/1X,2D24.6)
  STOP
  END

```


APPENDIX D.2


```

C K. SCHMIDT PROGRAM TO COMPUTE POLES OF LUMPED LINE MODEL
C LUMPED MODEL OF LOSSY LINE
C "L" SECTION LINE
C SHORT CIRCUITED TERMINATION
C VIEWED FROM CAPACITOR AT INPUT
C CONSTANT R,L, AND C ASSUMED (POSS. SEQUENCE)
C TYPICAL 765KV LINE PARAMETERS
C LENGTH=100 MILES, R=0.2251 OHMS/MILE, L=0.00145 HENRYS/MILE
C C=2.1*10-8 FARADS/MILE
C W=CCOMPLEX PCLES OF THE MODEL
C F=CCOMPLEX PCLES OF THE ACTUAL LINE 100 MILES LONG
C D(1)"DENOMINATOR OF DRIVING PT. IMPEDANCE POLYNOMIAL
C
C
C COMPLEX*8 F(100)/100*(0.0,0.0)/
C COMPLEX*8 G,Q,S,T,W(60)/60*(0.0,0.0)/,CC,GG,DD
C REAL*4 H(62)/60*0.0/
C REAL*8 A(60,60)/3600*0.0/,B(60,60)/3600*0.0/
C REAL*8 D(60)/60*0.0/,R(60)/60*0.0/,E(60)/60*0.0/,P(60)/60*0.0/
C "INC" IS THE INCREMENT IN GENERATING THE "D" POLYNOMIAL AND IN
C OBTAINING ITS ROOTS
C "M" IS THE MAX. NO. OF SECTIONS IN THE MODEL
C READ(5,100)M,INC
C
C 100 FORMAT(2I3)
C TO GENERATE "D" IT'S NECESSARY TO GEN. A AND B POLYS
C A(2,1)=1.0
C B(1,1)=1.0
C THE ABOVE ARE THE COEFFICIENTS OF THE FIRST A AND B POLYS
C THE FOLLOWING DOUBLE LOOP GENERATES THE A AND B POLYS
C DO 40 K=2,M
C L=K+1
C N=K+1
C DO 20 I=1,N
C IF(I.EQ.1) GO TO 11
C GO TO 25
C 11 A(1,K)=-R(1,K-1)

```

```

F.1*0001
E.1*0002
E.1*0003
E.1*0004
E.1*0005
E.1*0006
E.1*0007
E.1*0008
E.1*0009
E.1*0010
E.1*0011
E.1*0012
E.1*0013
E.1*0014
E.1*0015
E.1*0016
E.1*0017
E.1*0018
E.1*0019
E.1*0020
E.1*0021
E.1*0022
E.1*0023
E.1*0024
E.1*0025
E.1*0026
E.1*0027
E.1*0028
E.1*0029
E.1*0030
E.1*0031
E.1*0032
E.1*0033
E.1*0034
E.1*0035
E.1*0036

```



```

      B(1,K)=A(1,K-1)
      GO TO 30
25  IF(I.EQ.2) GO TO 12
      GO TO 26
12  A(2,K)=A(1,K-1)-B(2,K-1)
      R(2,K)=R(1,K-1)+A(2,K-1)
      GO TO 30
26  IF(I.EQ.K) GO TO 13
      GO TO 27
13  A(1,K)=A(1-1,K-1)+B(1-2,K-1)
      B(1,K)=B(1-1,K-1)+A(1,K-1)
      GO TO 30
27  IF(I.EQ.L) GO TO 13
      A(1,K)=A(1-1,K-1)+B(1-2,K-1)-B(1,K-1)
      B(1,K)=B(1-1,K-1)+A(1,K-1)
30  CONTINUE
40  CONTINUE
      C
      THE FOLLOWING LOOPS GENERATE THE "D" POLY AND CALL DPRBM
      DO 70 K=1,M,INC
      DO 60 I=1,K
      IF(I.EQ.K) GO TO 61
      GO TO 65
61  D(I)=B(K,K)
      GO TO 60
65  D(I)=B(I,K)-B(1,K-1)
60  CCNTINUE
      J=K-1
      CALL DPRBM(D,60,R,E,P,J,IFP)
      DO 601 IP=1,50
      H(IP)=R(IP)
601  CCNTINUE
      DO 66 IN=1,J
      G=(75.0,C.0)
      Q=(6560000,C,C.0)
      S=(1.0,C.0)
      T=(-2.64,C.0)

```

```

E.1*0037
E.1*0038
F.1*0039
E.1*0040
E.1*0041
E.1*0042
E.1*0043
E.1*0044
E.1*0045
F.1*0046
E.1*0047
E.1*0048
E.1*0049
E.1*0050
E.1*0051
E.1*0052
E.1*0053
E.1*0054
E.1*0055
E.1*0056
E.1*0057
E.1*0058
E.1*0059
E.1*0060
E.1*0061
E.1*0062
E.1*0063
E.1*0064
E.1*0065
E.1*0066
E.1*0067
E.1*0068
E.1*0069
E.1*0070
E.1*0071
E.1*0072

```



```

      KSQD=J**2
      W(IN)=T+CSQRT(G-Q*KSQD*(S-H(IN)))
      CCNTINUE
66  WRITE(6,800)J,IER
800  FORMAT('CFGR',I3,'SEC. THE ERROR CODE FROM SUBROUTINE IS',I3)
500  WRITE(6,500)I
      FORMAT('CFGR',I3,'SEC. THE COEF,ROOTS(RE),ROOTS(IM),2 POLES ARE')
      DO 80 I=1,K
      WRITE(6,700)D(I),R(I),E(I),W(I)
700  FORMAT('/IX,5D23.12)
      CCNTINUE
80  CONTINUE
70  CONTINUE
      DO 90 N=1,100,2
      F(N)=(-8.66,0.0)+CD SQRT((75.0,0.0)-8090000.0*(N**2))
90  CONTINUE
      WRITE(6,701)
701  FORMAT('1 THE 1ST 50 POLES OF THE REAL SHORTED LINE ARE')
      WRITE(6,900) (F(N),N=1,100,2)
900  FORMAT('/IX,2D24.6)
      STOP
      END
E.1*0073
E.1*0074
E.1*0075
E.1*0076
E.1*0077
E.1*0078
E.1*0079
E.1*0080
E.1*0081
E.1*0082
E.1*0083
E.1*0084
E.1*0085
E.1*0086
E.1*0087
E.1*0088
E.1*0089
E.1*0090
E.1*0091
E.1*0092
E.1*0093

```


APPENDIX D.3


```

C      K. SCHMIDT PROGRAM TO CCMPUTE POLES OF LUMPED LINE MODEL
C      LOSSLESS LINE MODEL
C      "L" SECTION LINE
C      CPEN TERMINATION
C      CP=POS.SEC. CAPACITANCE(F/MI) OF TYPICAL 765KV LINE
C      LP=PCS.SEC. INDUCTANCE(H/MI) OF TYPICAL 765KV LINE
C      WL=ANG. FREQ. CF MODEL POLE*(LENGTH OF ACTUAL LINE IN MILES)
C      WRL=ANG.FREQ. CF ACTUAL LINE*(LENGTH IN MILES)
C      C(I)"DENCMINATOR OF DRIVING PT. IMPEDANCE POLYNOMIAL
C
C      REAL*4 LP
C      REAL*8 WL(60)/60*0.0/,WRL(100)/100*0.0/
C      REAL*4 H(60)/60*0.0/
C      REAL*8 A(60,60)/3600*0.0/,B(60,60)/3600*0.0/
C      REAL*8 D(60)/60*0.0/,R(60)/60*0.0/,E(60)/60*0.0/,P(60)/60*0.0/
C      "INC" IS THE INCFREMENT IN GENERATING THE "D" POLYNOMIAL AND IN
C      OBTAINING ITS RCCTS
C      "M" IS THE MAX. NO. OF SECTIONS IN THE MODEL
C      READ(5,100)M,INC
C      100 FORMAT(2I3)
C      TO GENERATE "D" IT'S NECESSARY TO GEN.A AND B POLYS
C      A(2,1)=1.0
C      B(1,1)=1.0
C      THE ABOVE ARE THE COEFFICIENTS OF THE FIRST A AND B POLYS
C      THE FOLLOWING DOUBLE LOOP GENERATES THE A AND B POLYS
C      DO 40 K=2,M
C      L=K+1
C      N=K+1
C      DO 30 I=1,N
C      IF(I.EQ.1) GO TO 11
C      GO TO 25
C      11 A(1,K)=-E(1,K-1)
C      B(1,K)=A(1,K-1)
C      GO TO 30
C      25 IF(I.EQ.2) GO TO 12

```

```

E.2*0001
E.2*0002
E.2*0003
E.2*0004
E.2*0005
E.2*0006
E.2*0007
E.2*0008
E.2*0009
E.2*0010
E.2*0011
E.2*0012
E.2*0013
E.2*0014
E.2*0015
E.2*0016
E.2*0017
E.2*0018
E.2*0019
E.2*0020
E.2*0021
E.2*0022
E.2*0023
E.2*0024
E.2*0025
E.2*0026
E.2*0027
E.2*0028
E.2*0029
E.2*0030
E.2*0031
E.2*0032
E.2*0033
E.2*0034
E.2*0035
E.2*0036

```



```

GO TO 26
12 A(2,K)=A(1,K-1)-B(2,K-1)
   B(2,K)=B(1,K-1)+A(2,K-1)
GO TO 30
26 IF(I.EQ.K) GO TO 13
   GO TO 27
13 A(1,K)=A(I-1,K-1)+B(I-2,K-1)
   B(1,K)=B(I-1,K-1)+A(I,K-1)
GO TO 30
27 IF(I.EQ.L) GO TO 13
   A(1,K)=A(I-1,K-1)+B(I-2,K-1)-B(I,K-1)
   B(1,K)=B(I-1,K-1)+A(I,K-1)
30 CONTINUE
40 CONTINUE
   LP=0.C0145
   CP=2.1*1C*(-8.0)
   DO 90 N=1,50
     WRL(N)=(3.141592*N)/(SQRT(LP*CP))
50 CONTINUE
   WRITE(6,701)
701 FORMAT('1 THE 1ST 50 POLES (EXCLUDING WRL=0) OF THE ACTUAL OPEN
      1 LINE ARE')
   WRITE(6,900) (WRL(N),N=1,50)
900 FORMAT(/1X,C24.6)
      C THE FOLLOWING LOOPS GENERATE THE "D" POLY AND CALL DPRBM
      DO 70 K=1,M,INC
        J=K+1
      DO 60 I=1,J
        IF(I.EQ.1) GO TO 61
        IF(I.EQ.J) GO TO 62
        D(I)=B(I,K)-B(I-1,K)
        GO TO 60
      61 D(I)=B(I,K)
        GO TO 60
      62 D(I)=-B(K,K)
      60 CONTINUE
E.2*0037
E.2*0038
E.2*0039
E.2*0040
E.2*0041
E.2*0042
E.2*0043
E.2*0044
E.2*0045
E.2*0046
E.2*0047
E.2*0048
E.2*0049
E.2*0050
E.2*0051
E.2*0052
E.2*0053
E.2*0054
E.2*0055
E.2*0056
E.2*0057
E.2*0058
E.2*0059
E.2*0060
E.2*0061
E.2*0062
E.2*0063
E.2*0064
E.2*0065
E.2*0066
E.2*0067
E.2*0068
E.2*0069
E.2*0070
E.2*0071
E.2*0072

```



```

CALL CPREM(C,6C,R,E,P,K,I,IER)
DO 601 IP=1,50
  F(IP)=R(IP)
601 CCNTINUE
DO 66 IN=1,K
  Q=K
  WL(IN)=Q*SQRT(2*(1.0-H(IN))/(LP*CP))
66 CONTINUE
  WRITE(6,800)K,IER
800 FORMAT('CFOR',I3,'SEC. THE ERROR CODE FROM SUBROUTINE IS',I3)
  WRITE(6,500)K
500 FFORMAT('CFOR',I3,'SEC. THE COEFS,ROCTS(RE),ROOTS(IM),a POLES ARE')
  DO 80 I=1,J
    WRITE(6,700) C(I),R(I),E(I),WL(I)
700 FORMAT(/IX,4D23.12)
80 CONTINUE
70 CONTINUE
STOP
END

```

```

E.2*0073
E.2*0074
E.2*0075
E.2*0076
E.2*0077
E.2*0078
E.2*0079
E.2*0080
E.2*0081
E.2*0082
E.2*0083
E.2*0084
E.2*0085
E.2*0086
E.2*0087
F.2*0088
E.2*0089
E.2*0090
E.2*0091

```


APPENDIX D.4


```

C      K. SCHMIDT PROGRAM TO COMPUTE POLES OF LUMPED LINE MODEL
C      LOSSLESS LINE MODEL
C      PI SECTIONS
C      SHORT CIRCUITED TERMINATION
C      CP=POS.SEQ. CAPACITANCE(F/MI) OF TYPICAL 765KV LINE
C      LP=POS.SEQ. INDUCTANCE(H/MI) OF TYPICAL 765KV LINE
C      WL=ANG. FREQ. OF MODEL POLE*(LENGTH OF ACTUAL LINE IN MILES)
C      WRL=ANG. FREQ. OF ACTUAL LINE*(LENGTH IN MILES)
C      D(1)"DENOMINATOR OF DRIVING PT. IMPEDANCE POLYNOMIAL
C
C      REAL*4 LP
C      REAL*8 WL(60)/60*0.3/.WRL(100)/100*0.0/
C      REAL*4 H(60)/60*0.0/
C      REAL*8 A(60,60)/3600*0.0/.B(60,60)/3600*0.0/
C      REAL*8 D(60)/60*0.0/.R(60)/60*0.0/.E(60)/60*0.0/.P(60)/60*0.0/
C      "INC" IS THE INCREMENT IN GENERATING THE "D" POLYNOMIAL AND IN
C      OBTAINING ITS ROOTS
C      "M" IS THE MAX. NO. OF SECTIONS IN THE MODEL
C      READ(5,100)M,INC
C      100 FORMAT(2I3)
C      TO GENERATE "D" IT'S NECESSARY TO GEN.A AND B POLYS
C      A(2,1)=1.0
C      B(1,1)=1.0
C      THE ABOVE ARE THE COEFFICIENTS OF THE FIRST A AND B POLYS
C      THE FOLLOWING DOUBLE LOOP GENERATES THE A AND B POLYS
C      DO 40 K=2,M
C      L=K+1
C      N=K+1
C      DO 30 I=1,N
C      IF(I.EQ.1) GO TO 11
C      GO TO 25
C      11 A(1,K)=-B(1,K-1)
C      B(1,K)=A(1,K-1)
C      GO TO 30
C      25 IF(I.EQ.2) GO TO 12

```

E.3*0001
 E.3*0002
 E.3*0003
 E.3*0004
 E.3*0005
 E.3*0006
 E.3*0007
 E.3*0008
 E.3*0009
 E.3*0010
 E.3*0011
 E.3*0012
 E.3*0013
 E.3*0014
 E.3*0015
 E.3*0016
 E.3*0017
 E.3*0018
 E.3*0019
 E.3*0020
 E.3*0021
 E.3*0022
 E.3*0023
 E.3*0024
 E.3*0025
 E.3*0026
 E.3*0027
 E.3*0028
 E.3*0029
 E.3*0030
 E.3*0031
 E.3*0032
 E.3*0033
 E.3*0034
 E.3*0035
 E.3*0036


```

      GO TO 26
12  A(2,K)=A(1,K-1)-B(2,K-1)
      B(2,K)=B(1,K-1)+A(2,K-1)
      GO TO 30
26  IF(I.EQ.K) GO TO 13
      GO TO 27
13  A(I,K)=A(I-1,K-1)+B(I-2,K-1)
      B(I,K)=B(I-1,K-1)+A(I,K-1)
      GO TO 30
27  IF(I.EQ.L) GO TO 13
      A(I,K)=A(I-1,K-1)+B(I-2,K-1)-B(I,K-1)
      B(I,K)=B(I-1,K-1)+A(I,K-1)
30  CONTINUE
40  CONTINUE
      LP=0.00145
      CP=2.1*10**(-8.0)
      DO 90 N=1,100,2
      WRL(N)=(3.1415927*N)/(2*SORT(LP*CP))
90  CONTINUE
      WRITE(6,701)
701  FORMAT('1 THE 1ST 50 POLES OF THE REAL SHORTED LINE ARE')
      WRITE(6,900) (WRL(N),N=1,100,2)
900  FORMAT(/1X,D24.6)
      THE FOLLOWING LOOPS GENERATE THE "D" POLY AND CALL DPRBM
      DO 70 K=1,M,INC
      J=K+1
      DO 60 I=1,J
      D(I)=A(I,K)
60  CONTINUE
      CALL DPRBM(D,60,R,E,P,KI,IER)
      DO 601 IP=1,50
      H(IP)=R(IP)
601  CONTINUE
      DO 66 IN=1,K
      Q=K
      WL(IN)=Q*SORT(2*(1.C-H(IN))/(LP*CP))

```

C

E.3#0037
 E.3#0038
 E.3#0039
 E.3#0040
 E.3#0041
 E.3#0042
 E.3#0043
 E.3#0044
 E.3#0045
 E.3#0046
 E.3#0047
 E.3#0048
 E.3#0049
 E.3#0050
 E.3#0051
 E.3#0052
 E.3#0053
 E.3#0054
 E.3#0055
 E.3#0056
 E.3#0057
 E.3#0058
 E.3#0059
 E.3#0060
 E.3#0061
 E.3#0062
 E.3#0063
 E.3#0064
 E.3#0065
 E.3#0066
 E.3#0067
 E.3#0068
 E.3#0069
 E.3#0070
 E.3#0071
 E.3#0072


```

66 CONTINUE
   WRITE(6,800)K, IER
800 FORMAT('0FOR', I3, 'SEC. THE ERROR CODE FROM SUBROUTINE IS', I3)
   WRITE(6,500)K
500 FORMAT('0FOR', I3, 'SEC. THE COEFS,ROOTS(RE),ROOTS(IM),2 POLES ARE')
      DO 80 I=1,JJ
   WRITE(6,700) D(I),R(I),E(I),WL(I)
700 FORMAT(/1X,4D23.12)
80 CONTINUE
70 CONTINUE
   STOP
   END

```

```

E.3*0073
E.3*0074
E.3*0075
E.3*0076
E.3*0077
E.3*0078
E.3*0079
E.3*0080
E.3*0081
E.3*0082
E.3*0083
E.3*0084

```


APPENDIX D.5


```

C      K. SCHMIDT PROGRAM TO COMPUTE POLES OF LUMPED LINE MODEL
C      LOSSLESS LINE MODEL
C      PI SECTIONS
C      OPEN TERMINATION
C      CP=POS.SEQ. CAPACITANCE(F/MI) OF TYPICAL 765KV LINE
C      LP=POS.SEQ. INDUCTANCE(H/MI) OF TYPICAL 765KV LINE
C      WL=ANG. FREQ. OF MODEL POLE*(LENGTH OF ACTUAL LINE IN MILES)
C      WRL=ANG.FREQ. OF ACTUAL LINE*(LENGTH IN MILES)
C      D(I)"DENOMINATOR OF DRIVING PT. IMPEDANCE POLYNOMIAL
C
C      REAL*4 LP
C      REAL*8 WL(60)/60*0.0/,WRL(100)/100*0.0/
C      REAL*4 H(60)/60*0.0/
C      REAL*8 A(60,60)/3600*0.0/,B(60,60)/3600*0.0/
C      REAL*8 D(60)/60*0.0/,R(60)/60*0.0/,E(60)/60*0.0/,P(60)/60*0.0/
C      "WINC" IS THE INCREMENT IN GENERATING THE "D" POLYNOMIAL AND IN
C      OBTAINING ITS ROOTS
C      "M" IS THE MAX. NO. OF SECTIONS IN THE MODEL
C      READ(5,100)M,INC
C      100 FORMAT(2I3)
C      TO GENERATE "D" IT'S NECESSARY TO GEN.A AND B POLYS
C      A(2,1)=1.0
C      B(1,1)=1.0
C      THE ABOVE ARE THE COEFFICIENTS OF THE FIRST A AND B POLYS
C      THE FOLLOWING DOUBLE LOOP GENERATES THE A AND B POLYS
C      DO 40 K=2,M
C      L=K+1
C      N=K+1
C      DO 30 I=1,N
C      IF(I.EQ.1) GO TO 11
C      GO TO 25
C      11 A(1,K)=-B(1,K-1)
C      B(1,K)=A(1,K-1)
C      GO TO 30
C      25 IF(I.EQ.2) GO TO 12

```

```

E.4*0001
E.4*0002
E.4*0003
E.4*0004
E.4*0005
E.4*0006
E.4*0007
E.4*0008
E.4*0009
E.4*0010
E.4*0011
E.4*0012
E.4*0013
E.4*0014
E.4*0015
E.4*0016
E.4*0017
E.4*0018
E.4*0019
E.4*0020
E.4*0021
E.4*0022
E.4*0023
E.4*0024
E.4*0025
E.4*0026
E.4*0027
E.4*0028
E.4*0029
E.4*0030
E.4*0031
E.4*0032
E.4*0033
E.4*0034
E.4*0035
E.4*0036

```



```

GO TO 26
12 A(2,K)=A(1,K-1)-B(2,K-1)
   B(2,K)=B(1,K-1)+A(2,K-1)
GO TO 30
26 IF(I.EQ.K) GO TO 13
GO TO 27
13 A(I,K)=A(I-1,K-1)+B(I-2,K-1)
   B(I,K)=B(I-1,K-1)+A(I,K-1)
GO TO 30
27 IF(I.EQ.L) GO TO 13
   A(I,K)=A(I-1,K-1)+B(I-2,K-1)-B(I,K-1)
   B(I,K)=B(I-1,K-1)+A(I,K-1)
30 CONTINUE
40 CONTINUE
   LP=3.00145
   CP=2.1*10**(-8.0)
   DO 90 N=1,50
     WRL(N)=(3.141592*N)/(SQRT(LP*CP))
90 CONTINUE
   WRITE(6,701)
701 FORMAT('1 THE 1ST 50 POLES (EXCLUDING WRL=0) OF THE ACTUAL OPEN
      1 LINE ARE')
   WRITE (6,900) (WRL(N),N=1,50)
900 FORMAT(/1X,D24.6)
C THE FOLLOWING LOOPS GENERATE THE "DM" POLY AND CALL DPRBM
DO 70 K=1,M,INC
  JM=K+1
  JJ=K+2
DO 60 I=1,JJ
  IF(I.EQ.1) GO TO 61
  IF(I.EQ.2) GO TO 61
  IF(I.EQ.JM) GO TO 62
  IF(I.EQ.JJ) GO TO 63
  D(I)=(B(I-2,K)-B(I,K))
61 D(I)=-B(I,K)
GO TO 60

```

```

E.4*0037
E.4*0038
E.4*0039
E.4*0040
E.4*0041
E.4*0042
E.4*0043
E.4*0044
E.4*0045
E.4*0046
E.4*0047
E.4*0048
E.4*0049
E.4*0050
E.4*0051
E.4*0052
E.4*0053
E.4*0054
E.4*0055
E.4*0056
E.4*0057
E.4*0058
E.4*0059
E.4*0060
E.4*0061
E.4*0062
E.4*0063
E.4*0064
E.4*0065
E.4*0066
E.4*0067
E.4*0068
E.4*0069
E.4*0070
E.4*0071
E.4*0072

```



```

62 D(I)=B(K-1,K)
   GO TO 60
63 D(I)=B(K,K)
60 CONTINUE
   J=K+1
   CALL DPRBM(D,60,R,E,P,JM,IER)
   DO 601 IP=1,50
     H(IP)=R(IP)
601 CONTINUE
   DO 66 IN=1,J
     Q=K
     WL(IN)=Q*SQRT(2*(1.0-H(IN))/(LP*CP))
66 CONTINUE
   WRITE(6,800)K,IER
800 FORMAT('OFR',I3,'SEC. THE ERROR CODE FROM SUBROUTINE IS',I3)
   WRITE(6,500)K
500 FORMAT('OFR',I3,'SEC. THE COEFS,ROOTS(RE),ROOTS(IM),2 POLES ARE')
   DO 80 I=1,JJ
     WRITE(6,700) D(I),R(I),E(I),WL(I)
700 FORMAT(/IX,4D23.12)
80 CONTINUE
70 CONTINUE
   STOP
   END
E.4*0073
E.4*0074
E.4*0075
E.4*0076
E.4*0077
E.4*0078
E.4*0079
E.4*0080
E.4*0081
E.4*0082
E.4*0083
E.4*0084
E.4*0085
E.4*0086
E.4*0087
E.4*0088
E.4*0089
E.4*0090
E.4*0091
E.4*0092
E.4*0093
E.4*0094
E.4*0095
E.4*0096

```


APPENDIX D.6


```

C      K. SCHMIDT PROGRAM TO COMPUTE POLES OF LUMPED LINE MODEL
C      LUMPED MODEL OF LOSSY LINE
C      "L" SECTION LINE
C      SHORT CIRCUITED TERMINATION
C      VIEWED FROM INDUCTOR AT INPUT
C      TYPICAL 765KV LINE PARAMETERS
C      ELECTRICAL PARAMETERS ARE ZERO SEQUENCE VALUES
C      LENGTH=100.0MILES,R=0.51OHMS/MILE,L=0.0042 HENRYS/MILE
C      C=1.43*10**(-8) FARADS/MILE
C      W=COMPLEX PCLES OF THE MODEL
C      F=CCOMPLEX PCLES OF THE ACTUAL LINE 100 MILES LONG
C      D(1)"DENCMINATOR OF DRIVING PT. IMPEDANCE POLYNOMIAL
C
C      CCMPLX*E F(100)/100*(0.0,0.0)/
C      COMPLEX*E G,Q,S,T,W(60)/60*(0.0,0.0)/,CC,GG,DD
C      REAL*4 H(60)/60*0.0/
C      REAL*8 A(60,60)/3600*0.0/,B(60,60)/3600*0.0/
C      REAL*8 C(60)/60*0.0/,R(60)/60*0.0/,E(60)/60*0.0/,P(60)/60*0.0/
C      "INC" IS THE INCREMENT IN GENERATING THE "D" POLYNOMIAL AND IN
C      OBTAINING ITS ROOTS
C      "M" IS THE MAX. NO. OF SECTIONS IN THE MODEL
C      READ(5,1CC)"M,INC
C      FORMAT(2I3)
C      TO GENERATE "C" IT'S NECESSARY TO GEN.A AND B POLYS
C      A(2,1)=1.0
C      B(1,1)=1.0
C      THE ABOVE ARE THE CCEFFICIENTS OF THE FIRST A AND B POLYS
C      THE FOLLOWING COUPLE LCCP GENERATES THE A AND B POLYS
C      DO 40 K=2,M
C      L=K+1
C      N=K+1
C      DO 30 I=1,N
C      IF(I.EQ.1) GO TO 11
C      GO TO 25
C      11 A(1,K)=-B(1,K-1)

```

```

E.5*0001
E.5*0002
E.5*0003
E.5*0004
E.5*0005
E.5*0006
E.5*0007
E.5*0008
E.5*0009
E.5*0010
E.5*0011
E.5*0012
E.5*0013
E.5*0014
E.5*0015
E.5*0016
E.5*0017
E.5*0018
E.5*0019
E.5*0020
E.5*0021
E.5*0022
E.5*0023
E.5*0024
E.5*0025
E.5*0026
E.5*0027
E.5*0028
E.5*0029
E.5*0030
E.5*0031
E.5*0032
E.5*0033
E.5*0034
E.5*0035
E.5*0036

```



```

      B(I,K)=A(I,K-1)
      GO TO 30
25  IF(I.EQ.2) GO TO 12
      GO TO 26
12  A(2,K)=A(1,K-1)-B(2,K-1)
      B(2,K)=B(1,K-1)+A(2,K-1)
      GO TO 30
26  IF(I.EQ.K) GO TO 13
      GO TO 27
13  A(I,K)=A(I-1,K-1)+B(I-2,K-1)
      B(I,K)=B(I-1,K-1)+A(I,K-1)
      GO TO 30
27  IF(I.EQ.L) GO TO 13
      A(I,K)=A(I-1,K-1)+B(I-2,K-1)-B(I,K-1)
      B(I,K)=B(I-1,K-1)+A(I,K-1)
30  CONTINUE
40  CONTINUE
C    THE FOLLOWING LOOPS GENERATE THE "D" POLY AND CALL DPRBM
      DO 70 K=1,M,INC
      DO 60 I=1,K
      IF(I.EQ.K) GO TO 61
      GO TO 65
61  D(I)=B(K,K)
      GO TO 60
65  D(I)=B(I,K)-B(I,K-1)
60  CONTINUE
      J=K-1
      CALL DPRBM(C,60,R,E,P,J,IER)
      DO 601 IP=1,50
      H(IP)=R(IP)
601 CONTINUE
      DO 66 IN=1,J
      G=(27CC.C,C.G)
      C=(332CC00.0,0.0)
      S=(1.0,0.0)
      T=(-6C.9,0.0)

```

```

E.5*0037
E.5*0038
E.5*0039
E.5*0040
E.5*0041
E.5*0042
E.5*0043
E.5*0044
E.5*0045
E.5*0046
E.5*0047
E.5*0048
E.5*0049
E.5*0050
E.5*0051
E.5*0052
E.5*0053
E.5*0054
E.5*0055
E.5*0056
E.5*0057
E.5*0058
E.5*0059
E.5*0060
E.5*0061
E.5*0062
E.5*0063
E.5*0064
E.5*0065
E.5*0066
E.5*0067
E.5*0068
E.5*0069
E.5*0070
E.5*0071
E.5*0072

```



```

KSQD=K**2
W(IN)=T+CSQRT(G-C*KSQD*(S-H(IN)))
66 CONTINUE
WRITE(6,800)K,IER
800 FORMAT('OFCR',I3,'SEC. THE ERROR CODE FROM SUBROUTINE IS',I3)
WRITE(6,500)K
500 FORMAT('CFCR',I3,'SEC. THE COEFS,ROOTS(RE),ROOTS(IM),& POLES ARE')
DO 80 I=1,K
WRITE(6,700)D(I),R(I),E(I),W(I)
700 FORMAT(/IX,5D23.12)
80 CONTINUE
70 CONTINUE
DO 90 N=1,100,2
AA=-4100000.0*(N**2)
BB=0.0
CC=CMPLX(AA,BB)
GG=CMPLX(3700.0,0.0)
DD=CC+GG
F(N)=T+CSQRT(CC)
90 CONTINUE
WRITE(6,701)
701 FORMAT('1 THE 1ST 50 POLES OF THE REAL SHORTED LINE ARE')
WRITE(6,500) (F(N),N=1,100,2)
900 FORMAT(/IX,2D24.6)
STOP
END
E.5*0073
E.5*0074
E.5*0075
E.5*0076
E.5*0077
E.5*0078
E.5*0079
E.5*0080
E.5*0081
E.5*0082
E.5*0083
E.5*0084
E.5*0085
E.5*0086
E.5*0087
E.5*0088
E.5*0089
E.5*0090
E.5*0091
E.5*0092
E.5*0093
E.5*0094
E.5*0095
E.5*0096
E.5*0097
E.5*0098

```


LIST OF REFERENCES

In order Cited:

1. Djurdjevic, P. and Ruoss, E., Network Analysers for Studying Transient Phenomena in High-Voltage Networks, Brown Boveri Review, Vol. 55, No. 12, p. 734.
2. Cortain, R. and Koglin, H.J., Model for Demonstrating Problems in Transmission Systems and Power Stations, Siemens Rev. XXXVI (1969) No. 8, p. 315.
3. Clerici, A., Main Characteristics of TNA at CESI, letter dtd 1st August 1969 to Professor H.H. Woodson, M.I.T., Cambridge, Mass.
4. Peterson, H.A., Transients in Power Systems, Dover Publications Inc., New York, N.Y., 1966, Chapter 1-5, p. 29.
5. Wilson, G.L. and Bosack, D.J., Effects of Non Transposition on Steady-State Overvoltages on EHV Transmission Lines, Report No. 5 of the Power Systems Engineering Group, Department of Electrical Engineering, M.I.T., Cambridge, Mass.
6. Ibid. p. 15
7. Adler, R.B., Chu, L.J., and Fano, R.M., Electromagnetic Energy Transmission and Radiation, John Wiley and Sons, Inc., New York N.Y., 1960, Chapters 3, 4, 5 and 6.
8. Chipman, R.A., Theory and Problems of Transmission Lines, Schaum's Outline Series, McGraw-Hill Book Co., New York, N.Y. 1968.
9. Stevenson, W.D., Jr., Elements of Power System Analysis, McGraw-Hill Book Company, 1962, Ch. 5.
10. Marchenko, P.P., Electrical Characteristics of Transmission Lines Part 1, AEP and OVEC EHV Systems, Report No. 710, January 1967, American Electric Power Service Corporation, Appendix 4, Figure 7.
11. Wilson, G.L., Preliminary Calculation of UHV Line Parameters, AEP-ASEA Research Project, Report No. 1, January 30, 1970.
12. Wilson, G.L., Electric Power Systems Laboratory Line and Model Parameters Program, M.I.T., 1969. An unpublished program written for The Laboratory and maintained in Prof. Wilson's custody.
13. Legg, V.E., Analysis of Quality Factor of Annular Core Inductors, The Bell System Technical Journal, January, 1960.

14. Blinchikoff, H., Toroidal Inductor Design, Electro-Technology, November, 1964.
15. Legg, V.E., Magnetic Measurements at Low Flux Densities Using the A-C Bridge, The Bell System Technical Journal, Vol. 15, January, 1936, p.p. 39-63.
16. Winch, R.P., Electricity and Magnetism, Prentice Hall Inc., Englewood Cliffs, N.J., 1963, Chapters XVI and XVII.
17. M.I.T. Electrical Engineering Staff, Magnetic Circuits and Transformers, John Wiley and Sons, Inc., New York, 1943, p.p. 433ff.
18. Arnold Engineering Co., All About Arnold MPP Cores, Arnold Engineering Co., Bulletin PC-104D, Marengo Illinois.
19. Arnold Engineering Co., Arnold Silection Cores, Arnold Engineering Co. Bulletin SC-107B, Merengo, Illinois.
20. Arco Electronics, Inc., Precision Film Capacitors, Community Drive, Great Neck, New York, Catalog A-14, p. 9.
21. Von Hippel, A.R., Ed., Dielectric Materials and Applications, The M.I.T. Press, M.I.T., Cambridge, Mass., 1954.

Thesis
S33724 Schmidt

127269

Design of a non-trans-
posed power transmis-
sion line model.

24 SEP 71

DISPLAY

Thesis
S33724 Schmidt

127269

Design of non-trans-
posed power transmis-
sion line model.

thesS33724

Design of a non-transposed power transmi



3 2768 002 00374 1

DUDLEY KNOX LIBRARY